

Asia Pacific Research Initiative for Sustainable Energy Systems 2012 (APRISES12)

**Office of Naval Research
Grant Award Number N00014-13-1-0463**

Computational Fluid Dynamics (CFD) Applications at the School of Architecture, University of Hawaii: Summary & Conclusion for Occupant Comfort in Naturally Ventilated Spaces

Task 7

Prepared For
Hawaii Natural Energy Institute

Prepared By
Sustainable Design & Consulting LLC, UH Environmental Research and
Design Laboratory, UH Sea Grant College Program & HNEI

February 2016



Computational Fluid Dynamics (CFD) Applications at the School of Architecture,
University of Hawaii:

Modeling and Validating Thermal Comfort in Naturally Ventilated Spaces

Project Phase 1 – 7.C

Task 7.c.7: Project Summary Report and Presentation for Phase 7.c (Phase 3)

Project Deliverable No. 15:

Summary of the Research Project and Presentation of Results of Phase 3

Prepared for:

Hawaii Natural Energy Institute
School of Ocean and Earth Science and Technologies
University of Hawaii at Manoa

in support of:

Contract #N000-14-13-1-0463

February 11, 2016

Prepared by:

Manfred J. Zapka, PhD, PE (Lead author/editor) ⁽¹⁾

Tuan Tran, D. Arch ⁽²⁾

Eileen Peppard, M. Sc. ⁽³⁾

James Maskrey, MEP, MBA, Project Manager ⁽⁴⁾

Stephen Meder, D. Arch, Director ⁽²⁾

(1) Sustainable Design & Consulting LLC, Honolulu, Hawaii

(2) Environmental Research and Design Laboratory (ERDL), School of Architecture, University of Hawaii

(3) University of Hawaii Sea Grant College Program

(4) Hawaii Natural Energy Institute Honolulu, Hawaii

ACKNOWLEDGEMENTS

The authors would like to thank the Office of Naval Research (ONR) and Hawaii Natural Energy Institute (HNEI) for their support and funding of the research work conducted under this project.

The authors would like to thank students and staff members of the Environmental Design & Research Laboratory (ERDL) for their assistance in carrying out parts of this research study.

The contributions and support of the following companies are greatly appreciated for offering free or discounted products to conduct the work of the Research Program:

- *Cd-Adapco* for the use of the CFD software STAR-D+CCM+
- *Barcol USA* for the significant discounts of their radiant cooling panels.
- *Big Ass Fans* for the use of one of their high performance Haiku ceiling fans
- *National Gypsum* for the use of their innovative change phase material (PCM) boards

ACRONYMS AND UNITS

ACRONYMS

3D	Three Dimensional
3D-Cad	Three Dimensional Computer Aided Design
ABL	Atmospheric Boundary Layer
ASHRAE	American Society of Heating, Refrigerating, and Air-Conditioning Engineers
BPG	Best Practice Guidelines
BRG	Gypsum Ceiling System
CAD	Computer Aided Design
CFD	Computational Fluid Dynamics
clo	Clothing insulation
Cp	Pressure Coefficient
DNS	Direct Numerical Simulations
ERDL	Environmental Design and Research Laboratory, University of Hawaii at Manoa
FDM	Finite Difference Method
FEM	Finite Element Method
FVM	Finite Volume Method
GUI	Graphical User Interface
HIG	Hawaii Institute of Geophysics
HNEI	Hawaii Natural Energy Institute
HVAC	Heating, Ventilation, and Air Conditioning
LES	Large Eddy Simulation
met	Metabolic rate
ONR	Office of Naval Research
PDE	Partial Differential Equation
PMV	Predicted Mean Vote
PPD	Predicted Percentage Dissatisfied
UHM	University of Hawaii at Manoa
V	Velocity
WDR	Wind-driven Rain
WS	Weather Station

UNITS:

DC	Direct Current
ft	Foot or feet
hz	Hertz
m	Meter
m/s	Meter per second
mph	Miles per Hour
Pa	Pascal
sqft	Square Feet

TABLE OF CONTENTS

ACRONYMS AND UNITS

EXECUTIVE SUMMARY AND OVERALL CONCLUSIONS..... 1

SECTION 1 - OVERVIEW OF RESEARCH PROJECT 8

SECTION 2 - SUMMARY BRIEF OF PREVIOUSLY COMPLETED PHASE 1..... 22

 2.1 Brief Summary of fundamentals of Wind Movement Around Buildings 23

 2.2 CFD Process Workflow 24

 2.3 Using Oceanside Windy Location as a Temporary Wind Tunnel 26

 2.4 Investigations of Wind Patterns Around a Building – Simulations 30

 2.5 Investigations of Wind Patterns Around a Building – Field Measurements 33

 2.6 Investigations of Wind Patterns Around a Building – Validation of CFD Simulations 36

 2.7 Main Conclusions of Part 1 of the Research Project..... 40

SECTION 3 - SUMMARY BRIEF OF PREVIOUSLY COMPLETED PHASE 2..... 42

 3.1 Basics of Air Flow through Internal Spaces 43

 3.2 Basic Considerations of CFD Simulations for Internal Spaces..... 44

 3.3 Initial Internal CFD Investigations to Develop a Generic Workflow..... 47

 3.4 Final Internal Air Movement Investigation at the Selected Building – Measurements..... 50

 3.5 Final Internal Air Movement Investigation at the Selected Building – CFD Simulations 52

 3.6 Final Internal Air Movement Investigation at the Selected Building – CFD Validation..... 55

 3.7 Process to Predict Natural Ventilation Performance of Spaces..... 57

SECTION 4 – SUMMARY OF PHASE 3 61

 4.1 Value Proposition of Comfort Islands 61

 4.2 Basics of Human Thermal Comfort 64

 4.3 Scope of Work in Part 3 of the Research Project..... 67

 4.4 Test-set up for Occupant Comfort 69

 4.5 Generic CFD Workflow for Comfort Assessment 73

 4.6 Air Flow Measurements Around Person 79

 4.7 CFD and Experimental Investigation of Air Movement without Test Subjects..... 80

4.8 CFD Simulations and Measurement of Radiant Heat Transfer Without Test Subject 83

4.9 Comfort Test with Human Test Subjects – Methodology and Results..... 86

4.10 Performance and Ranking of Comfort Enhancement Measures 88

EXECUTIVE SUMMARY AND OVERALL CONCLUSIONS

This report summarizes the research work of the Computational Fluid Dynamics (CFD) research project (Research Project) which is sponsored by the Hawaii Natural Energy Institute (HNEI) and the Office of Naval Research (ONR). The Research Project endeavors to apply advanced building modeling in the context of alternative building conditioning at the Environmental Design and Research Laboratory (ERDL), University of Hawaii at Manoa.

The research work of the Research Project, which was conducted in three parts, made important contributions to the understanding of the thermal performance of primarily naturally ventilated buildings. In this context “primarily naturally ventilated” buildings are buildings that might have a mechanical assist ventilation system available for periods of insufficient external wind induced driving forces for air movements inside of buildings.

Conventional mechanical space conditioning fulfills three main functions, space cooling, dehumidification and ventilation. In naturally ventilated buildings the energy demand for these three functions are avoided, since the state of outdoor air entering the buildings is not changed and ventilation is induced by external environmental conditions. Assist ventilation requires some quantity of energy, but this energy demand is significantly lower than mechanical ventilation in a conventional HVAC system.

Hawaii’s tropical climate is characterized by extended periods of warm and moist weather. Buildings in such a tropical climate have both a high sensible cooling energy demand and a high latent energy demand for dehumidification of the outdoor air supply brought into the building. As warm and moist outdoor air supply is cooled, its relative humidity rises. In order to achieve acceptable relative humidity levels, moisture must be expelled. Conventional dehumidification is accomplished by cooling the air below its dew point and separating condensate from the air. This process requires significant energy. Insufficient dehumidification can cause or contribute to a range of problems in building operations, including health related problems for occupants, such as mold and sick-building syndrome.

The drawback of naturally ventilated buildings is the dependence on external environmental conditions when it comes to safeguarding acceptable indoor environmental quality. In low wind conditions, ventilation rates cannot be maintained. At times, high outdoor temperatures coupled with high humidity levels (weather conditions which are frequently encountered in Hawaii) will cause unacceptable indoor environmental conditions.

The challenge and opportunity in energy efficient building design is to combine natural building ventilation with limited mechanical measures that will improve indoor thermal comfort and ventilation conditions enough to successfully compete with conventional HVAC. When we say “compete” we must be aware that in a tropical climate it is nearly impossible for natural ventilation to provide indoor conditions that resemble conventional HVAC performance for most of the year.

Conventional HVAC provides an artificial indoor environmental condition that can be continuously maintained. Maintaining such an artificial environment requires, of course, significant energy. Natural ventilation, on the other hand, creates an indoor environmental condition which is attuned to external and natural environmental conditions. Therefore, conventional HVAC and natural ventilation represent two opposites in terms of technical building equipment, and a difference in how occupants experience the built environment.

Recent developments in the understanding of alternative occupant comfort systems show differences from the understanding of conventional building cooling and conditioning. The conventional understanding of comfort basically asserts that uniform thermal conditions are sufficient to provide occupants with acceptable indoor thermal experiences. On the other hand, recent developments in comfort standards describe occupant comfort experiences on a more personalized basis. These new approaches to comfort include an appreciation that occupants want to have more control of their thermal sensation, and that they can adapt to changing environmental conditions and still feel comfortable.

The research work carried out during the three parts of the project consisted of the following processes:

Part 1 – External CFD Investigations: The work investigated modeling and validation of wind patterns around buildings. Natural ventilation in buildings is maintained by wind pressures on the building and by a temperature difference between outdoor and indoor air temperatures. For the research work, only wind induced ventilation (“cross ventilation”) was considered. For effective cross ventilation, a pressure difference between external openings in the building envelope is required as a driving force to convey air through interior spaces. The most effective of these external openings are on the windward and leeward sides of the building.

The investigations of wind patterns around buildings included assessments of how wind patterns are affected by the building structure under different wind approach conditions. CFD simulations were carried out to predict the wind patterns.

At the start of project work on Part 1, scoping CFD investigations were carried out to develop a simulation workflow, which was to be used in the final external CFD simulations to predict wind patterns around a selected building. The scoping CFD simulations used a car placed at a windy nearshore parking lot. This selection of wind obstacle (e.g. the car, a small SUV) and the site with steady wind conditions proved to be a cost-effective substitute for the controlled test conditions of a wind-tunnel. The results of the scoping CFD simulations were validated with measurements around the car. Final CFD simulations were validated with measurements of wind velocities around and pressure distribution on a selected building on the University of Hawaii Manoa (UHM) campus.

The data consistency between final CFD simulation results and measurements at the selected building was good, considering the external test conditions and type of instrumentation available to the research team. Each CFD simulation was carried out under steady state conditions, which means

with constant wind approach direction and velocity. Actual wind conditions, however, were non-steady in nature. Comparisons between CFD simulations and measurements were carried out by using statistical analysis of wind records, and using several steady state CFD simulations, each with different wind approach conditions. Using several CFD simulations with varying wind conditions, which were weighted in accordance with frequency distribution of recorded wind approach directions and speeds, was done to reflect the probabilistic nature of the real world wind conditions at the test site.

Some steady-state CFD simulations revealed important non-steady wind phenomena which develop around buildings. Pressure measurements indicated that certain wind conditions produced differential pressure fluctuations between external openings, which seriously affected cross ventilation in buildings. These detected pressure fluctuations were of such short periods that cross ventilation would basically be impeded by rapidly reversing pressures on opposite sides of the building. The likely consequences for cross ventilation could mean that air volumes were basically “stuck” in the building since a constant supply of outdoor air flow is necessary to ensure satisfactory air changes in the building.

The results of the investigations confirmed that building designers can obtain important insights in the wind patterns and pressure distributions around buildings through the use of advanced CFD simulations. This design information will enable designers to identify optimum orientation of building relative to the primary wind approach and size and place openings in the building envelope.

Part 2 – Internal CFD Investigations: Part 2 investigated air movement through interior spaces. The main objective of the investigations in Part 2 was to identify how internal air movement was affected by external wind conditions and internal pathways. External wind conditions are the driving forces for internal air movement. Internal pathways affect the amount of air flow rates through interior spaces. Given the same wind induced external driving forces, internal air flow pathways with the lowest pressure losses cause the highest air flow rates.

The project team developed a CFD simulation workflow for internal air movement. For these initial CFD investigations, a test site of another ERDL project was used. Measures of air flow properties at this test set-up were used to validate the CFD simulation workflow. The test site for these initial CFD workflow tests was a naturally ventilated space on the UHM campus. The test space included a large number of internal columns, cubicle partitions and furniture. The test space was temporarily equipped with two banks of (2) 30” diameter, 6000 cfm, propeller-blade exhaust fans. These two fan banks were used to augment natural air flow through the test space, including night flushing to improve thermal comfort for occupants. The two exhaust fan banks were installed at the leeward side of the test space. When the external openings on the leeward side were sealed, air flow through the space was carried out by the exhaust fans. This controlled and steady-state air flow condition was used to quantify mass flow rates, which could be compared to predicted mass flow rates in the initial CFD simulations.

The initial CFD simulation results were compared against the actual measured flow rates. The analysis of the CFD simulation results and the comparison with measurement indicated that general flow patterns on the space could be predicted. The data consistency of absolute air velocity values between CFD predictions and measurements was limited. The CFD simulation used a very large coupled computational mesh which included the interior space and some extent of exterior space. The large size of the mesh required significant computational resource and the research team had to implement several simplifications to the model to render CFD calculation manageable.

The final internal CFD simulations were conducted at the same building where the external CFD investigations were carried out in Part 1. This selection of naturally ventilated test space was advantageous since it allowed correlation of external wind patterns and internal air movements.

The test site consisted of three naturally ventilated classrooms which were interconnected by a central hallway. Five test scenarios were investigated. The test scenarios were defined by different internal air flow pathways, which included internal doorways and louvered wall sections. CFD simulation results of air flow under the test scenarios were verified by using the mass balance of inflow and outflow of the central hallway. The central hallway was used as a control volume in the data analysis. Air flow rates derived by CFD simulations were compared with air flow measurements and good data consistency was detected for the control volume, assuring high quality CFD solutions.

The work culminated in the development of a procedure to predict long term natural ventilation effectiveness based on CFD simulations and long term wind records. With this procedure, the building designer can determine the percentage of exceedance of natural ventilation rates for a particular space. For example, it can be determined if the probability of effective natural ventilation of spaces is sufficiently high enough to only rely on natural ventilation or if a mechanical assist ventilation system would be required.

Conclusions from Part 2 of the Research Project are summarized in the following section providing insight into the use of advanced building modelling. The procedures developed under Part 2 will provide the building designer with effective tools to optimize designs of naturally ventilated buildings.

Part 3 – Occupant Comfort in Naturally Ventilated Spaces: The work under Part 3 investigated occupant comfort in naturally ventilated spaces. The basic premise of the investigations was the performance of so-called “comfort islands”, a term used by the project team. These comfort islands are spaces inside non-conditioned spaces where equipment is installed to provide localized comfort improvements above the level that is experienced in the remainder of the non-conditioned space. The value proposition of comfort islands is that by avoiding conditioning the entire space and only providing comfort enhancement measure on a limited localized scale significant energy can be saved.

Two types of comfort enhancement technologies were investigated. The first technology was a high performance ceiling fan. The second was an array of radiant cooling surfaces that were placed close to the occupant and which were operated at surface temperature above the dew point, in order to avoid condensation. A windowless room was temporarily transformed to a comfort chamber that had two desks where test subjects could sit during comfort tests. One of the spaces, the test station, was equipped with the two comfort enhancement measures and the other, the control station, did not have any comfort enhancement. The control station provided baseline conditions, which were used to determine the effectiveness of comfort improvements by the two tested comfort enhancement measures. The test set-up was designed and built to accommodate the specific requirements of the two comfort enhancement measures.

Project work included development of a generic comfort simulation workflow and the application of this workflow to a set of 14 test scenarios. The 14 test scenarios were systematic combinations of the two comfort enhancement measures at different indoor environmental conditions. The simulations of the test scenarios quantified thermal performance of the comfort level and predicted occupant comfort. Selected simulations were compared to measurements. Data consistency between simulations and actual measurements fluctuated across simulations, but was generally satisfactory.

The experimental portion of the investigations under Part 3 included comfort tests with a large group of test participants. Test participants were recruited from students and staff members of the University of Hawaii Manoa campus. The tests participants spent time in the comfort chamber while they experienced baseline conditions and comfort enhancement measures. Comfort surveys recorded their thermal sensation and comfort experiences under five experimental test scenarios. The five experimental test scenarios were four settings of comfort enhancement measures plus one baseline scenario.

The results of the comfort tests indicated that acceptable indoor comfort could be achieved in the non-conditioned test spaces when comfort enhancement measures were used. The results of the investigation provided the basis for deciding what comfort enhancement measure provided the largest comfort improvement. A two tier ranking system was developed and applied to identify the most effective measure. The result of the ranking concluded that the use of ceiling fans was the single most effective comfort enhancement technology within the test environment. The use of actively cooled radiant surfaces, which were operated at higher than dew point temperatures, provided only limited improvements in localized comfort.

The investigations concluded that the concept of comfort islands is a viable and potentially important concept to improve comfort in non-conditioned or naturally ventilated spaces. Naturally ventilated spaces with comfort islands can be viable alternatives to fully conditioned spaces.

OVERALL CONCLUSIONS:

Part 1 – External CFD Investigations: The results of the investigations of Part 1 confirmed that building designers can obtain important insights in the wind patterns and pressure distributions around buildings through the use of advanced CFD simulations:

- A naturally ventilated building needs sufficient pressure differentials between external openings to provide the required driving forces for air movements through the buildings.
- Based on results of external CFD simulation the designer can conclude whether the placement and shape of the building can provide good natural ventilation effectiveness.
- Placement and shape of the building includes building orientation relative to primary wind approach direction, wind interactions with adjacent structures and placement and size of external openings.
- While investigations in the wind tunnel used to be the preferred method of identifying good wind design of building, CFD simulation are becoming more and more important. The project develops a good design framework for CFD simulations to predict wind patterns around the buildings.

Part 2 – Internal CFD Investigations: The results of the investigations of Part 2 showed that CFD simulations can successfully predict air movements in naturally ventilated buildings.

- The precise prediction of air flow through buildings is necessary to assess the amount of air changes per time period. Such an assessment determines whether or not the naturally ventilated spaces provides code conformant ventilation rates.
- The project work on Part 2 culminated in a proposed procedure to predict long-term natural ventilation performance of the building based on CFD simulations combined with long-term wind records.
- The outcome is a prediction of the probability that a certain air change in the building can be accomplished by natural ventilation alone, or if additional mechanical assist ventilation would be required.
- This application of CFD simulation can be an important design tool for energy saving buildings which rely primarily on natural ventilation.

Part 3 – Occupant Comfort in Naturally Ventilated Spaces: The results of the investigations of Part 3 confirmed that occupant comfort can be attained in naturally ventilated spaces at any time if comfort enhancement measures, or “comfort islands”, are added to the spaces.

- Typically, naturally ventilated spaces provide insufficient occupant comfort during times of insufficient wind and hot outdoor climate. The research work identified that ceiling fans and combinations of ceiling fans with actively cooled surfaces can provide the significant comfort enhancement in naturally ventilated spaces.

- The comfort enhancement through comfort islands can render natural ventilation as a viable alternative to mechanical space cooling and ventilation.
- The investigation also concluded that comfort simulations can successfully predict the level of comfort improvements.

Recommendations for future research and development of comfort islands: Follow-up research into the effectiveness of comfort islands may benefit from the following:

- Using a larger test space.
- Follow-up tests should use radiant barriers to shield test participants from high radiant temperatures of the surrounding walls and ceiling to improve the effectiveness of radiant surfaces installed around the test subject.
- A dedicated thermal comfort software product should be used in lieu of the generic CFD program that was used during all three parts of the Research Project.
- Validation of the comfort simulations could greatly benefit from the use of an instrumented manikins.

SECTION 1 - OVERVIEW OF RESEARCH PROJECT

The research project “Computational Fluid Dynamics (CFD) Applications at the Environmental Research and Design Laboratory (ERDL), University of Hawaii” studied the effectiveness of advanced simulations procedures. Advanced simulation can provide important design input of predicting certain performance aspects of naturally ventilated building. Advanced simulations can also identify the effectiveness of innovative space conditioning technologies, which can enhance occupant thermal comfort while at the same time saving energy for space cooling and ventilation. Results of advanced building simulations and actual measurements of important building performance parameters were conducted in parallel in order to allow validation of theoretical predictions through experimental data.

The research work was carried out by ERDL with funding by and active participation of the Hawaii Natural Energy Institute (HNEI).

The project was segmented in three main sections, each of which was subdivided into four work tasks for a total of 12 work tasks. For each of the work task a final report was prepared. Figure 1.1.1 illustrates the three parts of the Research Project. Part 1 investigated wind movement and resulting pressures around a building. Part 2 investigated wind induced air movements through a naturally ventilated building. Part 3 investigated occupant thermal comfort in non-conditioned spaces. All three parts used CFD simulations and validation through experimental tests.

Project statistics:

- The project work was conducted over a period of two years, from July 2013 through October 2015.
- The research team included three ERDL and HNEI researchers, three post-doctoral fellows (architecture) and 10 engineering and architectural graduate and undergraduate students.
- The results of the project work were documented in 20 projects reports, 15 FINAL and 5 DRAFT reports.
- The entire project documentation which was presented in the report was 3,500 pages; 2,600 pages of which were prepared in the 15 final reports.

Summaries of the project reports are presented in Table 1.1

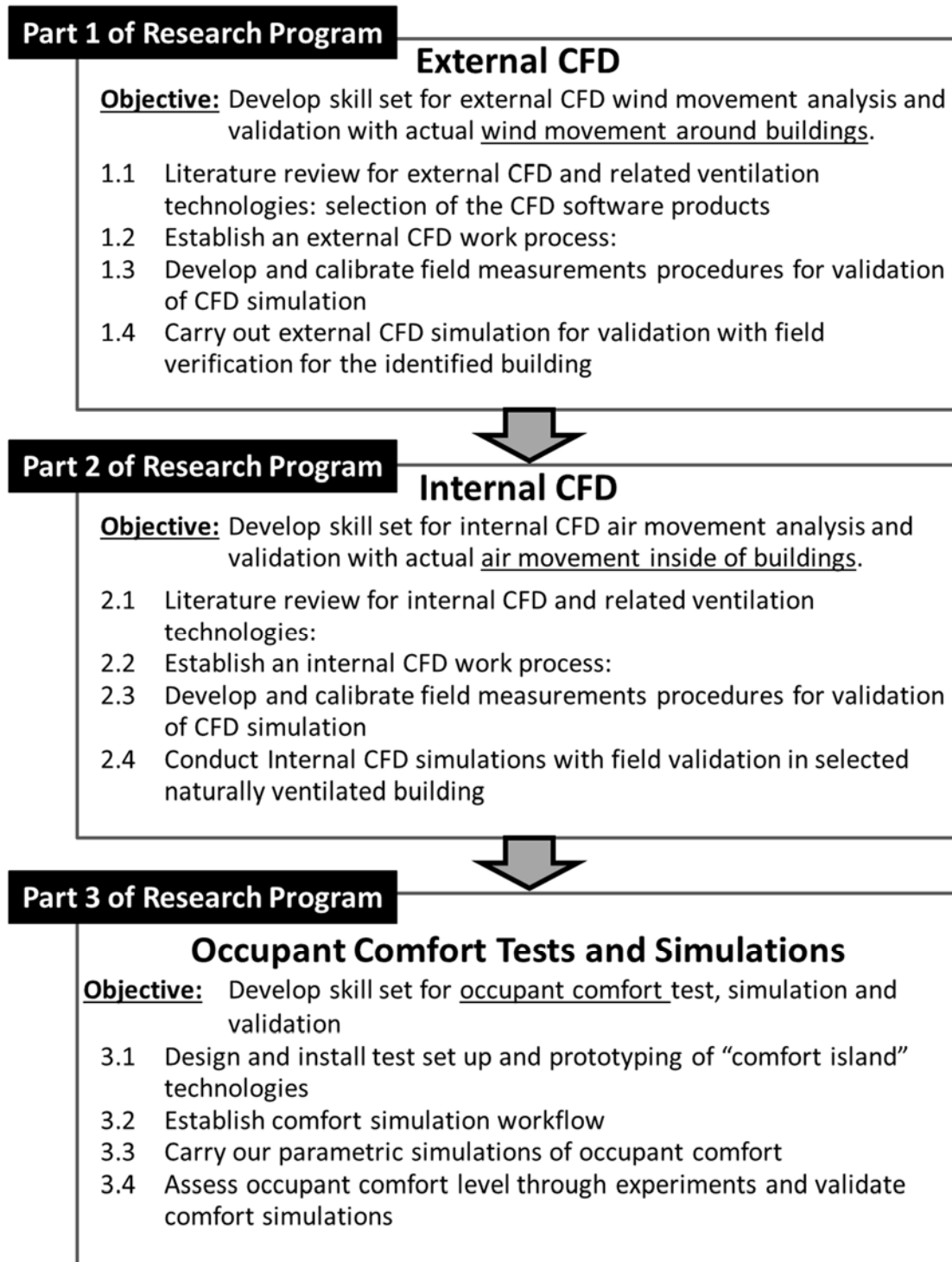


Figure 1.1.1: Process Flow Scheme of Three Phases of the Research Project

Table 1.1: Summaries of project reports published in the course of this research project

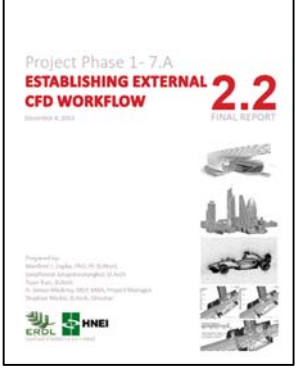
Project Deliverable No.	Title and Description of Project Report	Cover page
Phase 1 of the Research Project – External CFD Applications External CFD applications investigated		
1	<p>Literature Review of External CFD (170 pages): The report presents the result of a comprehensive literature review of simulating wind movement around buildings. The main research work presented in this report were as follows:</p> <ul style="list-style-type: none"> • Review of basic processes of wind movements around buildings, including but not limited to topics addressing atmospheric boundary layer, mechanism of wind induced pressures, effects of building geometry on wind regime, basics of urban wind comfort. • Review of assessment methods of air movement around buildings, including an assessment of the effectiveness of CFD compared with other prediction methods • Review of the state of the art and trends in external CFD applications, including but not limited to basics consideration of CFD calculation processes, verification and validation, tasks required for CFD pre-processing, solver and post processing. 	 <p>Cover page of the Project Deliverable 1</p>
2.1 DRAFT and 2.2 FINAL	<p>DRAFT and FINAL Report² Establishing External CFD Workflow (282 pages for FINAL report): The report presents a work flow for external CFD simulations. The workflow was used to model wind movements around buildings and the resulting wind velocities and wind induced pressure distribution on the building envelope. The main project work topics presented in this report are:</p> <ul style="list-style-type: none"> • Review fundamentals of CFD calculations and modeling as it applies to buildings in Hawaii. • Review different approaches to build and adjust CFD meshing, evaluate different mesh geometries and determine the best suitable model geometries (including façade appurtenances) for air flow and wind induced pressure phenomena around buildings. 	 <p>Cover page of the Project Deliverable 2.2 (Final report)</p>

Table 1.1: Summaries of project reports published in the course of this research project

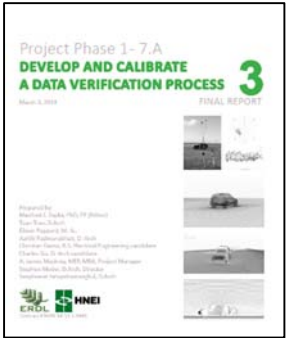
Project Deliverable No.	Title and Description of Project Report	Cover page
	<ul style="list-style-type: none"> Evaluate required capabilities of the candidate CFD software products as they apply to CFD applications in Hawaii climate. Evaluate various ways to post-process (visualize) CFD data, both basic as well as more advanced CFD visualization functions. Select a CFD software product based on a project specific ranking procedure. 	
3	<p>Develop and Calibrate a Data Verification Process (for External CFD Simulations) (186 pages): The report presents project work that was conducted to establish a data acquisition and analysis methodology for wind movement and wind induced pressure distribution around structures. The main project work topics presented in this report are:</p> <ul style="list-style-type: none"> One site for the shakedown tests was selected from several candidate sites. The selected site needed the logistics and steady wind conditions to serve as a quasi “wind tunnel” for wind movement and pressure distribution measurements around a simple test structure. Initial CFD simulations were performed using most probable wind direction and speeds at the test site. The initial simulations provided locations where instrumentation was placed during tests to validate CFD results. A comprehensive search for candidate instrumentation and final selection of instruments to measure wind, direction, wind speed and differential pressure. Preparing and calibrating the selected instruments in the laboratory and develop and test the data acquisition procedures before the instruments were to be deployed in the field for shakedown tests. Shakedown tests of instruments were conducted at the selected site on three days. A comprehensive data analysis process was tested in the process of the shakedown testing. 	 <p>Cover page of the Project Deliverable 3</p>

Table 1.1: Summaries of project reports published in the course of this research project

Project Deliverable No.	Title and Description of Project Report	Cover page
	<ul style="list-style-type: none"> The results of final CFD simulations and actual field measurements of wind velocity and differential pressures around the test structure were compared. The comparison of CFD simulation and experimental results confirmed that the external CFD workflow was suitable for the final tests. 	
<p>4.1 DRAFT and 4.2 FINAL</p>	<p>External CFD Simulation & Field Validation for Selected Building (282 pages for FINAL report): The report presents project work that was conducted to carry out a comprehensive series of CFD simulation runs to predict wind movement and resulting pressures around a selected building. Actual measurement of wind velocity and differential pressures at the selected building were used to validate the theoretical predictions. Validated CFD procedures successfully predicted most probable wind movement and pressure differentials for historical wind data at the tests site. The main research work tasks presented in this report were as follows:</p> <ul style="list-style-type: none"> Select a naturally ventilated building for which wind induced wind patterns and pressure differentials were studied through CFD analysis and measurements in the field. (The same naturally ventilated building was to be studied in Phase 2, internal CFD, in regard to air movement due to external wind). Carrying out CFD simulations using the geometry of the selected building and wind approach direction and velocity as boundary conditions. For the final CFD simulations work flow procedures developed during the initial CFD simulations were fine-tuned and applied for a series of incident wind conditions. Measure actual wind induced velocities around the selected building and pressure differentials between opposite building sides. Validate the CFD simulations with the field measurements. Carry out a final set of CFD simulations to determine the wind movement and resulting pressure distribution on the building envelope for the most probable incident wind direction and speed, based on longer term wind data at the site. 	 <p>Cover page of the Project Deliverable 4.2 (Final report)</p>

Table 1.1: Summaries of project reports published in the course of this research project

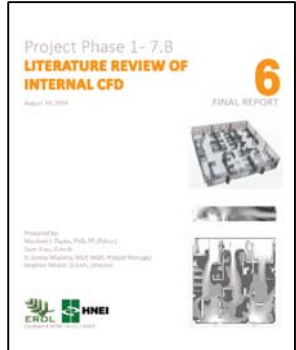
Project Deliverable No.	Title and Description of Project Report	Cover page
5	<p>Summary and Conclusion of Project Phase 1 – External CFD (122 pages):</p> <p>The summary report describes the applied research work that was carried out for Phase 1 of the research project – External CFD Applications. The project work included modeling of air movement around buildings with CFD and validating the theoretical CFD results through full-scale measurements in the field.</p>	 <p>Cover page of the Project Deliverable 5</p>
<p>Phase 2 of the Research Project – Internal CFD Applications</p> <p>Internal CFD applications investigated air movement in building which were produced by wind movement around the building and by mechanical exhaust fans. Actual measurements were used for validation of theoretical predictions</p>		
6	<p>Literature Review of Internal CFD (140 pages)</p> <p>The report presents the result of a comprehensive literature review of simulating air movement inside buildings, where the air movements are driven by external wind around buildings. The main research work tasks presented in this report were as follows:</p> <ul style="list-style-type: none"> • Conduct a comprehensive review of scientific and technical literature concerning airflow inside of buildings with the help of Computational Fluid Dynamics (CFD) investigations. Emphasis air movement inside naturally ventilated buildings. • Identify and evaluate CFD simulation settings used in previous investigations. • Determine main airflow phenomena and thermal conditions in buildings as they relate to naturally ventilated buildings and determine appropriate ways to simulate these. 	 <p>Cover page of the Project Deliverable 6</p>

Table 1.1: Summaries of project reports published in the course of this research project

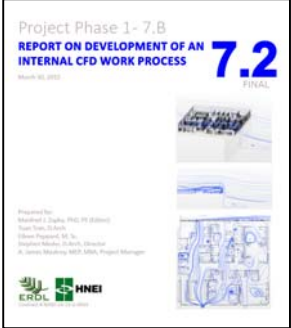
Project Deliverable No.	Title and Description of Project Report	Cover page
	<ul style="list-style-type: none"> Evaluate how building designers have been using advanced numerical simulations for quantitative assessment of building performance. Assess the potential of using CFD simulations as alternatives to wind tunnel investigations. 	
<p>7.1 DRAFT and 7.2 FINAL</p>	<p>Development of an Internal CFD Work Flow Process (193 pages for FINAL report): The report presents project work that developed a generic work flow for internal CFD applications. The workflow was used to model air movements through naturally ventilated spaces. Predicting air movement through spaces allowed assessment of air exchange rates and the effectiveness of natural ventilation of spaces under specific external wind conditions and internal air pathways. The main work topics presented in this report are:</p> <ul style="list-style-type: none"> Different CFD simulation settings for modeling internal air movement were tested to determine sensitivity of parameters and convergence performance of the simulations. A large room on the University of Hawaii Manoa campus was used to carry out full scale validation test of internal CFD simulations. The room was equipped with a temporary exhaust fan system which was used to establish controlled forced ventilation conditions that were used for validation of test results. This test set up was used to assess the contribution of mechanical assist ventilation in naturally ventilated spaces. Different combinations of inlet and outlet conditions were used. This included different variations of inlet windows open and different combinations of exhaust fans to establish air flow pathways through the room. Measurement of airflow velocity of the different forced ventilation scenarios provided data for validation for CFD simulations. 	 <p>Cover page of the Project Deliverable 7.2 (Final report)</p>

Table 1.1: Summaries of project reports published in the course of this research project

Project Deliverable No.	Title and Description of Project Report	Cover page
	<ul style="list-style-type: none"> Develop the final CFD workflow based on comparison between theoretical air flow predictions and actual measurements. Determine the effectiveness of different post processing procedures of CFD simulations to obtain qualitative and quantitative determination of the CFD solutions. 	
8	<p>Report on Development of Data Acquisition Procedures for Internal CFD Simulation Validation (69 pages)</p> <p>The report presents project work that was concerned with the development and testing of data acquisition procedures for measurements of internal air movement conditions. The main work topics presented in this report are:</p> <ul style="list-style-type: none"> A suitable test space for the measurements and validation of the internal CFD workflow was selected. The test space was the naturally ventilated room where another ERDL project investigated occupant comfort. Use the test space and the temporarily installed mechanical assist ventilation to provide controlled mass flow rate which could be used for CFD simulation validation. Install an array of instrumentation and data acquisition in the test space with which pertinent environmental parameters as well as air movement velocities could be measured. Conduct air movement measurements with different air flow pathways established with a combination of windows open and closed and with different fan operating speeds. Compare the measured air flow data with the theoretical CFD predictions to carry out data validation. 	 <p>Cover page of the Project Deliverable 8</p>

Table 1.1: Summaries of project reports published in the course of this research project

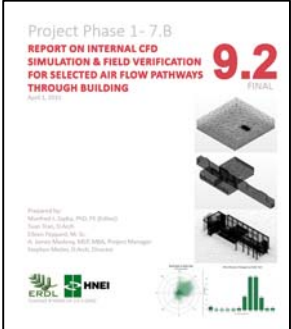
Project Deliverable No.	Title and Description of Project Report	Cover page
<p>9.1 DRAFT and 9.2 FINAL</p>	<p>Report on Internal CFD Simulation & Field Verification for Selected Air Flow Pathways through Building (166 pages for FINAL report): The report presents project work that carried out a comprehensive series of CFD simulation runs to predict air movement through a cross ventilated building. The selected building was a naturally ventilated building on the University of Hawaii Manoa campus. Actual measurement of air movements through the spaces of the selected building were used to validate the theoretical predictions. Validated CFD procedures created most probable air exchanges for naturally ventilated spaces based on historical wind data at the test site. The main work topics presented in this report are:</p> <ul style="list-style-type: none"> • Utilize appropriate spaces in a naturally ventilated building on the University of Hawaii Manoa campus, as a test site to carry out CFD simulation at the full scale prototype. • Equip the test site with temporary closures of internal air flow pathways in order to create fully controlled test environment of the naturally ventilated building spaces. • Perform a comprehensive series of CFD simulations of internal air movement through different air flow pathways using measured external wind conditions. • Validate theoretical CFD predictions with measured air flow conditions in the naturally ventilated spaces. Create the same boundary conditions in the experimental investigations that were used in the CFD simulations. • Develop and test a building design methodology where effectiveness of air changes in naturally ventilated spaces can be predicted based probability of external wind movement conditions. 	 <p>Cover page of the Project Deliverable 9.2 (Final report)</p>

Table 1.1: Summaries of project reports published in the course of this research project

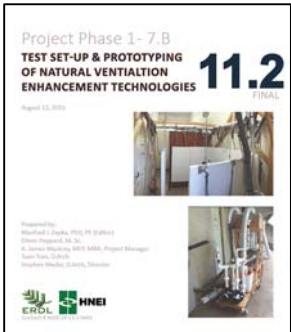
Project Deliverable No.	Title and Description of Project Report	Cover page
<p>10</p>	<p>Summary and Conclusion of Project Phase 2 – Internal CFD (109 pages): The summary report describes the applied research work that was carried out for Phase 2 of the research project – Internal CFD Applications. The project work included modeling of air movement through cross ventilated building spaces with Computational Fluid Dynamics (CFD) and validating the theoretical CFD results through full-scale experimental measurements in these spaces.</p>	 <p>Cover page of the Project Deliverable 10</p>
<p>Phase 3 of the Research Project – Occupant Comfort Tests and Simulations Occupant comfort investigation were carried out in a temporary comfort test chamber. A series of comfort enhancement technologies were tested in the comfort test chamber at internal temperatures and humidity levels which emulated conditions in naturally ventilated spaces at the University of Hawaii with reported occupant discomfort. Thermal comfort simulations were carried out and validated against a series of comfort tests with human test subjects.</p>		
<p>11.1 Draft and 11.2 Final</p>	<p>Test Set-up and Prototyping of Natural Ventilation Enhancement Technologies (180 pages for FINAL report): The report presents project work of designing, building and Starting up a test set-up for occupant comfort studies. A room at on the University of Hawaii Manoa campus was temporarily transformed into thermal comfort chamber. The test set-up allowed testing of thermal comfort with human test subjects. The main work topics presented in this report are:</p> <ul style="list-style-type: none"> • Design a test set-up that was flexible to allow for a range of test scenarios for thermal comfort enhancement technologies, also referred to as “comfort islands”. The test set-up had to fit into a relatively small room that was temporarily converted into a comfort chamber. • Design and build a prototype installation of an innovative cooling technology for use with comfort islands. This prototype was an array of actively cooled radiant panels which were situated around a test subject in an otherwise 	 <p>Cover page of the Project Deliverable 11.2 (Final report)</p>

Table 1.1: Summaries of project reports published in the course of this research project

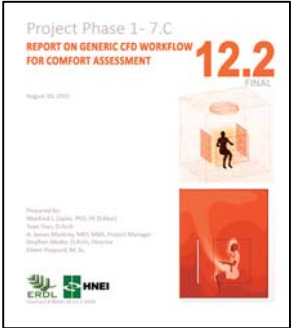
Project Deliverable No.	Title and Description of Project Report	Cover page
	<p>un-conditioned space. The space was held at high internal temperature and humidity levels.</p> <ul style="list-style-type: none"> • Install, calibrate and operate a large instrumentation array to measure the indoor environmental conditions at which the test set-up would be operating during the comfort tests. The environmental conditions had also to serve as boundary conditions for the series of comfort simulations. • Develop a test plan for human comfort studies that could be carried out at the test set-up. 	
<p>12</p>	<p>Report on Generic CFD Workflow for Comfort Assessment (92 pages): The report presents project work to develop a generic work flow for occupant thermal comfort. The workflow was used to model occupant comfort levels. The main work topics presented in this report are:</p> <ul style="list-style-type: none"> • Review procedures of modelling thermal comfort for building occupants in the literature and use applicable procedure in these comfort simulations. • Determine appropriate metrics that were used to quantify thermal comfort. • Develop a procedure to compare comfort simulations results with results obtained from thermal comfort experimental tests. • Develop CFD procedures to calculate sensitive convective and radiative heat transfer rates in the test set up. A precise quantification of convective and radiative heat transfer rates is typically not obtainable under standardized assessment occupant of comfort levels. • Develop CFD workflow procedures so that they can be readily applied in for final comfort tests. 	 <p>Cover page of the Project Deliverable 12</p>

Table 1.1: Summaries of project reports published in the course of this research project

Project Deliverable No.	Title and Description of Project Report	Cover page
<p>13</p>	<p>Parametric CFD Investigations of Comfort and Environmental Conditions at the ERDL Test Site (240 pages)</p> <p>The report presents a series of parametric comfort simulations that were carried out for a range of tests conditions at the ERDL test site. For logistic reasons the comfort simulations had to be completed before the experimental comfort test were carried out. Therefore, the indoor environmental conditions that could be maintained at steady state during the comfort experiments were not known and could not be used as boundary conditions. The purpose of the parametric comfort investigations was to provide comfort predictions at anticipated indoor environmental conditions of the test set-up. The main work topics presented in this report are:</p> <ul style="list-style-type: none"> • Apply the CFD comfort simulation workflow which was developed in Project Deliverable 12 and apply the simulation work flow to a range of thermal and air flow boundary conditions, which represented test conditions used in the experimental comfort tests. • Carry out CFD simulations to predict the physical (e.g. without human interactions) response of the ERDL test set-up to varying induced air flow and conjugate heat transfer conditions. • Create a series of CFD simulations using the geometry and fluid flow and heat transfer characteristics of the ERDL site using an estimated range of main test parameters that will be used in upcoming experimental test of the ERDL test site. • Carry out CFD simulations that will be used for two different purposes. One, obtain a more detailed description of the fluid flow field and heat transfer characteristics at the ERDL test site. Two, obtain a prediction of occupant comfort, based on averaged fluid flow and heat transfer phenomena as environmental condition input variables. 	 <p>Cover page of the Project Deliverable 13</p>

Table 1.1: Summaries of project reports published in the course of this research project

Project Deliverable No.	Title and Description of Project Report	Cover page
14	<p>Simulations and Testing of the Effectiveness of Ceiling Fans and Actively Cooled Radiant Panels as Comfort Enhancement Technologies at the ERDL Test Site <i>(370 pages)</i></p> <p>The report presents the results of the experimental comfort tests at the ERDL test site. The results of tests were used to determine the effectiveness of comfort enhancement technologies. The experimental tests were used to validate simulations of heat transfer and occupant comfort using the same indoor environmental conditions. The main work topics presented in this report are:</p> <ul style="list-style-type: none"> • Prepare the test equipment and instrumentation of a temporary internal comfort test set-up to carry out experiments on physical indoor environmental parameters and comfort test with human test subjects. • Conduct comfort tests with human test subjects using a range of test scenarios to determine the effectiveness of two comfort enhancement technologies at the ERDL test facility. • Obtain results of comfort tests as well as record a significant number of pertinent physical parameters in order to obtain an objective assessment of comfort supporting indoor environmental conditions. • Carry out a comprehensive data analysis, discuss results and come to conclusions on the validation process of the theoretical simulations results against results obtains in experimental investigations. • Perform validation of theoretical CFD predictions with actually measured phenomena in the controlled test environment of a specifically equipped test facility. • Develop a ranking procedure with which the effectiveness of the comfort enhancing measures could be assessed. Use the ranking procedure to select the most suitable comfort enhancement technology. 	 <p>Cover page of the Project Deliverable 14</p>

Table 1.1: Summaries of project reports published in the course of this research project

Project Deliverable No.	Title and Description of Project Report	Cover page
15	<p>Summary of the Research Project and Presentation of Results of Phase 3 (100 pages)</p> <p>The summary report describes the applied research work that was carried out during the three parts of the Research Project. Summarize the main results of Parts 1 and 2, and elaborate on part 3 of the Research Project – “Occupant Comfort Tests and simulations”. The project work of part 3 included designing and installing a comfort chamber in which the effectiveness of comfort enhancement technologies was investigated by means of experiments with human test subjects. Heat transfer and fan induced air movements as well as the comfort levels were simulated and were validated against the experimental results. The main work topics presented in this report are:</p> <ul style="list-style-type: none"> • Prepare the test equipment and instrumentation of a specifically furnished internal comfort test set-up to carry out experiments on physical indoor environmental parameters and comfort test with human test subjects. • Conduct comfort tests with human test subjects using a range of test scenarios to determine the effectiveness of two comfort enhancement technologies at the ERDL test facility. • Obtain results of comfort tests as well as results of pertinent physical parameter tests in order to obtain an objective assessment of comfort supporting indoor environmental conditions. • Carry out a comprehensive data analysis, discuss results and come to conclusions about the validation process of theoretical simulations results through results obtained in experimental investigations. • Perform validation of theoretical CFD predictions with actually measured phenomena in the controlled test environment of a specifically equipped test facility. • Develop a ranking procedure by which the level of effectiveness of the comfort enhancing measures was assessed and used to select the best comfort enhancement technology. 	 <p>Cover page of the Project Deliverable 15</p>

SECTION 2 - SUMMARY BRIEF OF PREVIOUSLY COMPLETED PART 1

This section presents the main results and conclusions of the work that was conducted under the Research Project Part 1 – External CFD Applications.

The main objective of the research work of Part 1 was developing and validating Computational Fluid Dynamics (CFD) simulation methodologies for wind movements around buildings in order to predict wind induced ventilation performance of buildings.

Wind forces and the resulting pressure distribution around the building envelope are the driving forces of air movement through naturally ventilated buildings. Therefore, the first necessary step in determining the anticipated ventilation effectiveness of naturally ventilated buildings is a good understanding of wind movement and wind induced pressures. The preferred conventional approach to determine these important design information has been through wind tunneling testing. Using numerical simulation with advanced CFD models is evolving as a powerful and alternative design tool.

The work in Part 1 of the Research Project evaluated CFD software products and tested their performance by comparing simulated and actually measured wind induced phenomena around a building on the University of Hawaii Manoa campus.

Part 1 of the Research Project consisted of four project tasks, 1.1 through 1.4, illustrated in Figure 2.1.

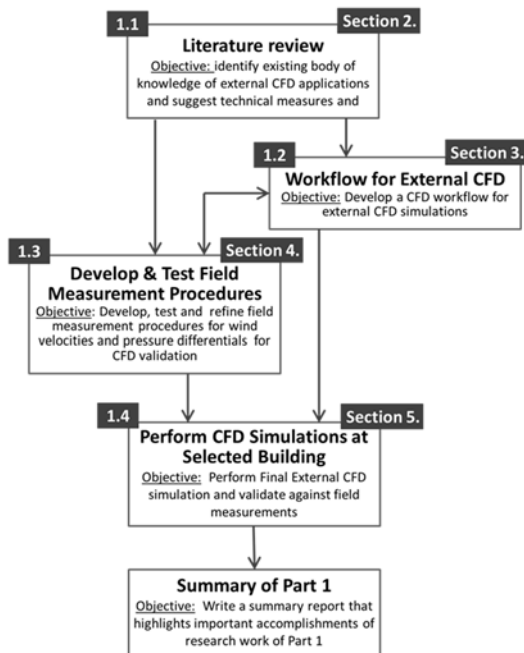


Figure 1: Process flow diagram of the project tasks during Phase 1 of the Research project

The work process in Figure 2.1 illustrates how project tasks 1.1 and 1.2 were carried out interactively. The workflow for external CFD was developed and continuously refined in project task 1.2, with validation from data obtained under project task 1.1.

2.1 Brief Summary of Fundamentals of Wind Movement Around Buildings

Flow patterns around buildings: The external wind movement generates site-specific pressure and wind velocity patterns around the building envelope. The pressure and velocity distribution is dependent on the wind speed, wind approach direction and the shape of the building. Flow patterns around simple geometries can be predicted using standardized design guidelines. For more complicated building patterns and especially with upwind and downwind flow obstruction present, prediction of wind velocity and pressure distribution around buildings requires analytical methods and/or wind tunnel test.

Figure 2.1.1 illustrates a typical pattern of wind movements around a simple rectangular building. Figure 2.1.2 shows downwash conditions caused by wind approach to the building.

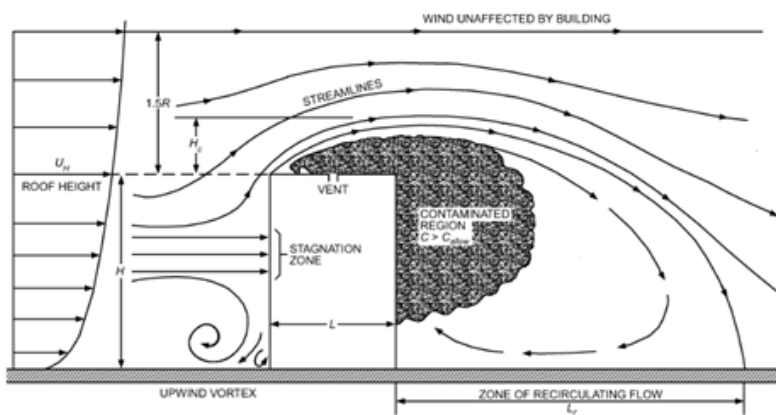


Figure 2.1.1: Typical pattern of wind movements around a rectangular building - vertical section

As wind impinges on a building, airflow separates at the building edges, generating recirculation zones over downwind surfaces (roof, side and downwind walls) and extending into the downwind wake.

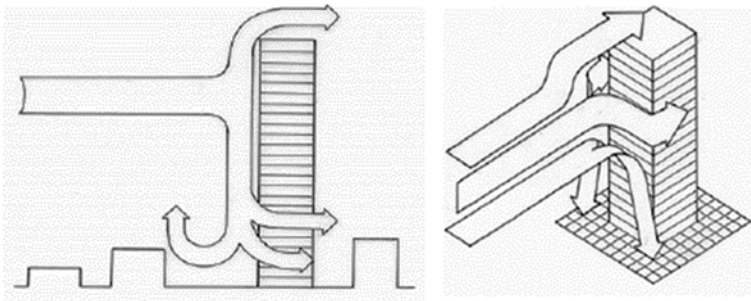


Figure 2.1.2: Flow patterns around buildings, typical downwash conditions

When a stream of wind strikes the surface of a tall building, a significant portion of the incident wind moves downward thus reaching the street / pedestrian level. This can create significant negative impact.

Wind patterns around buildings affect ventilation inside building, since wind forces are driving forces for internal air movement. Strong wind movement around buildings can even have negative effects on the safety of occupants.

There are two main environmental processes which cause naturally induced air movement through buildings. The first process is referred to as “Stack Effect” ventilation, where buoyancy forces lift warmer, and therefore lighter air to higher openings from where they leave the building. The displaced air draws in outside at lower building openings. The strength of the driving force behind stack effect ventilation are two main parameters, (1) the temperature difference of the warmer inside and colder outside air and (2) the vertical difference of openings between which the stack effect operates. Stack effect ventilation had a negligible effect on the buildings investigated in this research project.

The second ventilation process is wind driven ventilation, where a pressure differential drives the air flow through the building. The pressure distribution on the building envelope is dependent on the external wind movement, where upwind wind stagnation creates regions of higher pressure and downwind separation of the streamlines cause lower pressure regions. The distribution of higher and lower pressures on the building envelope needs to be studied to derive building designs that have effective pressure distributions. With complicated building geometry the wind movement and resulting pressure distribution around the building should be investigated with the help of CFD.

The project work was concerned in determining wind induced ventilation due to pressure differentials on the building envelope.

2.2 CFD Process Workflow

The project team established a specific process flow for CFD simulations. Figure 2.2.1 illustrates the different steps of this work flow.

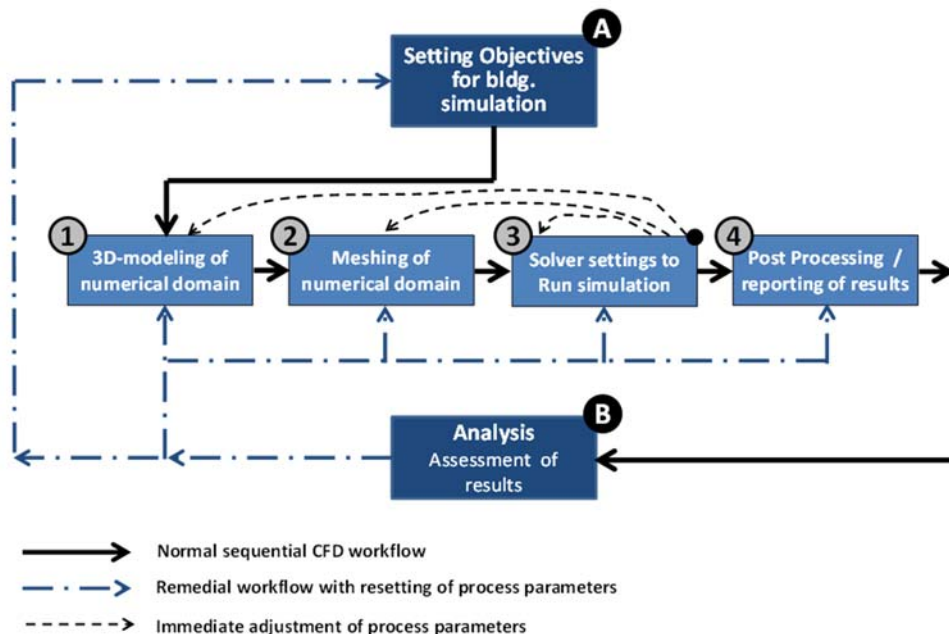


Figure 2.2.1: Generic workflow for external CFD, showing process steps involved

The process steps illustrated in Figure 2.2.1 are briefly described in the following table:

Process Steps ID	Description
A	Setting objectives for the CFD investigation; for example, the main objective might be determining the wind speed around buildings, the dispersion of exhaust from a building stack or the pressure distribution on the building envelope.
B	Upon completion of a CFD simulation results have to be examined regarding their consistency with the objectives , and design conclusions have to be drawn. The assessment of results determines whether results appear valid or if actual validation with measurements have been obtained.
1	3D-Modelling: Creating a suitable geometry of the computational domain. The computational domain represents the volume or mass of fluid. Only the fluid but not solid objects is subjected to the selected physics conditions, including suitable boundary conditions.
2	Meshing: Generating a suitable grid, or mesh, which represents the digitization of the numerical solution. The meshing occurs in two phases. (1) preparation of an “impermeable” surface mesh with a continuous mesh that surrounds all solid objects and therefore creates the boundaries of the fluid, (2) creation of the volume mesh which encompasses the extent of the fluid that is analyzed in the computational domain. The volume of the fluid is discretized into a large number of cells for which the governing equations are solved.
3	Solver & Simulation: Select appropriate solver setting to initiate and run the CFD simulations to ensure precise results and stable convergence. Important parameters include definition of boundary conditions and selection of turbulence model. If the solution does not show robust convergence, changes of the geometry, the mesh or the solver settings must be performed.
4	Post Processing: Using effective post processing options allows for ready interpretations and analysis of the converged solution. The value proposition of CFD is the ability to describe a fluid flow field and related physical effects at any point in the computational domain. Typically, CFD post-processing involves visual depictions of parameters, such as colored contour maps. Other post-processing options provide virtual "probes" which identify parameter values at desired locations.

2.3 Using Windy, Ocean Shore Location as a Temporary Wind Tunnel

The ERDL research team excelled in thinking out of the box and finding cost effective solution to logistical problems in conducting the investigations. This creativity uncovered cost effective options for carrying out project objectives of the project.

One example of this creative thinking was planning and execution of the initial field tests. In preparation of the field tests of wind pattern around a naturally ventilated building the team had to acquire expertise using the new wind measurement instrumentation and equipment to process field data. Using the controlled test environment of a wind tunnel, with its constant air movement, was the most effective method to acquire such expertise. Such a facility was not available to the ERDL research team and therefore the team opted to carry out the initial scoping tests at a location with constant wind conditions. The team selected an ocean side location with few obstructions to the prevailing trade winds.

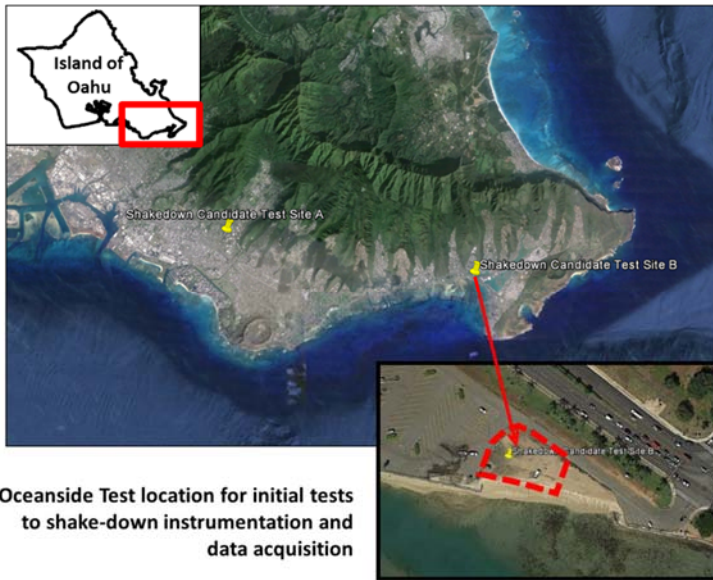
Since the measurements of a sufficiently strong wind pattern around a structure required a solid obstacle a small SUV was used as the test specimen. The use of the small SUV to house data acquisition equipment also had added logistical advantages.

An ocean side test location with exposure to strong and constant trade winds was used as a “substitute” wind tunnel. A small SUV served as a moveable structure to measure surrounding wind patterns that were generated by the strong and constant wind conditions.

The tests were conducted by temporarily fencing off an approximately 200 by 200 feet ocean side location and placing the small SUV with a surrounding instrument array. Three days with strong trade winds were used for the initial tests. Scoping CFD simulations with typical wind direction and speeds at the tests site identified suitable locations to place an eight anemometer array around the small SUV. At the days of the tests a weather station was installed at the site to measure actual wind conditions. The actual wind conditions were used for final CFD simulations against which the measured wind pattern parameters were validated.

Figures 2.3.1 shows the ocean side location and the small SUV that was used as wind obstruction. Figure 2.3.2 shows the SUV and instrumentations deployed around the SUV. Figure 2.3.3 shows the “real world” SUV and the 3D-model that was created for the CFD simulations using the actual wind conditions at the test location. Figure 2.3.4 shows the contour maps that were created with assumed wind conditions. These wind velocity contours were used to select suitable placement of instruments in the field, and around the SUV.

SECTION 2 - SUMMARY BRIEF OF PREVIOUSLY COMPLETED PART 1



Oceanside Test location for initial tests to shake-down instrumentation and data acquisition

Figure 2.3.1: Location of initial “shakedown” tests

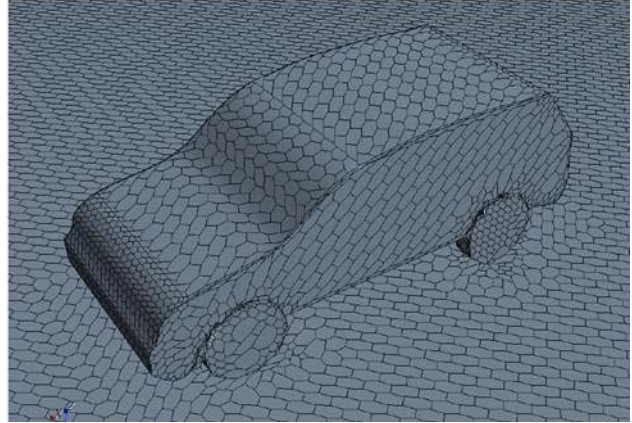
The initial shakedown tests were conducted to give the ERDL research team a good working knowledge of the instrumentation to measure wind patterns



Figure 2.3.2: Initial experimental tests to acquire working knowledge of instrumentation and data acquisition

- (a) The SUV at the test site close to the ocean
- (b) Placing instrumentation around the SUV
- (c) Weather station to measure wind conditions during the tests

Initial CFD simulations proved to be essential in preparing the shake-down testing and selecting instrument locations around the test structure (e.g. the small SUV).



“Test structure” used for the shakedown testing. A RAV (small SUV) served as an effective mobile structure around which to carry out the wind experiments

The “Test structure” shown as the CAD model for the CFD analysis

Figure 2.3.3: The test structure (= RAV-SUV) used for the initial “shakedown” testing

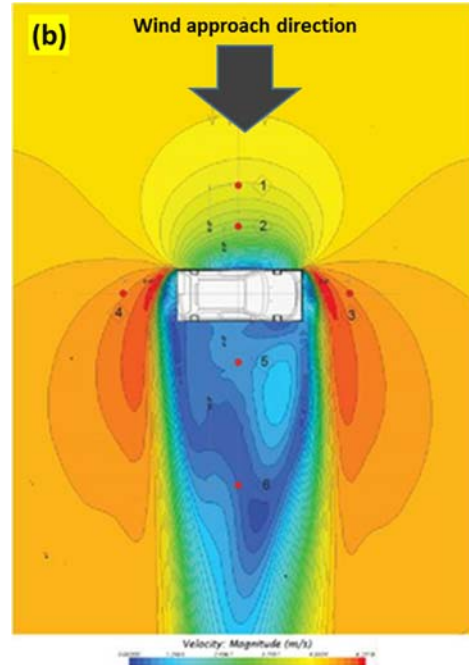
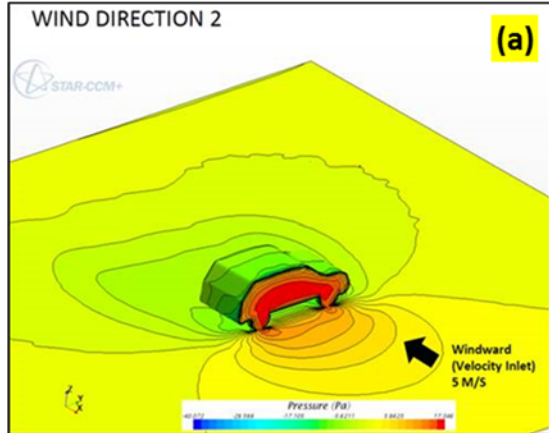


Figure 2.3.4: CFD analysis results of initial “shakedown” tests
 (a) Contours of equal pressure on the SUV surface and the ground
 (b) Contours of equal wind velocities around the SUV

Final CFD simulations of wind patterns surrounding the small SUV were conducted with measured wind conditions at the site. The CFD results were validated against the measured wind velocity and pressure data.

The final CFD simulation of the wind pattern around the test car (small SUV) used a higher mesh resolution for areas of interest than was used for initial scoping CFD simulations. Results of final CFD wind movement pattern showed very good data consistency with actual measurements of wind speed around the test car (small SUV). The CFD predictions for differential pressures around the test car did show smaller data consistency with actual pressure measurements.

Figure 2.3.5 shows two important aspects of the computational domain. Image (a) in Figure 2.3.5 shows the extent of the computational domain. The relatively large dimension of the domain in respect to the area of interests with the geometry of the small SUV in its center, was chosen to decrease the influence of the domain boundaries on the solution. Image (b) in Figure 2.3.5 shows the surface mesh of the small SUV used in the final CFD simulations. In comparison to the simple surface mesh used in the initial shakedown testing (e.g. see Figure 2.3.3) the surface mesh used for the final CFD simulation was significantly larger. Larger meshes inevitably feature a higher resolution and typically the CFD solution is more precise. Image (b) indicates that different mesh resolutions were used for different domain areas. Typically, in areas that have high flow gradient a higher mesh resolution was used.

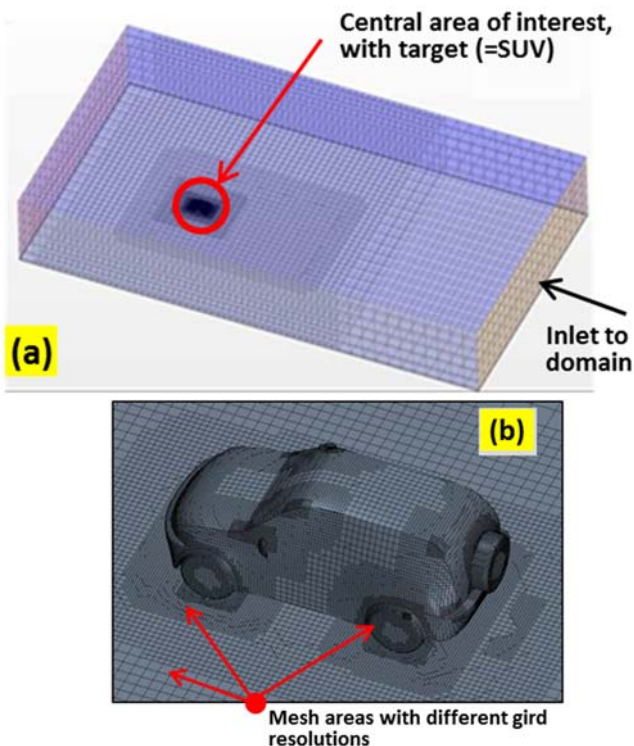


Figure 2.3.5: Aspects of the computational domain.

- (a) Extent of the computational domain; the target, e.g. the geometry of the small SUV, is located in the central portion of the domain.
- (b) Different grid (or mesh) resolutions were used for different areas of the computational domain. Typically, areas with high flow or pressure gradients, such as areas of flow separation or other flow discontinuities, require finer meshing.

Figure 2.3.6 shows an example of post-processing visualization using contour maps. The images (a) and (b) in Figure 2.3.6 indicate the spatial distribution of the wind velocity around the small SUV. While the contour maps provide a good indication about spatial distribution of wind velocities, extracting precise values for specific locations could only be accomplished by so-called virtual probes.

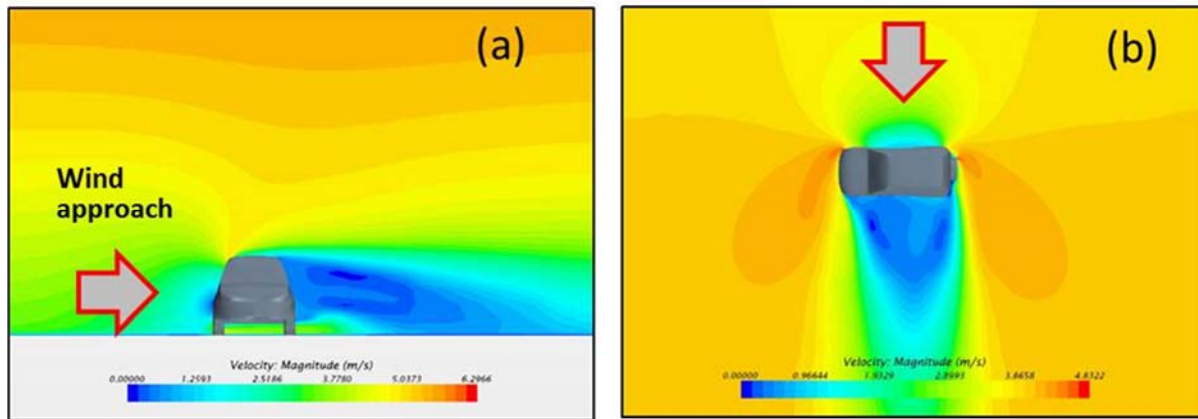


Figure 2.3.6: Air speed distribution around the test car due to wind from the side, (a) side view and (b) view from the top.

2.4 Investigations of Wind Patterns Around a Building – Simulations

The final investigations of wind movement around the selected building were carried out with the validated CFD workflow process. The naturally ventilated *Keller Hall* building was used as the test site for final external CFD simulations. The Keller Hall building is located at a central location on the University of Hawaii Manoa (UHM) Manoa campus. Figure 2.4.1 shows the location of Keller Hall on the Manoa campus.

The primary wind direction to the campus are from the North-East. Trade winds pass over the Ko’olau Range and approach the campus from North through the Manoa valley, where the campus is located. A weather station was erected on the roof of Keller Hall for long-term data recording. The weather station collected data over a six-month period, which coincided with the experimental investigations of Parts 1 and 2 of the Research Project.

As was done for the initial shakedown tests with the small SUV, initial scoping CFD simulations were carried out for the Keller Hall investigations with approximate wind conditions and with a coarse computational grid. The results of these wind pattern simulations indicated preferred locations where anemometers were placed during the field measurements. The CFD simulations produced representative wind velocity at physical locations that corresponded with virtual locations within the computation grid. Figure 2.4.2. shows the locations where anemometers were placed during the wind measurements around Keller Hall.

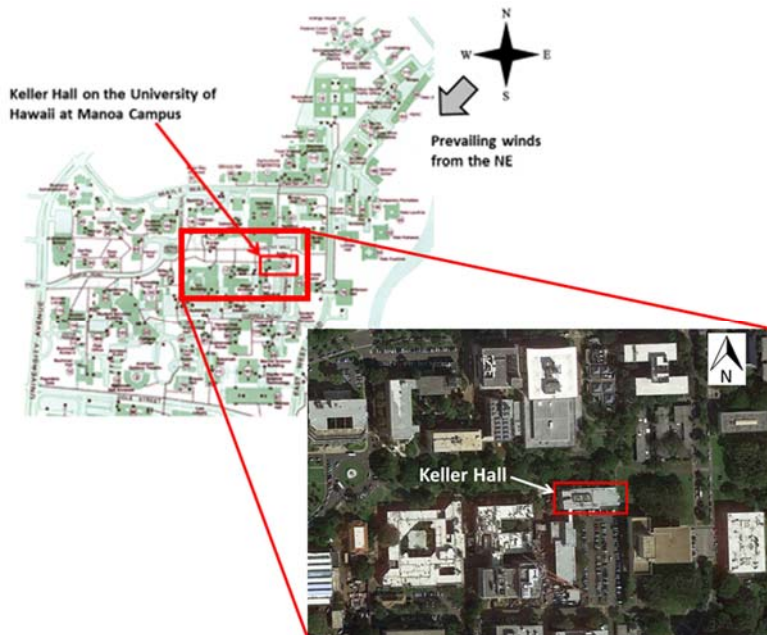


Figure 2.4.1: Location of Keller Hall, a naturally ventilated building, on the University of Hawaii Manoa campus.

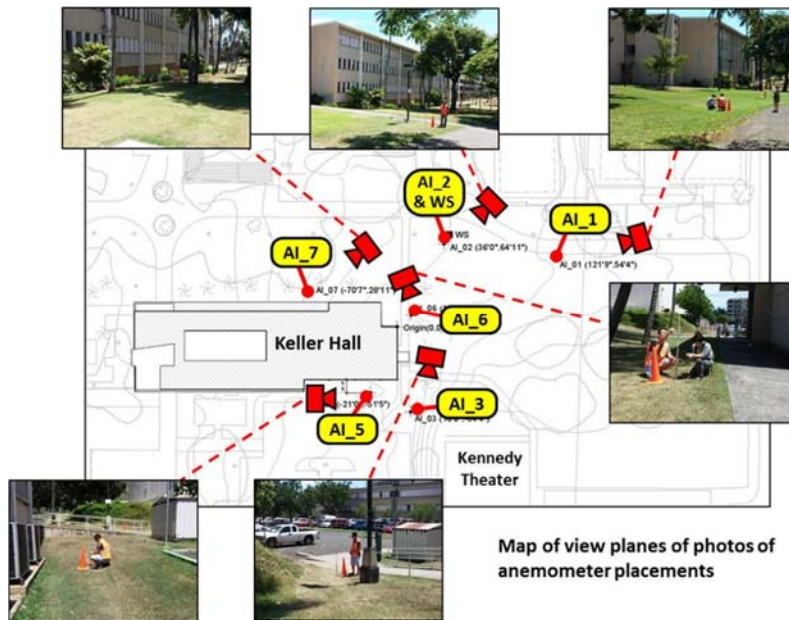


Figure 2.4.2: Locations of anemometer around Keller Hall during the wind velocity measurements.

(AL x) indicate the placement of anemometer with the corresponding index.

(WS) indicates the location of the portable weather station which was installed during the field tests.

CFD simulations of wind patterns around Keller Hall were carried out for three wind approach directions, North, North-East and East. These three wind approach directions had the largest probabilities in long-

term wind history of the site. Each wind directions used in the CFD simulations had representative wind speeds.

Figure 2.4.3 shows wind velocities around Keller Hall and adjacent buildings derived from the CFD solution for Northerly wind approach. Figure 2.4.3 illustrates that several buildings adjacent to Keller Hall were included in the computational domain in order to include interactive effect of their geometries on wind patterns around Keller Hall. Figure 2.4.4. shows a more detailed view of wind velocity distribution around Keller Hall

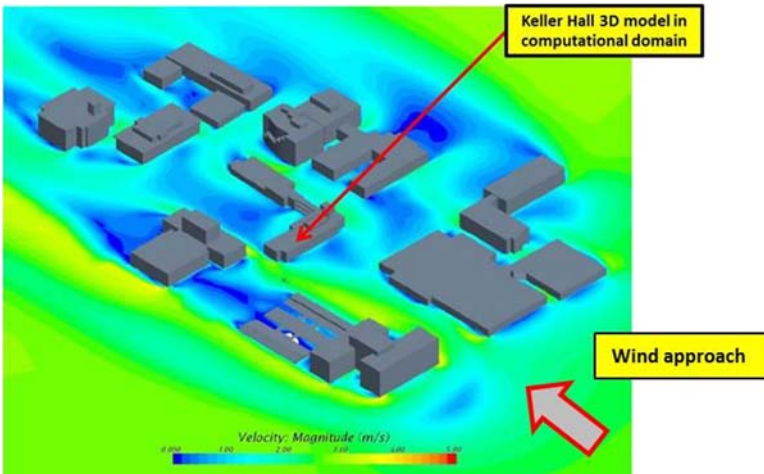


Figure 2.4.3: Isometric View (from NE) of Wind Velocity Contour Map for a Northerly wind approach

The colored contour map indicates the wind speed around the Keller Hall and surrounding buildings for a North wind approach direction. The horizontal slice (e.g. contour map) is referenced to the horizontal plane at 1m height above finishing level of the 1st floor of Keller Hall.

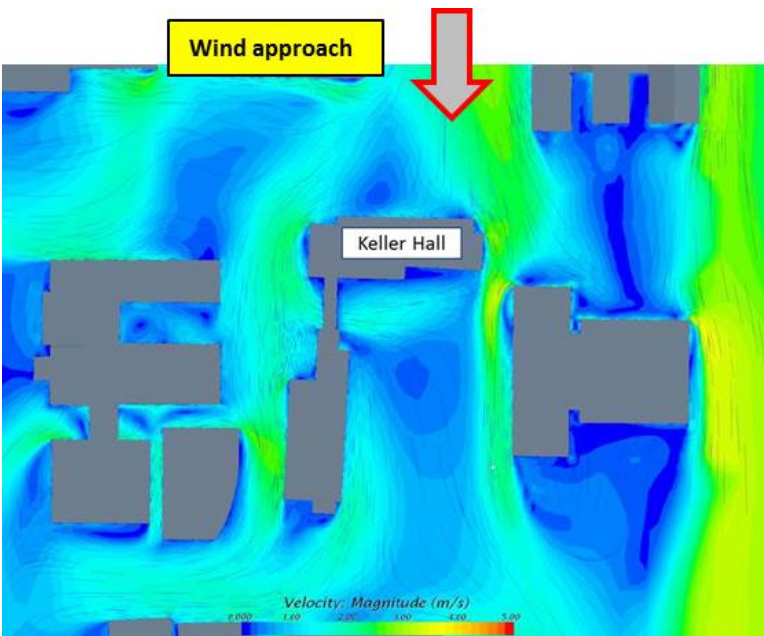


Figure 2.4.4: Plan View of Detailed Wind Velocity Stream Map around Keller Hall

Blue colors indicate small wind velocities. Green and yellow higher wind velocities, in this order. It can be seen in the figure that with Northerly approach directions there are sections of accelerated wind movement to the West and East of Keller Hall. In the North of the building wind stagnation occurs which results in decelerated wind movement. In the South of the building there are areas of slow wind movement, as a result of large scale eddies around the building.

Virtual probes, so-called “presentation grids”, were used to determine specific wind speeds at selected locations inside the computational domain. Of importance were predicted wind velocities at locations in the CFD domain which corresponded to locations where anemometers were placed during the field measurements. Local average wind velocity data was derived by using a 2D-matrix of 24 nodes (e.g. 6x6 data point matrix; 1 foot by 1 foot in size) in the computational domain. Figure 2.4.5 illustrates the use of presentation grids to extract localized wind velocities and average them.

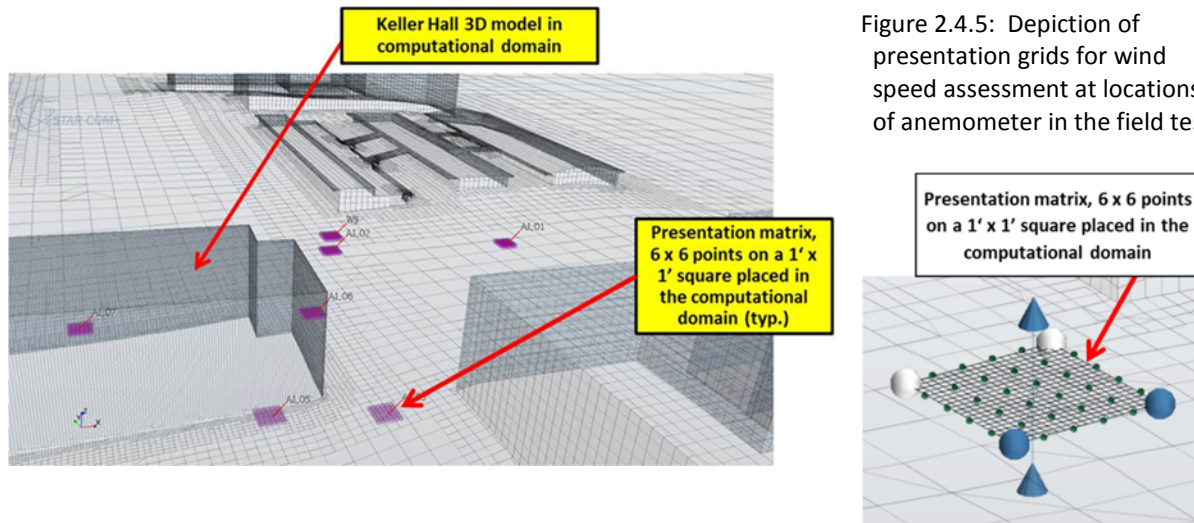


Figure 2.4.5: Depiction of presentation grids for wind speed assessment at locations of anemometer in the field tests

2.5 Investigations of Wind Patterns Around a Building – Field Measurements

The field measurements included data collection of wind conditions around the Keller Hall building and differential pressures between the North and South façade of Keller Hall.

Data of the **wind and weather measurements** around Keller Hall included three types of instrumentation:

- Weather station on Keller Hall roof, which collected long-term wind and weather data for the project site over a period of six months.
- Temporary weather station at ground level, which was installed on the windward side and adjacent to Keller Hall. The station was installed during the field measurements.
- Hot-wire anemometers, measured wind speeds at the selected sensor location around Keller Hall.

Figure 2.5.1 shows an example of the long-term wind condition record measured by the weather station on Keller Hall roof. The depiction of wind conditions in Figure 2.5.1 is a combination of a so-called wind rose and a probability frequency diagram.

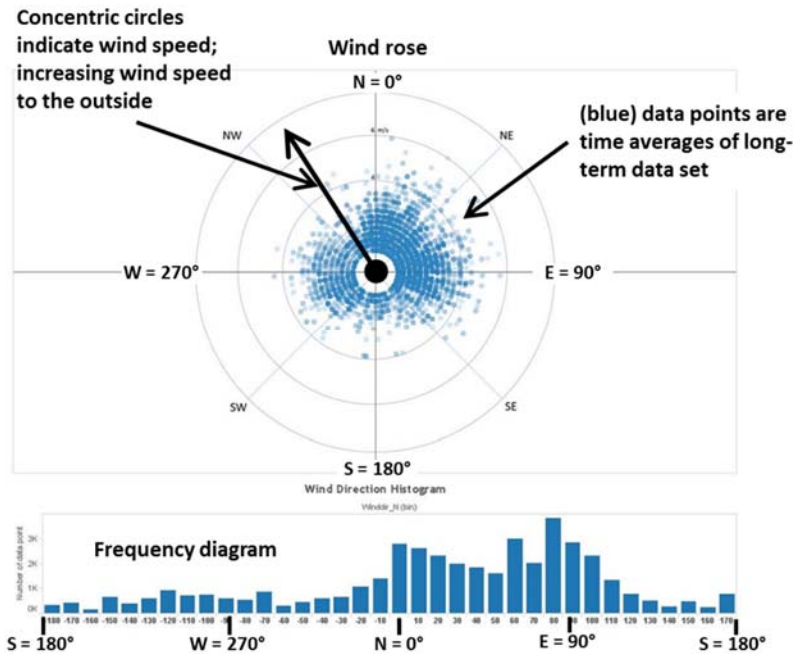


Figure 2.5.1: Definition of wind conditions measured by the weather station on Keller Hall roof

- The wind rose indicates the wind direction for the data point along a 360 degree circle, with north being 0° and South 180°.
- The wind rose indicates the wind speed by the position of data points on concentric circles. Increasing wind speed is outwards.
- The wind direction frequency diagram indicates the percentage of all data points falling into a 10° data bin.

Figure 2.5.2 shows a series of wind rose and frequency diagram representations of the actual data record. Figure 2.5.2 shows four wind rose and frequency diagram representations. One representation shows all data points and the three remaining show data-filtered representations. The data-filter process shows only data points which exceed a certain threshold wind speed. This type of data representation allowed determining the primary wind approach direction. In image (d) of Figure 2.5.2 the data record with a filter of wind speed larger than 4 m/sec suggests two ranges of main wind approach direction. One range had a center direction of around 45° and the second range at 90°. An additional important wind approach range with a center direction of around 0° was identified in image (c) of Figure 2.5.2.

The CFD simulations were run with three main approach directions of 0° (North), 45° (North-East) and 90° (East). Experimental wind speed data measured around Keller Hall was directionally filtered for these three main approach directions. A +/- 10° range window with a declining weight function was used to attribute higher weights, e.g. more importance, to wind data centering around the main wind approach directions.

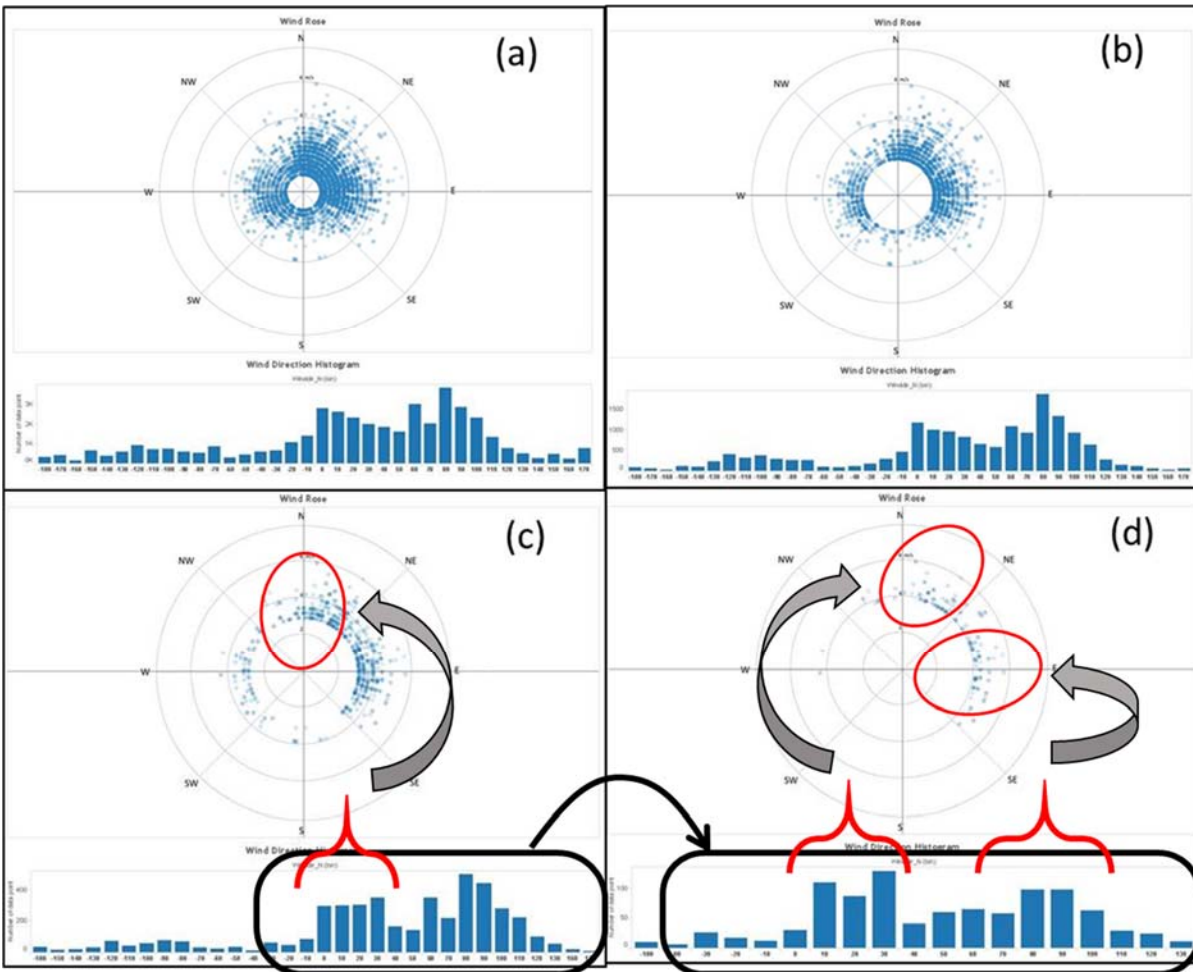


Figure 2.5.2: Data sets obtained for wind direction and speed from the weather station on the roof of Keller Hall, (a) entire date set, (b) only data for wind speed larger than 2 m/sec, (c) only data for wind speed larger than 3 m/sec, (d) only data for wind speed larger than 4 m/s

Differential pressure measurements on Keller Hall façade: Differential pressures were recorded between several locations on the North and South façade of Keller Hall over a period of three months. Figure 2.5.3 shows locations of the differential pressure measurements. Measurements of the wind induced differential pressures were a significant challenge because of the extremely low pressure differential values. The differential pressures were measured by differential pressure transducers which were placed at the midpoint of long pressure tubing. One pressure tubing terminal was fitted to each tubing end. The terminals were specially designed and manufactured by the project team. Figure 2.5.4 shows one set of pressure transducers, pressure tubing and pressure tubing terminals.

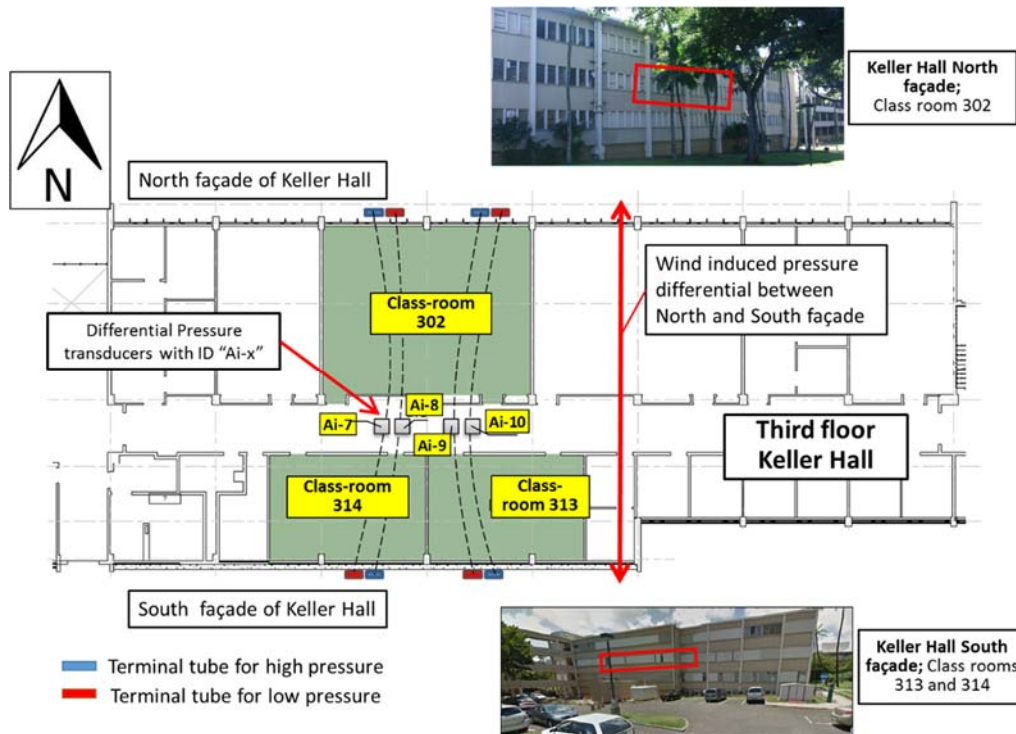


Figure 2.5.3: Measurement of differential pressures between North and South façade of Keller Hall

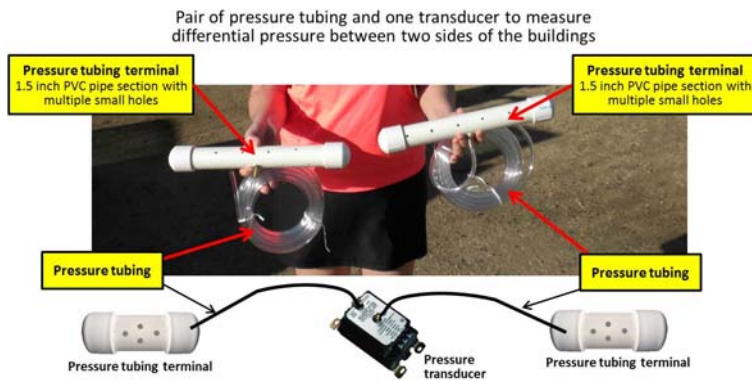
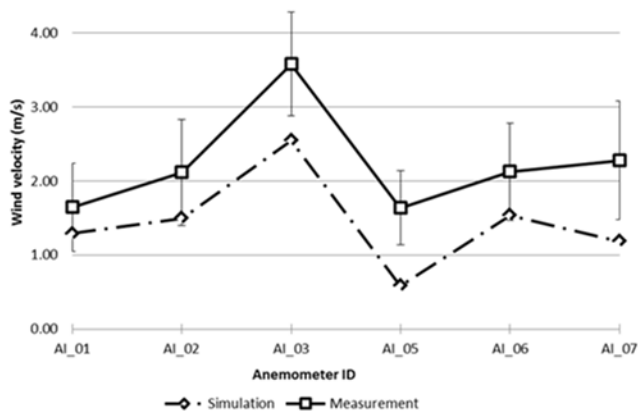


Figure 2.5.3: Instrumentation used for differential pressure measurements.

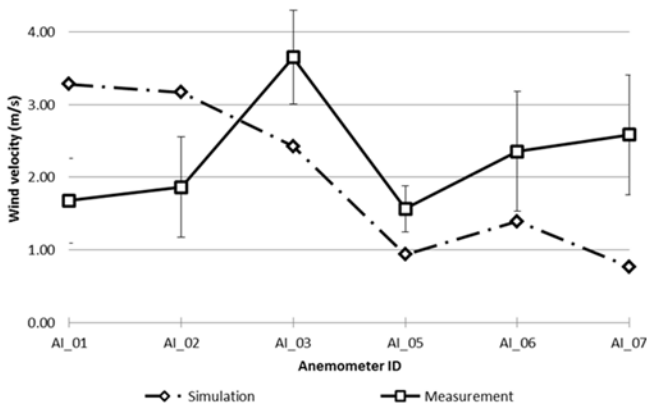
One instrumentation set included a differential pressure transducer that was placed at the midpoint of pressure tubing. The ends of tubing were fitted with terminals, that were made of 1.5 inch PVC pipe sections with multiple holes. The main function of terminal was to provide pressure averages at the sampling point.

2.6 Investigations of Wind Patterns Around a Building – Validation of CFD Simulations

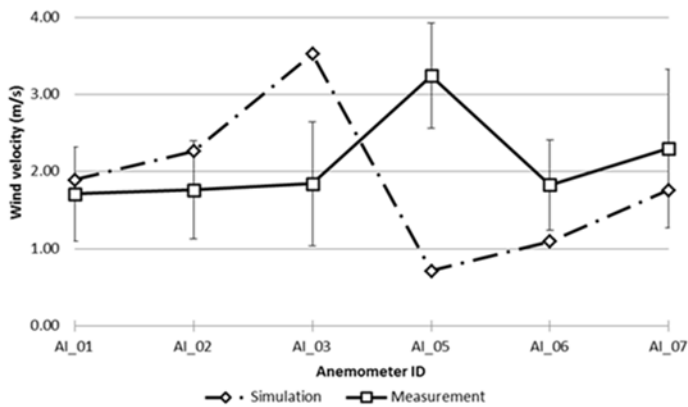
The results of CFD simulations for wind patterns and wind induced differential pressures were validated against the data-filtered wind measurements. Figures 2.6.1 shows a comparison of the CFD simulated and filtered wind measurement records for the three main wind approach directions and the for an approach wind speed of 4 m/sec.



Measurements only include filtered North wind data

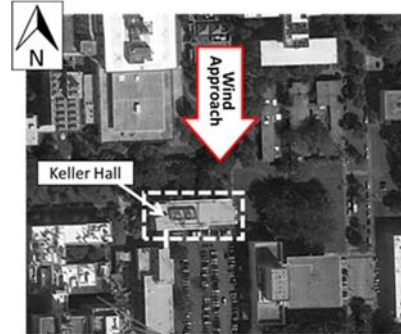


Measurements only include filtered East wind data

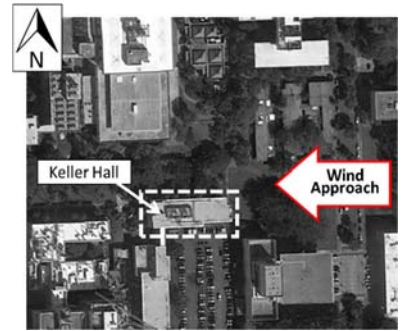


Measurements only include filtered North-East wind data

Comparison between averaged wind velocity for field measurements and simulation (medium grid resolution) wind is approaching from the North.



Comparison between averaged wind velocity for field measurements and simulation (medium grid resolution) wind is approaching from the East.



Comparison between averaged wind velocity for field measurements and simulation (medium grid resolution) wind is approaching from the North-East.

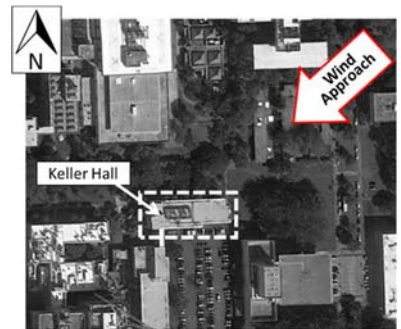


Figure 2.6.1: Validation of CFD simulations of **wind speed** around Keller Hall through filtered wind approach data

In Figure 2.6.1 the comparison of representative values obtained by CFD simulation and field measurements depict the most consistent data trend for wind approaching the Keller Hall from the North.

Figure 2.6.2 shows a comparison of the CFD simulated and measured long term differential pressures for wind approach direction for selected combinations of windward and leeward façade locations.

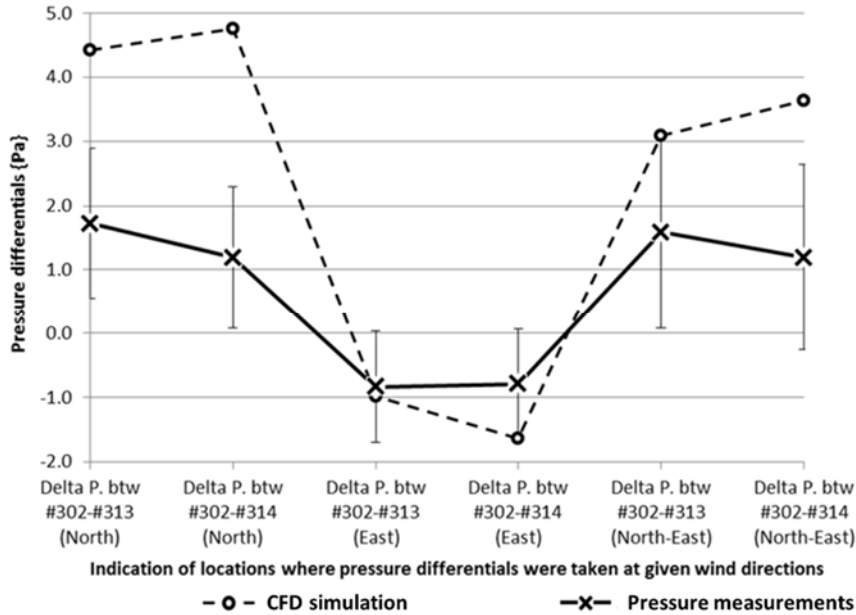


Figure 2.6.2: Validation of CFD simulations of differential pressures in Keller Hall facades through filtered wind approach data

Measurements of differential pressures referred to in the figures are filtered pressure data for wind approach from North to East.

Positive pressure differential values indicate higher pressures on the North façade. Negative pressure differential values indicate higher pressures on the South façade.

Figure 2.6.2 indicates differences of values for differential pressures obtained through measurements and CFD simulations. The results suggest that the CFD simulations over predict pressure differentials for wind approaching from the North and the North-East. Measured and calculated values for wind coming from the East both indicate a negative differential pressure, which means that, at average, higher pressures are produced on the South façade. It should be noted how small the pressure differentials are between the North and South façade. Reliable measurements of such small pressures are quite difficult and reasons for the diverging measured and calculated values could be pressure transducer limitations at such small pressure differentials.

A pressure fluctuation phenomenon was observed which indicated changing positive pressures between the North and South façade with periods of pressure reversals between 20 and 60 seconds. This fluctuating pressures can negatively affect the effectiveness of natural ventilation. The record in Figure 2.6.3 shows a correlation between fluctuation of differential pressures and the observed recorded wind direction. In Figure 2.6.3 the data for wind direction indicates changes in the order of 100 degrees within 10 minutes of recorded time. The resulting pressure differentials indicate that wind pressures build up on opposite sides of the building with periods between 20 and 60 seconds.

Observations of differential pressure fluctuations were repeated during measurements of internal air movement, when the research team encountered air flow reversal from northward to southward inside Keller Hall. The causes for these pressure variations and resulting air flow reversal observations inside the building are not conclusive from the data obtained. It is likely that large eddy formations induced by primarily East winds were contributing to the observed variations in pressure fields.

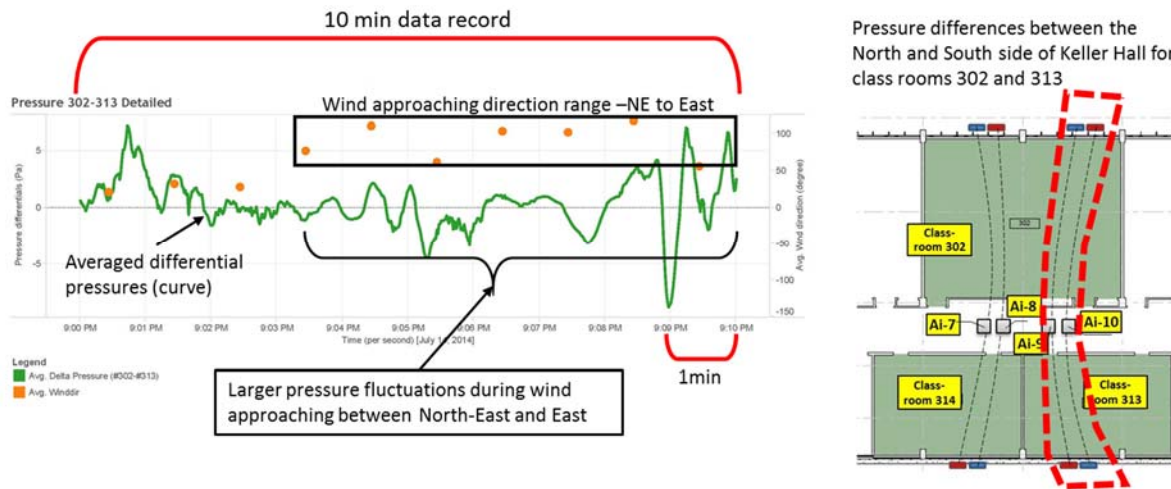


Figure 2.6.3: Example of a differential pressure data record; shows the location of the two pressure tubing terminals in relation to the transducer and a shorter record of the differential pressures between two locations on the North and South facades of Keller Hall.

2.7 Main Conclusions of Part 1 of the Research Project

The main objectives of Part 1 of the Research Project were investigations of wind movement and wind induced pressure distributions around buildings. The investigations included theoretical predictions of wind patterns around objects and buildings using means of Computational Fluid Dynamics (CFD) simulations. The results of the CFD simulations were compared with actual measurements.

The following conclusions could be drawn:

- CFD simulations of external wind movement around buildings are an increasingly important design tool for the build environment. The effectiveness of natural ventilation processes can be predicted by CFD simulations of wind movement around buildings and wind induced pressure distributions on the building façade.
- Reliable external CFD simulations are dependent on a range of simulations parameters and procedures which include appropriate choices of the following:
 - Size of computational domain has to include areas of interest, e.g. the building that is investigated, and adjacent structures to account for interactions in the flow field. There has to be sufficient distances to horizontal and vertical domain boundaries. The 3D-model of the investigated building has to be prepared with more detail than the adjacent structures.
 - Mesh sizes have to be selected with the appropriate resolution to give good solutions. Benchmark simulations were conducted with coarse, medium and fine mesh sizes. Finer mesh resolutions required significantly longer computational resources than coarser meshes but gave better solutions. The research team selected the type of mesh size that gave the best results for the least computational time.
 - Solver setting significantly affect the CFD simulation performance. Benchmark simulations were conducted to identify the most effective turbulence model.
 - The 3D-building model had an opaque or impermeable geometry in the CFD model. This means that air flow through the building was neglected for the external CFD simulations.
- Wind patterns measured around the investigated building depended on the direction and strengths of the approaching wind. Due to the non-stationarity of the incident wind, the resulting wind speed vectors are also non-stationary. The type of CFD simulations used in this investigations, however, used steady state conditions. Therefore, CFD results did not have a time dependency. In order to compare the real world wind conditions and CFD simulations using the same wind approach conditions, the wind measurement data had to be conditioned. Data conditioning included averages and data filters to compare only those measured wind data that corresponded with the approaching wind speed and direction used in the CFD simulations.

- Data consistency of CFD predictions results and actual measurements of wind velocities and pressures typically differed at various levels. The project team found data consistencies that ranged between good and medium. The CFD team identified several reasons for data deviations between theoretical predictions and actual measurements. One of the reasons was the type of hot-wire anemometers used in the field measurements. The type of anemometer used could not determine wind direction but only the absolute wind speed. These anemometers were also sensitive to the wind direction relative to the sensor orientation. Data consistency for differential pressures were also found to be limited. The reason for the limited data consistency were the very low differential pressure values, which were difficult to measure, although the research team had purchased very sensitive differential pressure transducers.
- Through observations and data analysis important non-stationary flow patterns could be identified around buildings. These time-dependent flow phenomena likely resulted from large scale eddies that were created downwind by wind-structure interactions. The most important consequence for natural ventilation is that fluctuating pressures around the building impede a constant wind induced air movement through the building. This phenomenon needs to be more investigated in future projects.

The Main Conclusion of Part 1 are as follows:

- CFD simulations provide important understanding of wind movement around building and are therefore becoming important design tools for the build environment
- The CFD simulations carried out in this investigation were validated against field measurements of wind speed. Good to medium data consistency was found for wind speed; less data consistency was found for differential pressures between opposite building facades.
- Non-stationary wind movement was detected through measured data. This phenomenon causes pressure fluctuations, which can impede natural ventilation in a building.

SECTION 3 - SUMMARY BRIEF OF PREVIOUSLY COMPLETED PART 2

This section presents the main results and conclusions of the project work that was conducted under Part 2 of the Research Project – Internal CFD Applications.

The main objective of Part 2 of the Research Project was development and validation of Computational Fluid Dynamics (CFD) simulation methodologies for wind induced air movements through naturally ventilated buildings.

Air movement through buildings are driven by external wind conditions and the resulting pressure distribution around the building envelope. Along the internal flow pathways through the building flow obstacles contribute to pressure losses. With the same external wind driving force a higher cross ventilation rates can be achieved by minimizing energy losses along internal pathways. CFD simulations can be used to determine air movement rates through spaces while considering external and internal air movement conditions.

The work in Part 2 compared simulated and actually measured wind induced air flow through naturally ventilated spaces of a building on the University of Hawaii Manoa campus.

Part 2 of the Research Project was carried out in four work tasks, 2.1 through 2.4, as illustrated in Figure 3.1.

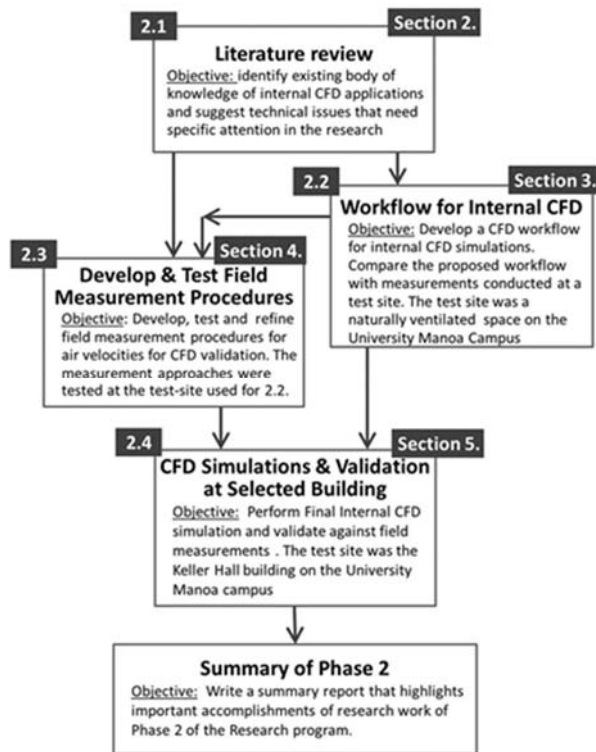


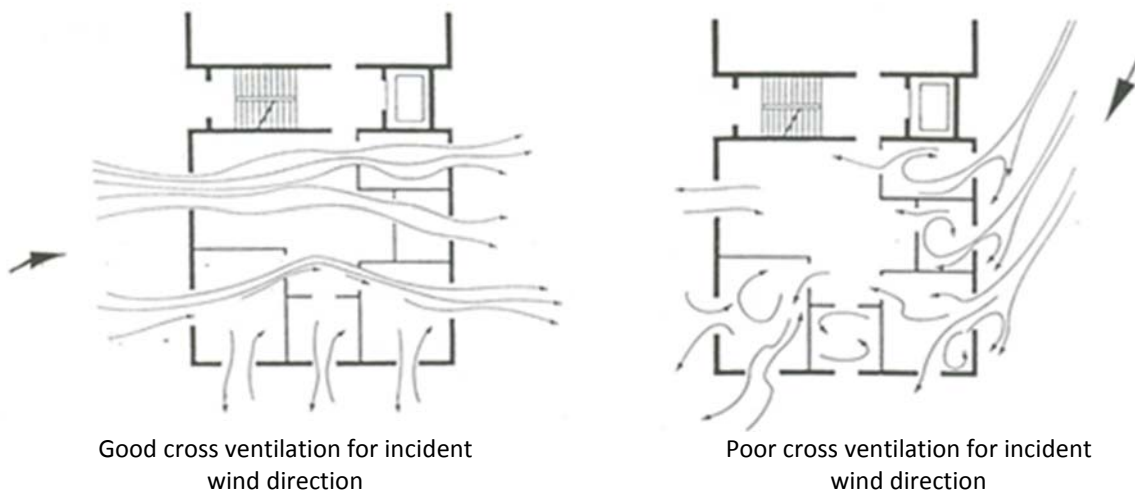
Figure 3.1: Process flow diagram of the project tasks during Phase 2 of the Research Project

The work process in Figure 4.1 illustrates how project tasks 2.1 and 2.2 were carried out interactively. The resulting workflow for internal CFD was used in project task 2.4 to predict internal air flow phenomena through the selected building. CFD simulation results were validated with data measured under project task 2.4.

3.1 Basics of Air Flow through Internal Spaces

The investigation of internal air flow under natural ventilation conditions was the main objective of Part 2 of the Research Project. Air flow rate in naturally ventilated buildings is a function of external driving forces and the effectiveness of internal pathways to convey the air flow with the least amount of pressure losses.

Figure 3.1.1 shows an example of a layout of spaces that has good cross ventilation for one particular wind approach direction, while under a different wind approach natural ventilation is less effective. This example illustrates that a building layout should allow good ventilation performance for a range of wind directions. In areas where there is a predominant wind direction layout should be optimized for this wind approach while making provisions for secondary wind approaches.



3.1.1: Effectiveness of cross ventilation under different wind directions

Minimizing pressure losses of opening is important to maximize air flow rates. External openings allow air to enter and leave the building. Internal openings allow air flow between spaces. Figure 3.1.2 illustrates how the configuration of an opening affects air flow rates. External and internal openings in buildings can be described with discharge coefficient. In Figure 3.1.2 the largest discharge coefficient causes the highest flow through the opening, while the driving forces of air flow is the same for all cases depicted in Figure 3.1.2. The technical literature presents a comprehensive treatment of discharge characteristics for openings in mechanical systems. Widespread information of discharge performance of typical openings in natural ventilation is not as readily available. CFD simulations provided important design information on air flow characteristics in naturally ventilated spaces, which the available technical literature does not readily provide.

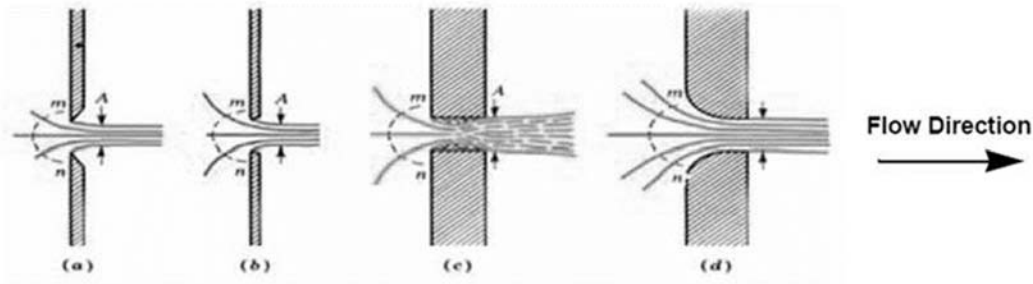


Figure 3.1.2: Discharge coefficients for orifices (noted as C_d) with the same diameter but with different inlet geometries

3.2 Basic Considerations of CFD Simulations for Internal Spaces

Achieving good solutions of internal CFD simulations hinges on basic consideration of what physical parameters have to be modelled. The basic question is *What do we want to obtain from the prediction?* As an example, the room as depicted in Figure 4.2.1 should be investigated. Both pictures in Figure 4.2.1 show the same room, one with many details the other devoid of any furniture. If the nature of the CFD analysis is air intrusion in the vicinity of a window, then simplification can reduce the amount of objects to be modelled inside the space. If an intricate airflow in the room is required, involving complex thermal plumes, much more interior objects need to be included in the CFD model. Much care has to be taken that simplification matches the objectives and the computer resources involved.



(a) Office situation with all details



(b) Simplified office situation

Figure 3.2.1: Comparison of situations to be modeled with different degrees of simplification

Using an appropriate mesh or computational grid can significantly affect the solution. In the present Research Project meshes of different resolutions, or in other works meshes with different numbers of cells, were used. The mesh with a higher number of cell has a higher resolution. In benchmark simulations it was found that using a higher resolution mesh did not necessarily result in better convergence than a mesh with a fewer number of cells.

Several turbulence models were used in the present project. Typically, high-level turbulence models require more computational resources. The commonly used k- ϵ -model has limitations that can be overcome with the use of SST model. For this research project both the k- ϵ and the SST turbulence models were used in benchmark simulations.

The selection of boundary conditions significantly affected the calculation performance and quality of the CFD solution. During the development of the workflow for internal CFD simulations the research team tested several boundary conditions and selected the more effective boundary conditions. For the modelling of internal air movement which are driven by external environmental conditions it was important to consider the air intake into the building.

There are two domain approaches to predict internal airflow phenomena through the use of CFD analysis. The first approach is called “domain decoupling” or “decoupled” approach, where wind induced air flow conditions on the exterior of the building are analyzed, which produces results in regard to pressure distribution and wind speeds. These results are then used as boundary condition for the CFD simulation of the interior space. The advantage of the decoupled approach is that it requires fewer computational resources than the coupled approach. The disadvantage is that internal airflow cannot be precisely predicted, especially close to free flow openings. The second approach is the so-called “coupled” approach where the exterior and interior space is combined into one computational domain.

In CFD simulations of cross-ventilation, involving large openings as in the case of our present investigations, a major issue of concern is the accurate modeling of the interaction between the outdoor wind flow around the buildings and the indoor air flow inside the buildings. Both types of flows interact with each other at the ventilation openings. Figure 3.2.2 illustrates the difference between the coupled and uncoupled domains as used in CFD simulations.

The research team opted to employ a combination of the coupled and decoupled domain approach. Figure 3.2.3 illustrates the approach selected for the present investigation if indoor air flow. Under this selected approach the outdoor domain is kept relatively small, but of sufficient size to account for wind induced pressure and free flow conditions in the vicinity of the windward openings.

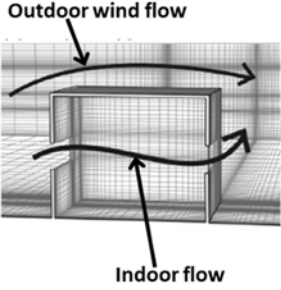
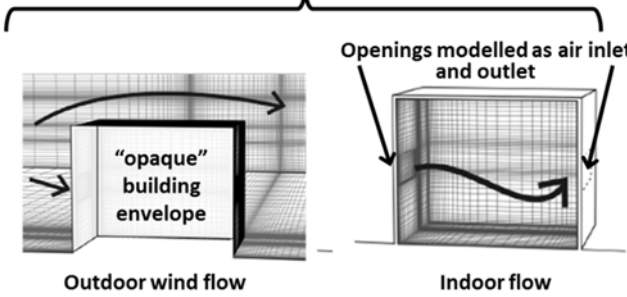
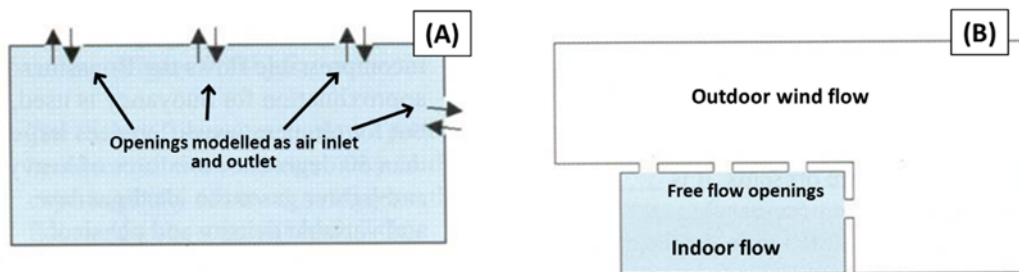
<p>COUPLED simulation for internal CFD simulations</p> 	<p>DECOUPLED simulation for internal CFD simulations</p> 
<p>In the COUPLED simulation approach the outdoor wind flow and indoor air flow are modeled as one “coupled” computation domain.</p>	<p>In the DECOUPLED simulation approach the outdoor wind flow and indoor air flow are modeled as two different or “segregated” computational domains. For the outdoor flow simulation, the building envelope is “opaque”, meaning external openings are not passing any air flow to the interior. For the indoor flow simulation, openings are modelled as inlet and outlet interfaces.</p>
<p>Advantages: The wind induced driving forces phenomena such as stagnation of flow on the windward side are correctly modeled. The air flow in the vicinity of building envelope openings are modelled in detail.</p>	<p>Advantages: Significantly less computational resources are required than in COUPLED approach. The outdoor flow simulation provides the pressure distribution on the building, which can be used to set the boundary conditions of the building envelope openings. Due to the segregation of the outdoor and indoor domain, the indoor meshes can have more resolution and can consider more geometry, details.</p>
<p>Disadvantages: Combining the outdoor and indoor domains requires significant computational resources.</p>	<p>Disadvantages: The mass transfer and pressure effects of the outdoor flow cannot be considered in detail, which makes it impossible correctly model indoor airflow close to external openings.</p>

Figure 3.2.2: Coupled and decoupled approach for analysis of wind-induced cross-ventilation of buildings



(B) is the correct boundary conditions by enlarging the computational domain (area in blue is the smaller domain shown in (A)). The blue area is the area indoor flow which is the area of interest.

Figure 3.2.3: Examples of boundary conditions in free flow openings

3.3 Initial Internal CFD Investigations to Develop a Generic Workflow

Following the same approach as for external CFD investigation a generic CFD workflow was developed for the internal CFD simulations. The results of the generic internal CFD workflow were to be validated by measurements of indoor airflow data. Using this validation approach also served the purpose of developing specific instrumentation and data acquisition procedures for indoor air movements.

The test set-up of another ERDL project was used to carry out the internal CD workflow development and data acquisition shake-down tests. This test location was located in the third floor of the at Sinclair Library on the University of Hawaii Manoa campus. A 5,000 square feet naturally ventilated space was fitted with a temporary mechanical assists ventilation to investigate contribution of increased air flow on occupant comfort. The mechanical assists ventilation allowed a controlled test environment where the air discharge could be controlled by four propeller fans. Figure 3.3.1 show images of the space layout and the propeller fans.

The test measurements in Room 301, which were carried out in conjunction with the CFD work flow development (Section 3), provided the team with an opportunity to fine tune the measurement procedures before the final internal CFD investigations were conducted.

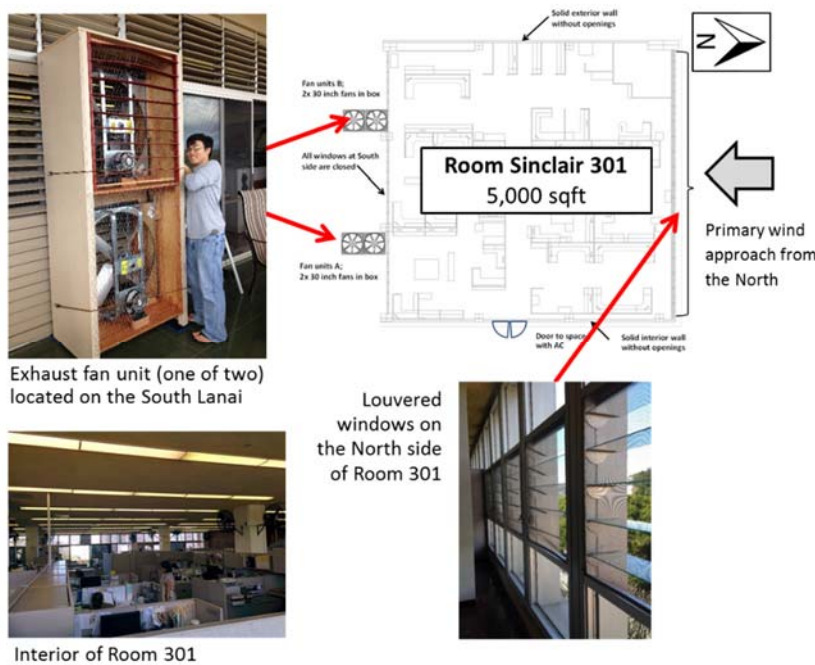


Figure 3.3.1: Location of the initial investigations of indoor air flow

The test site was the third floor of the Sinclair Library in the University of Hawaii Manoa campus. A temporary system of four exhaust fans were installed at the South lanai. These fans increased the cross ventilation through in the normally naturally ventilated space.

Both the coupled and decoupled simulation process was investigated. Figures 3.3.2 and 3.3.3 illustrate the computational domains used for the decoupled and coupled simulation approach, respectively.

Benchmarking results indicated that the coupled domain approach was the preferred approach. The meshes sizes of the decoupled and coupled domains differed significantly. The decoupled domain mesh had 2.5 million cells. The coupled domain mesh with and without furniture (e.g. mainly internal cubicle partitions) had 16 and 4.4 million cells, respectively.

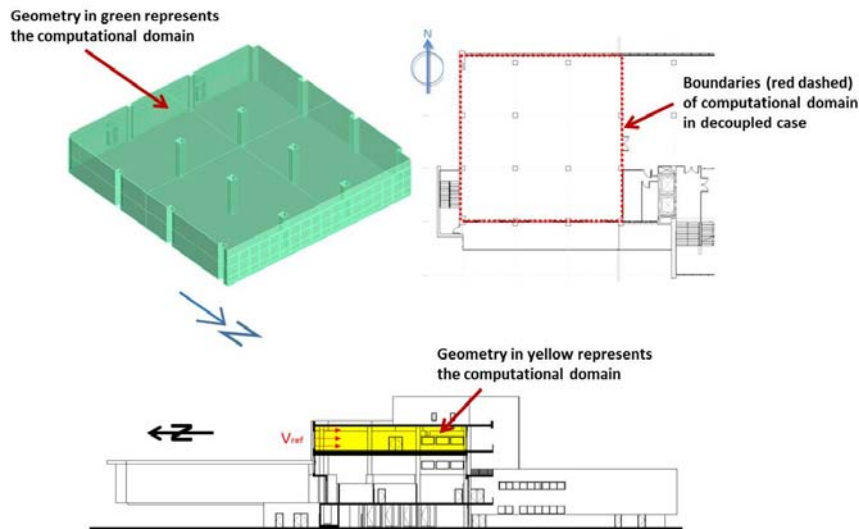


Figure 3.3.2: Geometry modeled for the **DECOUPLED** domain case

The image illustrates the 3D model of Room 301. Since the decoupled domain case was used only for benchmarking, no internal structures, e.g. furniture and cubicle partitions, were included in the model.

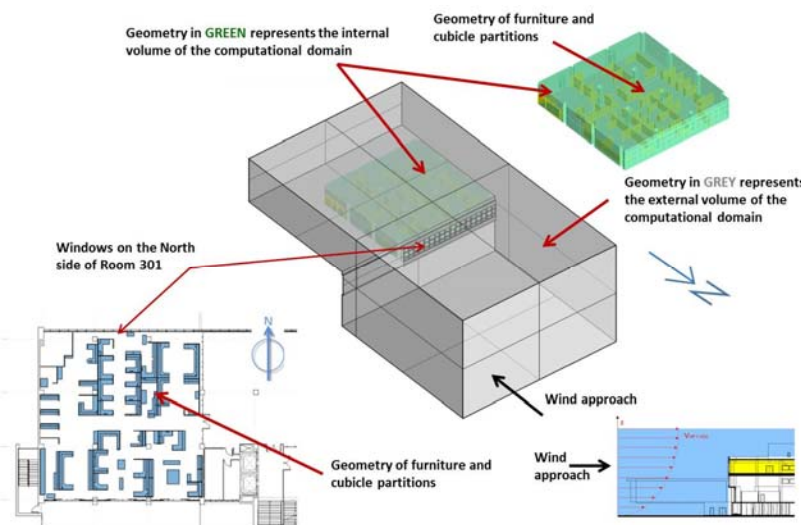


Figure 3.3.3: 3D CAD model illustration of the **COUPLED** domain CFD; case with furniture

Note: The coupled domain simulations were run with TWO cases, one with and the other without furniture and cubicle walls included.

One of the most important findings of the initial CFD simulations was the performance of turbulence models. Figures 3.3.4 and 3.3.5 indicate the convergence characteristics and the resulting air flow

calculated with the two turbulence models Realizable k-ε turbulence model and the SST k-ω turbulence model.

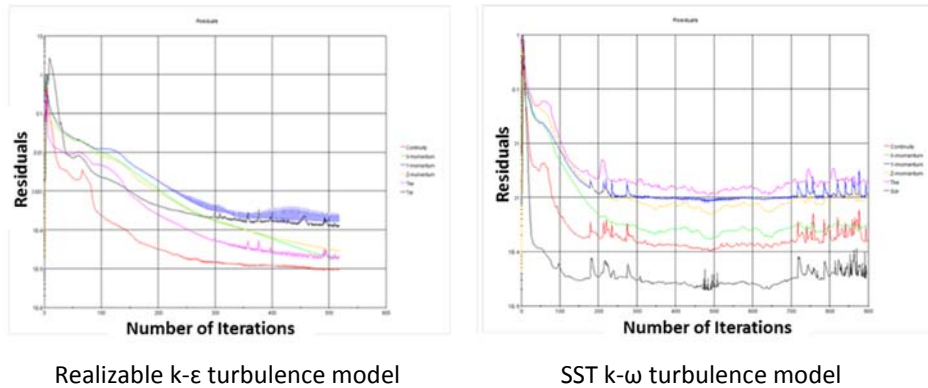
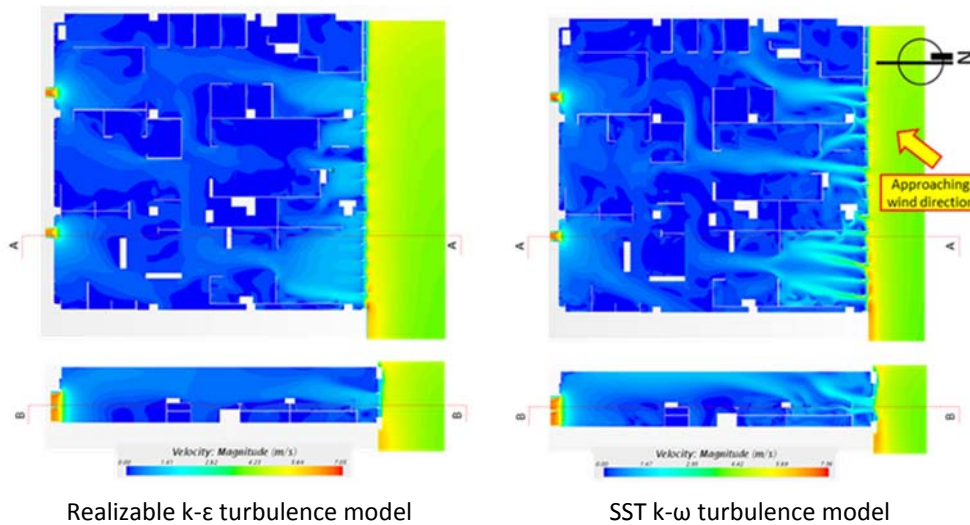


Figure 3.3.4: Residuals plot of CFD solutions of two different turbulence models.



NOTE: the k-ε turbulence model shows a more robust convergence performance while the SST k-ω turbulence model defines the air flow pattern in more detail.

Figure 3.3.5: An example of airflow pattern from simulation results of two different turbulence models from the same CFD scenario

The CFD investigation of the air flow patterns inside Room 301 revealed very complex air movements, caused by numerous internal flow obstructions. The selected decoupled domain approach produced good results. Benchmarking of two turbulence models provided good insight in CFD solver setting selection. The lessons learned from the CFD investigation provided a good basis to develop a workflow that was subsequently used for final internal CFD investigations at Keller Hall.

3.4 Final Internal Air Movement Investigation at the Selected Building – Measurements

The test site for the final internal CFD investigations was a portion of third floor of Keller Hall. The Keller Hall building was previously used as a test site for the external CFD investigations under Part 1 of the Research Project. The prevailing trade winds approach the building from the North-East. The portion of the third floor that was used for the final internal CFD investigations included three naturally ventilated classrooms. Cross ventilation through these three classrooms passed through a hall way in the center of the building. Figure 3.4.1 shows the floor plan of the third floor and indicates the location of the three classrooms. Figure 3.4.1 also shows images depicting the three classrooms.

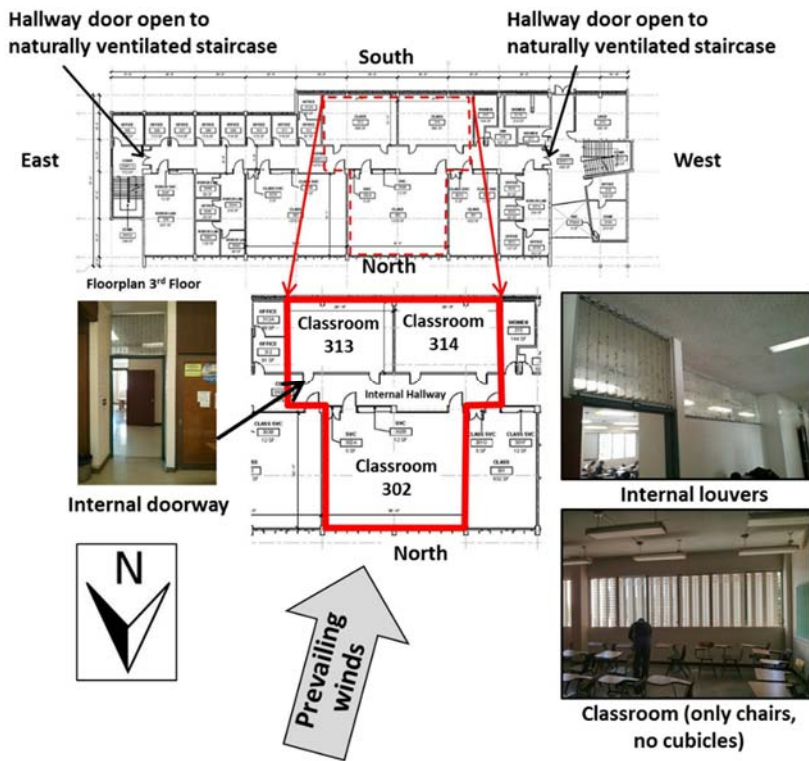


Figure 3.4.1: Test site for the final internal CFD investigations

The test site included three naturally ventilated classroom, which were separated by a central hall way, which was also naturally ventilated.

Five test scenarios were selected for which CFD simulations and validation measurements were carried out. The test scenarios were defined by different combinations of open and closed doorways and open or closed internal louvered connections between the classrooms and the central hallway. The concept of a **control volume** is important in the understanding of the five test scenarios. In the control volume, under steady state conditions, the change in mass is zero. In our case the control volume was used to balance the net mass flow rate for the air moving from room 302 to the classrooms 313 and 314. The inlets and outlets of the control volume, e.g. the control surfaces, were internal doorways, louvered wall sections between classroom and hallway and sections of the hallway. For four of the five test scenarios the internal louvers, which were situated above the doors between the classrooms and the hallway, had to remain impermeable to air flow.

In preparation for experimental investigations internal louvers were temporarily sealed by plastic covers. Figure 3.4.2 shows the installation of the temporary plastic covers. Figure 3.4.3 show the placement of the anemometers. Since mass flow rates between the classrooms were of importance the air velocities in the internal doorway and hallways were measured.



Installing the temporary tarp to seal sections of the louvered openings; seen from classroom 302



Completed sealing of the louvered section

Figure 3.4.2: Images of preparing the test site for measurements of internal air flow – sealing of the internal louvered sections



Deploying the anemometers at the test site; anemometers placement in doorway of room 313 (A4)



Deploying the anemometers at the test site; placement of all anemometers inside the hallway for measurements under test Scenario 1.

(Note the extension cords were used to supply the excitation voltage as well as transmit the recorded data of the sensors to the data acquisition system)

Figure 3.4.3: Deploying the anemometers at the test site

The test site consisted of three interconnected and naturally ventilated classrooms. Cross ventilation produced air movement through internal openings, which included doorways, louvered wall sections and a central hallway. Air flow rates between spaces were determined by measuring air velocities in internal openings. This experimental set-up provided the team with a good opportunity to validate results of CFD simulations with measured data.

Wind approach velocity and direction were recorded concurrently with the tests of internal air movement. The environmental data, including wind conditions, were measured with a weather station on the Keller Hall roof. Figure 3.4.4 shows a long-term wind record, depicted by the wind rose and the wind direction histogram. The wind record indicates predominately North-East wind approach during the tests.

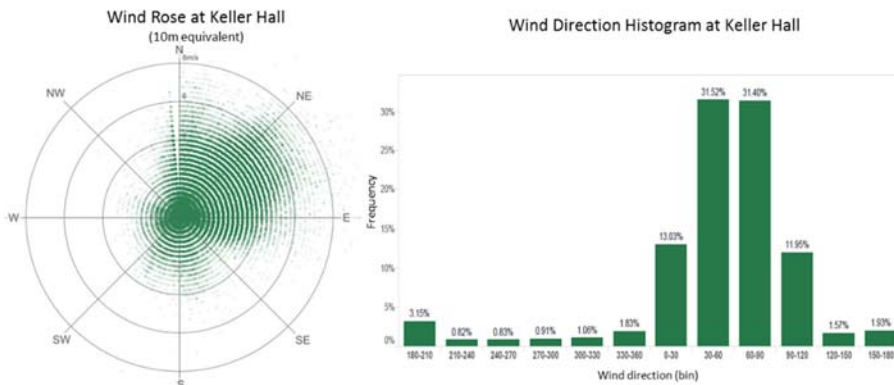


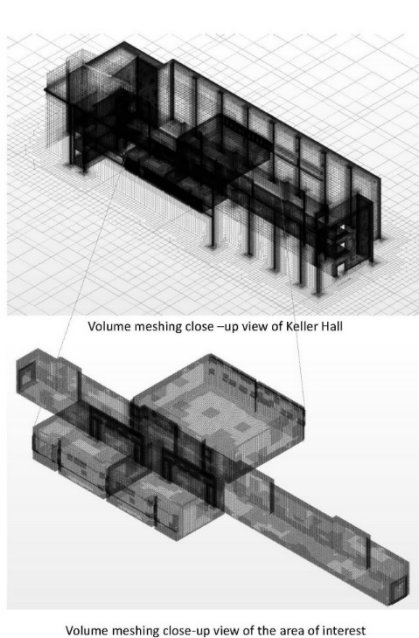
Figure 3.4.4: Wind observation for Keller Hall showing predominately N/E winds.

Prevailing winds during the experiments were coming from the North-East. This created good experimental conditions, since this wind approach direction has the least obstructions.

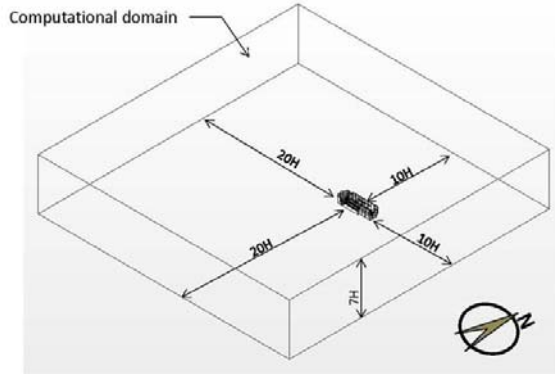
4.5 Final Internal Air Movement Investigation at the Selected Building – CFD Simulations

The simulations were carried out using a coupled domain approach. Three mesh sizes were benchmarked ranging from 10 to 19 million cells. During benchmarking the 10 million cell mesh produced approximately the same results as the higher resolution grids, while simulations with the higher resolution meshes required significantly longer simulation time until acceptable convergence. Therefore, the 10 million cell mesh was used. Figure 3.5.1 illustrates the mesh as well as the size of the computational domain.

Typical results of the simulations are depicted in Figure 3.5.2 and 3.5.3 as velocity contour maps in the horizontal and vertical plane. In Figure 3.5.2 open and closed doorways between classrooms and hallway are indicated.



(a) The mesh had 10 million cells, Grid sensitivity analysis revealed a good quality grid resulting in acceptable errors in the converged solution.



(b) Size of the computational domain; distance to upwind and downwind boundary was $20 H$ and $10 H$, respectively. Vertical distance was $7 H$. H is the height of the 3D-model of Keller hall in the computational domain

Figure 3.5.1: Volume mesh for the area close to Keller Hall (a) and size of computational domain (b)

Five test scenarios were used, where each scenario was defined as a combination of open and closed internal doorways and louvered wall sections. Table 3.5.1 defines the five test scenarios.

Label	Type	Room	Scenario 1	Scenario 2	Scenario 3	Scenario 4	Scenario 5
a0	Door	314	closed	open	open	open	open
a1	Door	302	closed	open	closed	open	open
a2	Door	314	closed	open	open	open	open
a3	Door	302	closed	open	open	open	open
a4	Door	313	closed	open	open	open	open
a6E	Door	Hall way	open	closed	closed	open	open
a6W	Door	Hall way	open	closed	closed	open	open
A	Clerestory	313	closed	closed	closed	closed	open
B	Clerestory	314	closed	closed	closed	closed	open
C	Clerestory	302	closed	closed	closed	closed	open

Table 3.5.1: Description of the five test scenarios as combinations of open and closed internal doorways and louvered wall sections (e.g. clerestory)

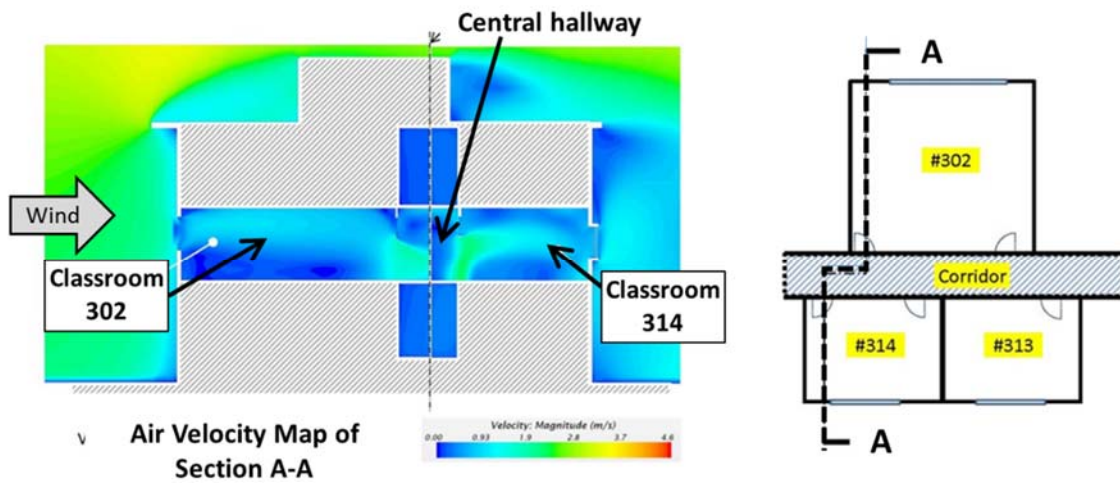
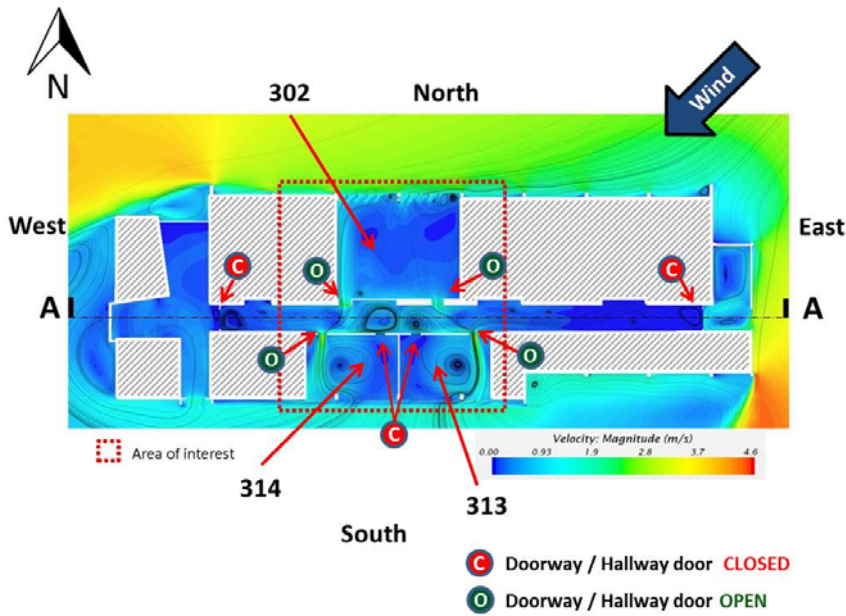


Figure 3.5.3: Sample Visualization of internal air flow – Velocity Contour Map on the vertical plane

The central hallway was defined as a control volume for air flow, with the internal doorways, hallway section and louvered wall sections representing the inlets and outlets, e.g. the control surfaces. The control volume was used to verify the conservation of mass assumption in the CFD analysis of the three interconnected classrooms and hall way under steady state conditions. Under steady state the net mass flow rate, e.g. sum of all mass flow into (positive) and out (negative) of the control volume has to be zero since no air is stored in the control volume. Figure 3.5.4 illustrates balancing of the control volume under steady state conditions, where the sum of flow rates 1 through 6 is zero. Figure 3.5.5 shows that mass flow for all five test scenarios were completely balanced and that residuals were very low. This fact indicated CFD solutions were conclusive.

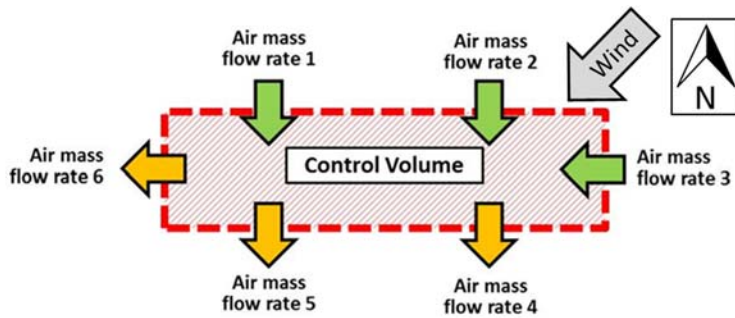


Figure 3.5.4: Definition of ass flow balancing of control volume approach used in the investigations

The central hallway in Keller Hall was defined as the control volume. The mass balancing shown in the figure is for a wind approach from the North to North-East. For winds from other directions the arrows could reverse.

Mass balance of the control volume:

	Scenario 1	Scenario 2	Scenario 3	Scenario 4	Scenario 5
In	147	513	431	639	1,189
Out	-147	-513	-431	-638	-1,189
Residual	0	0	0	1	0
Error	0.0%	0.0%	0.0%	0.2%	0.0%

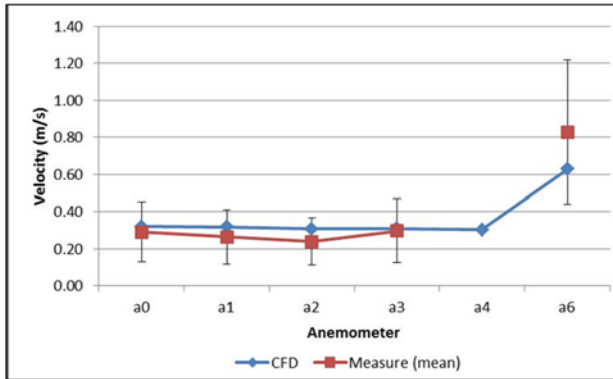
Inflow	into the control volume (positive value)
Outflow	from the control volume (negative value)

Figure 3.5.5: Results of mass flow balancing of a control volume for the five tests scenarios

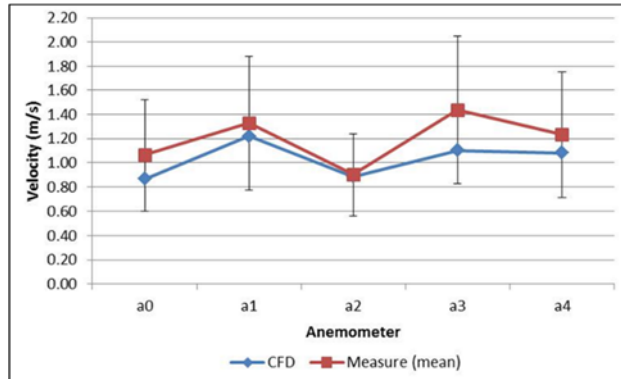
The CFD solutions showed ZERO or very low residuals and therefore ZERO or very low errors. This indicated CFD solutions were conclusive.

3.6 Final Internal Air Movement Investigation at the Selected Building – CFD Validation

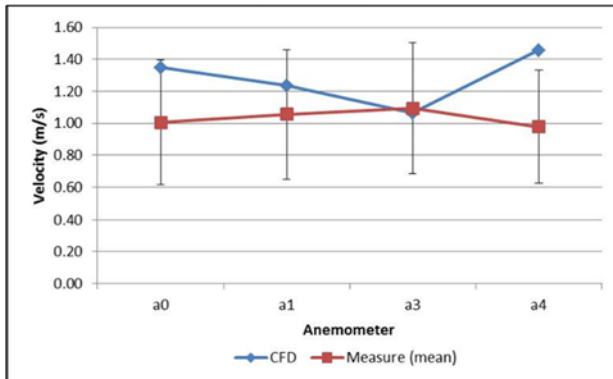
The CFD simulations were compared with experimental data. The CFD simulations for all five test scenarios used the same approach wind direction of 45° (e.g. North-East wind) but varying wind velocities for each test scenario. During each test scenario the wind velocities were measured by the weather station and one representative wind velocity for each of five test scenarios was defined. Figure 3.6.1 summarizes comparisons between CFD simulations and experimental data for all five test scenarios.



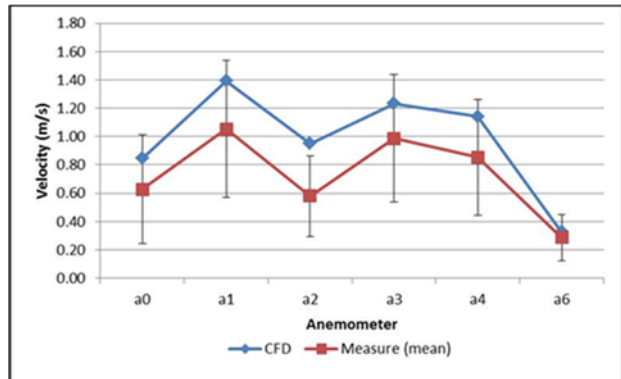
Test scenario 1



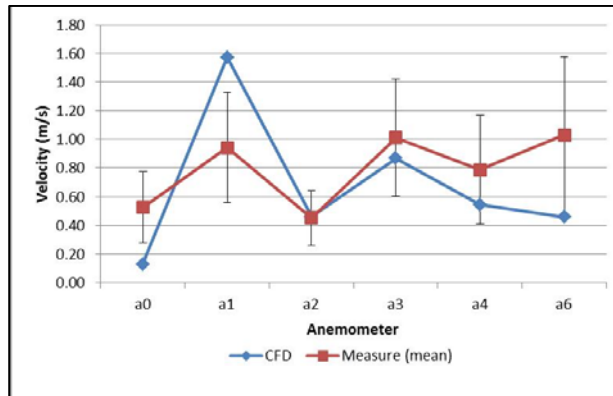
Test scenario 2



Test scenario 3



Test scenario 4



Test scenario 5

Figure 3.6.1: Comparisons of results of CFD simulations and experimental data for all five test scenarios.

Correlation of CFD simulations and experimental data was good. CFD derived velocity values represented averages derived over opening geometry. Measured data was taken at a height of 3' 6" above the floor.

The results of the CFD simulations and the measurements for the air velocities compared well. Overall, the validation of CFD results with actual measurements can be regarded as **successful**. The control volume approach proved that conservation of mass was achieved and the net mass flow rates on the control volume were zero. This verified that the CFD solution was a valid numerical solution.

3.7 Process to Predict Natural Ventilation Performance of Spaces

A method was developed to predict natural ventilation effectiveness in buildings. This method uses a combination of CFD simulations and long term wind records. In this method CFD simulations evaluate a series of so-called “unit responses” of air flow through interior spaces, which are valid for certain wind approach directions and wind speeds. As an example, a unit response air flow rate would be based on an average wind approach direction of 45° (North-East wind) and a wind speed of 1 m/sec. From the air flow rates and the interior volume values of air-changes-per-hour (ACH) are calculated. Long-term wind records are analyzed and wind direction and wind speed are expressed with probabilities of exceedance. The overall result of this procedure is an expression how many ACH happen in a certain space through natural ventilation over a period of time. Figure 3.7.1 illustrates the calculation procedure. The procedure steps A through E are described in the following.

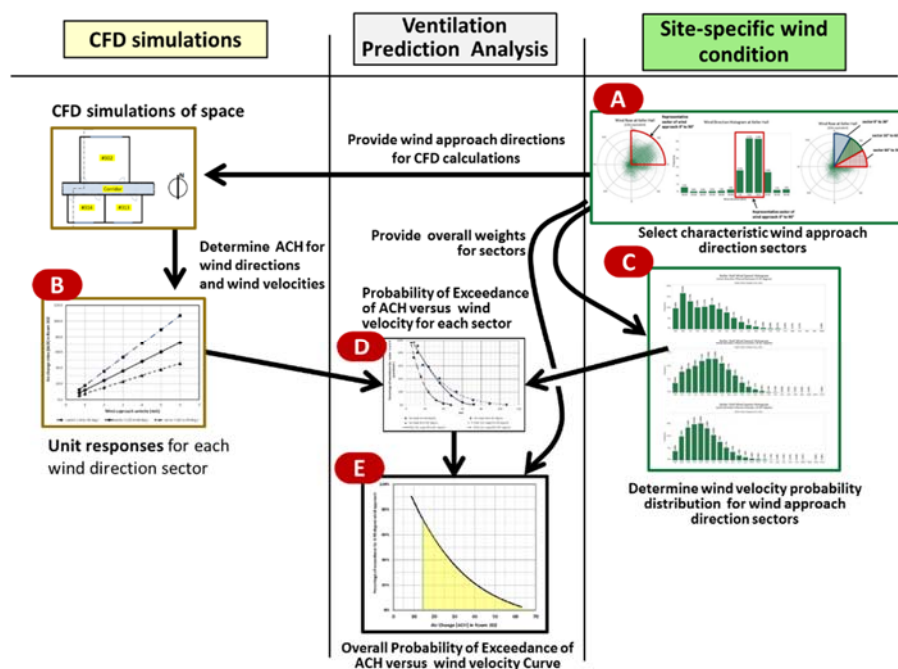
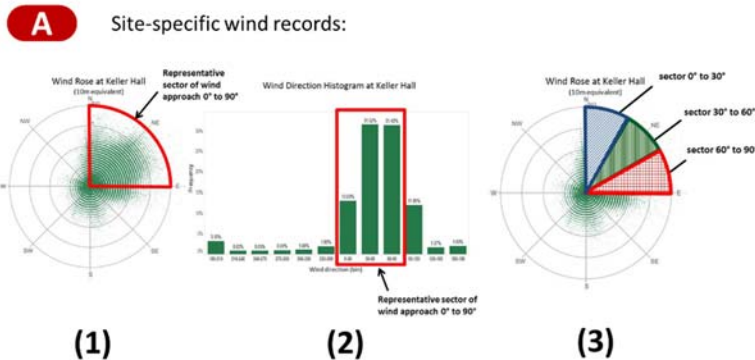


Figure 3.7.1: Procedure to determine the probability of exceedance for ACH

The process steps A through E are described in more detail

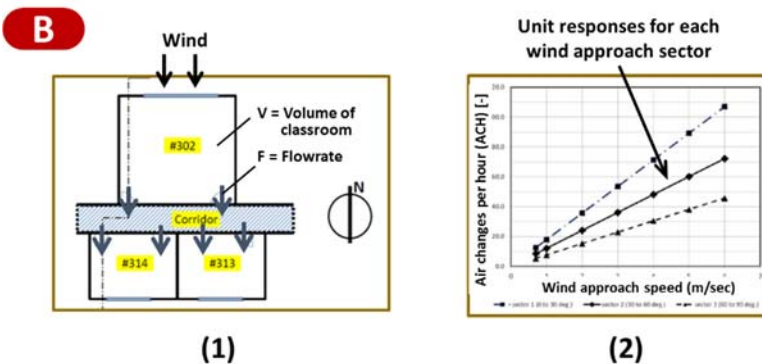


Note: Limiting the analysis to the primary wind direction lowers the complexity and scope of the assessment, while still providing good results.

Process Step A:

(1) and (2): The long-term site specific wind record is analyzed to determine primary wind directions. In the depicted case wind approach directions that ranged from 0° to 90° were identified as primary wind directions.

(3) The range of primary wind directions is subdivided into sectors. Each sector is assigned a wind approach direction which is the bisecting line of the sector. In the depicted case there are three sectors, each of which span over 30°. Therefore, sectors 1,2 and 3 have wind directions of 15°, 45° and 75°, respectively.



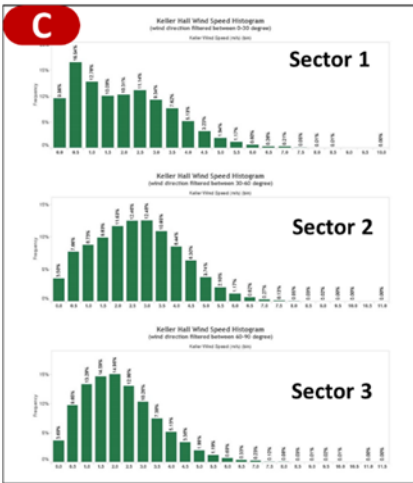
Air-changes-per-hour (ACH) is calculated by dividing Flowrate [cbm/h] by the volume [cbm] of the classroom that is assessed.

$$ACH = F / V \quad [1/h]$$

Process Step B:

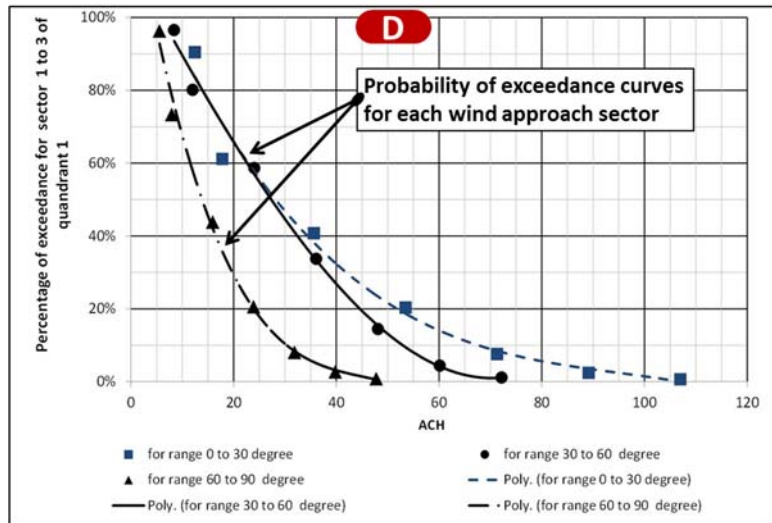
(1) CFD simulations are performed for each wind approach sector and unit wind speed. The flowrate through the room is determined.
 (2) For each room unit response graphs are plotted as functions of unit wind speed (x-axis) and ACH (y-axis). In the depicted diagram each graph represents a wind approach direction. For each graph unit wind approach speed were used in simulations.

SECTION 3 - SUMMARY BRIEF OF PREVIOUSLY COMPLETED PART 2



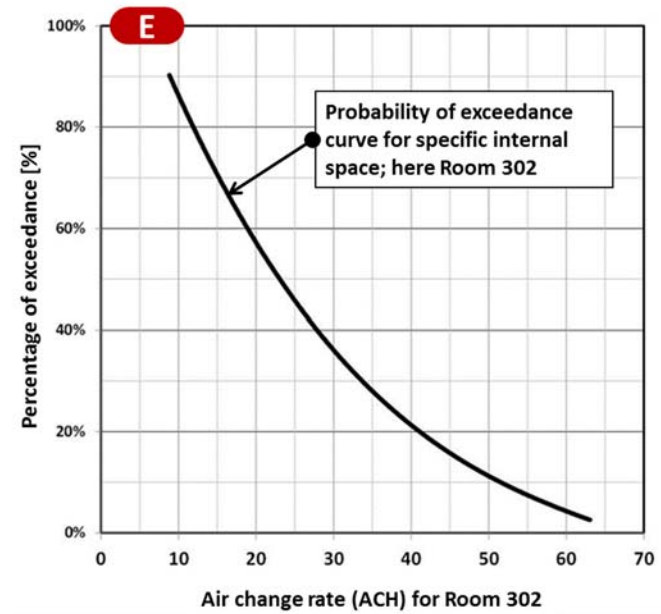
Process Step C:

For each wind approach sector, the probability distribution of wind speeds was determined.



Process Step D:

For each wind approach sector, the probability of exceedance of ACH was determined for each wind approach sector.



Process Step D:

The final probability of exceedance curve is obtained by a weighted average of the sector exceedance graphs. Weighting is done by assigning each sector an overall weight that corresponds to the sector's frequency probability in the long term wind record.

Figure 3.7.2 illustrates an example of determining the predicted air change rate for Room 302. A probability of exceedance of 75% corresponds to 14 air changes per hour (ACH).

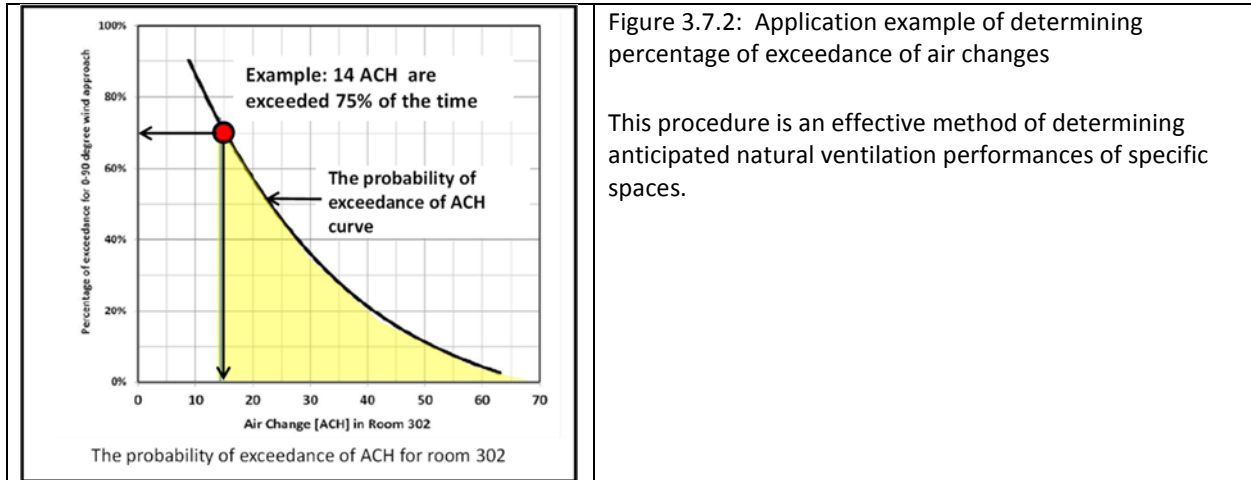


Figure 3.7.2: Application example of determining percentage of exceedance of air changes

This procedure is an effective method of determining anticipated natural ventilation performances of specific spaces.

A workflow to predict exceedance rates of air changes per hour (ACH) was developed during the studies and benchmarked using one classroom and one test scenario. The procedure included CFD calculations of unit responses, which were ACH values as a function of wind approach direction and wind approach speed. The unit response factors were determined for each wind approach sector. The unit responses were then correlated with the probability distribution long-term wind record at the site. The resulting was a graph of percentage exceedance versus air change rates (ACH), and therefore is an indicator of ventilation effectiveness based on probability of wind direction and velocities. This procedure, if more developed, can be an effective tool for the designer to assess the natural ventilation effectiveness of buildings.

SECTION 4 – SUMMARY OF PART 3

This section of the report summarizes Part 3 of the Research Project. Part 3 investigated the performance of comfort enhancement technologies, or “comfort islands” as they are referred to in this report, in unconditioned spaces. Unconditioned spaces that are not mechanically cooled or dehumidified represent challenges in regard to providing acceptable occupant comfort, especially in the hot and humid Hawaii climate.

4.1 Value Proposition of Comfort Islands

The basic premise of “comfort islands” in the context of this investigation is that significant energy can be saved by providing localized occupant comfort without fully conditioning an entire space. The typical application of comfort islands is in naturally ventilated spaces. Naturally ventilated spaces have significantly lower energy demands in comparisons to energy intensive HVAC space conditioning. The disadvantage of naturally ventilated spaces is their lack of ability to continuously provide acceptable levels of thermal comfort and space ventilation. Natural ventilation is following outdoor environmental thermal and humidity conditions, which can change significantly over time. Natural ventilation is dependent on sufficient wind movement, which represents driving forces for space ventilation, and wind is by nature intermittent.

Occupants of naturally ventilated space react differently to thermal comfort conditions than occupants of fully conditioned spaces. The approach of “adaptive comfort” correlates the level of thermal discomfort a person can tolerate to the long term exposure of the occupant to either cold or warm outdoor climate. In essence, adaptive comfort postulates that occupants living in a warm climate can tolerate higher internal operative temperatures than occupants who are used to colder climate. Depending on the site and type of building there are periods when thermal conditions in naturally ventilated spaces surpass temperatures that are deemed tolerable even under the adaptive comfort standards. If periods outside the adaptive comfort zone are occurring too often the soundness of the natural ventilation conditioning approach can be called into question. Therefore, measures to assist the natural ventilation processes and providing a satisfactory basic comfort level at all times can add significant value to reliance on natural ventilation.

Spaces with comfort islands combine advantages of conditioned and naturally ventilated spaces. They provide a certain level of comfort through energy efficient localized cooling, when natural ventilation alone cannot provide basic levels of comfort and space ventilation.

Figure 4.1.1 illustrates the main differences of naturally ventilated spaces, spaces with full mechanical cooling and ventilation and spaces with comfort islands.

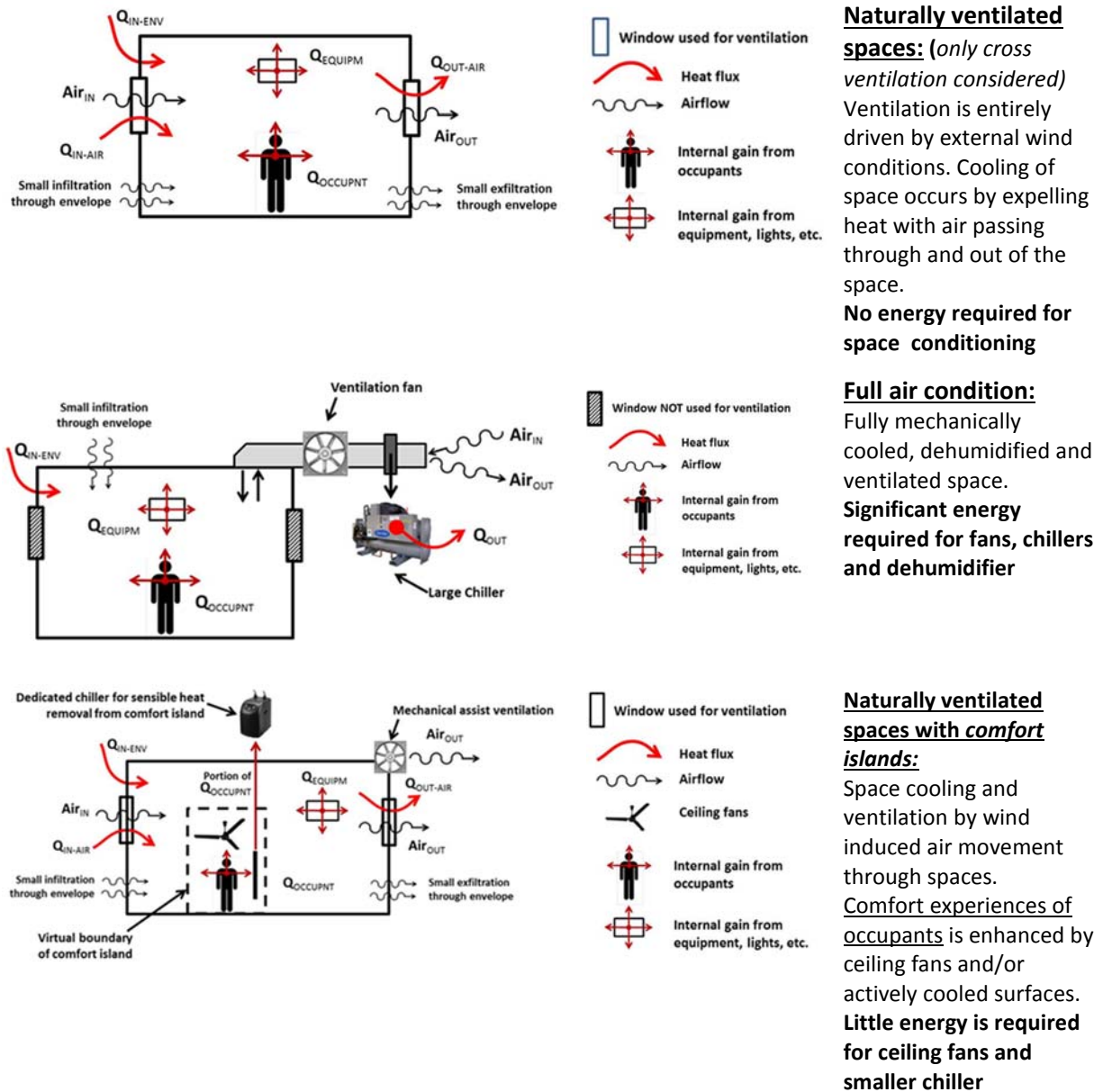


Figure 4.1.1: Description of physical processes used in comfort islands and comparison to conventional space conditioning

Table 4.1.1 shows anticipated energy savings when using comfort islands. The table compares the three modes of spaces conditioning listed in Figure 4.1.1. In addition, the table compares the mode with mechanical assist ventilation. In this latter case mechanical ventilation is operating during periods when external wind conditions are insufficient to provide sufficient ventilation.

Table 4.1.1: Projected energy savings for different types of space ventilation and cooling

Description of energy service for function of conditioning	Type of space conditioning and applied technology							
	A		B		C		D	
	Naturally ventilated space		HVAC conditioned space		Naturally ventilated space with comfort island		Naturally ventilated space with comfort island – and mechanical assist ventilation	
	Energy expenditures		Energy expenditures		Energy expenditures		Energy expenditures	
	Unit %	Overall %	Unit %	Overall %	Unit %	Overall %	Unit %	Overall %
Energy demand on level of entire space:								
Energy for space ventilation	0%	0%	100%	20%	0%	0%	35%	7%
Energy for sensible heat removal	0%	0%	100%	48%	0%	0%	0%	0%
Energy for latent heat removal	0%	0%	100%	32%	0%	0%	0%	0%
Total energy demand on space level >>>	0%		100%		0%			7%
Energy demand on level of occupant:								
Energy for sensible heat removal	N/A	N/A	N/A	N/A	35%	17%	35%	17%
Energy for latent heat removal	N/A	N/A	N/A	N/A	0%	0%	0%	0%
Total energy demand on space level >>>	0%		0%		17%			17%
Total energy used to provide comfort in space >>>	0%		100%		17%			24%
Energy saved relative to full space conditioning >>>	100%		0%		83%			76%

Note:

Unit % of energy expenditures indicates that x% of energy has to be spend relative to this specific heat removal function.
 Overall % of energy expenditures indicates that x% of energy has to be spend relative to the total energy.
 All values are relative to the energy demands of a full space conditioning.

The concept of comfort islands was investigated in this project. In comparison to full mechanical space cooling, dehumidification and ventilation the use of comfort island can potentially save up to 80% of energy to provide the occupants with acceptable comfort conditions. Conventional space conditioning focuses on providing the same comfort conditions throughout an entire space. Comfort islands in conjunction with natural ventilation provide localized comfort conditions. **The use of comfort islands is a paradigm shift from the conventional space conditioning towards more energy saving space conditioning technologies.**

4.2 Basics of Human Thermal Comfort

Thermal comfort is described as the absence of sufficient heat transfer to the environment. In warm climates, such as in Hawaii, this means that the human body cannot reject enough heat to keep the heat balance of the body within a preferable range. Since the investigations conducted under this research project are concerned with achieving thermal comfort in naturally ventilated spaces under hot and humid climate, only mechanisms of heat rejection from the human body are considered.

In warm climates the human body has to continuously lose (reject) body heat to the environment to maintain thermal equilibrium

There are several mechanisms available to the human body to regulate body temperature within an acceptable range and reject heat to the outside environment. Figure 4.2.1 illustrates the four main mechanisms that are relevant to the present investigations.

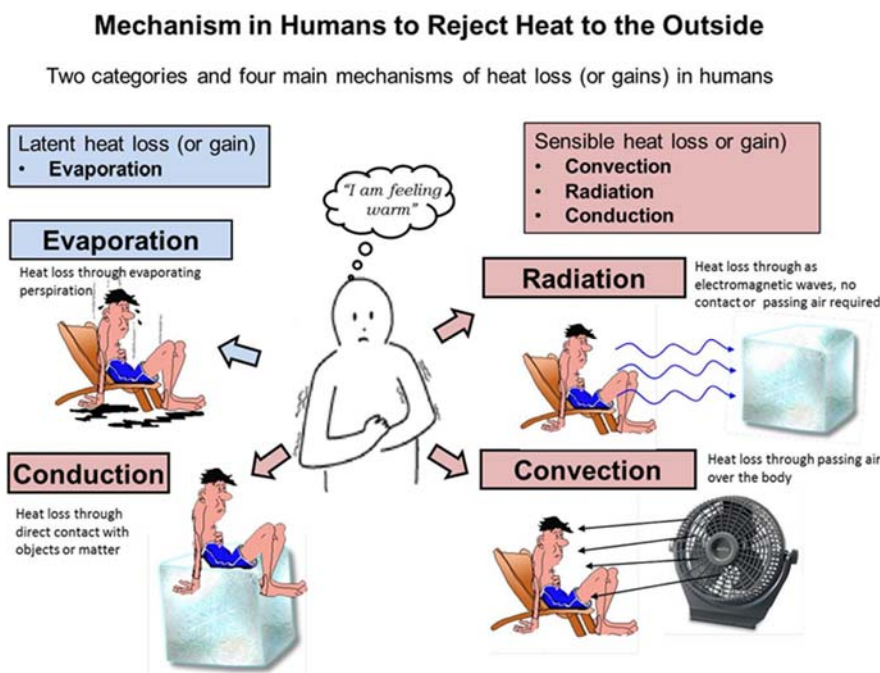


Table 4.2.1: Four main mechanisms of how the human body rejects heat to the outside environment

The two main categories of heat loss are sensible and latent heat loss. Sensible refers to changes in heat that we can “sense” such as measuring with a thermometer. This means the loss of heat energy goes hand-in-hand with a drop in temperature of an object that rejects heat. In latent heat loss the temperature of the object does not change since heat is used to initiate a phase change of water, e.g. evaporation of perspiration from the surface of the body.

Sensible heat loss mechanisms include convection, radiation and conduction and latent heat loss is evaporation. For all sensible heat loss processes the heat always flows from the warmer to the colder objects. The heat transfer rate is a function of the temperature difference between the body and the ambient air.

Sensible heat loss through convection: Under this process air is passing over the skin and heat is transferred to the passing air. The colder the air the more heat can be rejected from the body to the outside. The faster the air passes by the skin, even at the same air temperature, the more heat can be transferred, since the film resistance around the skin is reduced by the higher air speed.

Sensible heat loss through radiation: Under this process the body radiates heat energy to colder adjacent objects. The heat loss occurs through electromagnetic waves, the body basically “lights” up objects which have a lower surface temperature. The objects and body which exchange radiant heat must be in line of sight to each other. The rate of heat radiated to objects depends on the value of temperature difference between the body and the receiving objects, the relative orientation of the body and object, and the size of the object. It is important to remember that radiative heat loss happens at the speed of light (e.g. the speed of electromagnetic waves).

Sensible heat loss through conduction: Under this process the body losses heat energy through direct contact with a colder object or matter, which can be solid, liquid or gaseous. The rate of heat energy exchanged between the body and colder objects depends on the temperature difference and the overall resistance of materials to the conduction of heat through it.

Latent heat loss through evaporation: Under this process the body losses heat energy through evaporating water on the skin. The rate of heat loss is dependent on the amount of water that is evaporated, which in turn is dependent on the relative humidity of the ambient air and other factors such as air speed over the skin. Increased air speed significantly increases the amount of evaporation.

The experience of thermal comfort occurs on the individual level and two occupants in a room with the same thermal conditions might feel different thermal sensations. Standards have been developed to provide objective criteria of how a human will most likely experience thermal comfort. All of the relevant standards use six physics parameters that describe the predicted comfort level and provide a quantitative description. Figure 4.2.2 illustrates the six physical parameters. The parameters are furthermore discussed in the following:

Air temperature: Air temperature regulates a significant portion of convective and conductive heat transfer processes. The driving force for sensible heat loss is the difference between the skin temperature and the ambient air temperature. Air temperature is measured by conventional dry bulb temperature.

Radiant temperature: This is the temperature of surfaces of objects to which the human body rejects heat through electromagnetic waves, e.g. through radiation. The total amount of heat that is lost

through radiation from the human body is the sum of radiant heat loss to all relevant objects within the line of sight of the human body. In order to make the analysis easier the term “mean radiant temperature” (MRT) has been defined, which is the aggregated sum of radiant heat flux from objects that affect the body through radiant heat loss. The mean radiant temperature can be determined through a so-called “globe thermometer”.

Operative Temperature: Operative temperature is an expression that combines air and radiant temperature into one metric. Operative temperature is quantified as the weighted average of air and radiant temperature. When values of air and radiant temperatures do not deviate significantly, the operative temperature is the simple statistical mean of the air and radiant temperatures.

Metabolic rate: Metabolic rate, as it related to human comfort assessment, is the level of transformation of chemical energy into heat and mechanical work by metabolic activities within the human body. Metabolic rate is defined in “met” units, with 1 met being the rate generated by a sitting person at rest. Tables are available that provide met units for different activities. Examples are sleep and light office work as 0.7 met and 1.2 met, respectively.

Clothing insulation: Clothing insulation is the amount of thermal insulation created by clothing worn by a person. The value of clothing insulation is expressed in “clo” unit and can be determined by adding the value of any particular clothing worn by a person.

Relative humidity: Relative humidity (RH) is expressed as the ratio of the amount of water vapor in the air to the amount of water vapor at saturation pressure of air at the specific temperature and pressure. Relative humidity has significance to human comfort in a range of processes, such as impeded ability to reject heat through evaporation at higher RH values or feeling of itchiness and impacts on the respiratory system at very low RH values. RH is measured as a percentage.

Air speed: air speed is expressed as the average speed of air measured at points of reference. Higher air speed can lower the perceived temperature, enabling the set point in air conditioned spaces to be increased without the loss of comfort or raising acceptability limit for naturally ventilated spaces.

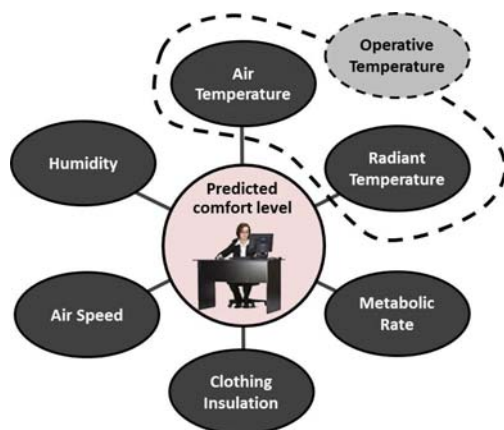


Figure 4.2.1: Six main parameters to assess thermal comfort levels

Human thermal comfort in internal spaces can be predicted statistically by using main comfort parameters and applying them to comfort standards. The result of predicted comfort suggests that a certain percentage of occupants will experience satisfaction with the thermal environment.

These six main parameters are used in conventional space conditioning to quantify thermal comfort levels. The thermal comfort standard used in these investigations is the so-called Predicted Mean Vote (PMV) index.

For naturally ventilated spaces another comfort standard, the so-called adaptive comfort index, was developed. The basic premise of adaptive comfort is that thermal comfort sensation is affected by prevailing outdoor temperatures. For prevailing hot weather this means that humans have a better predisposition for warmer indoor temperatures.

Figure 4.2.2 illustrates the use of adaptive comfort. Comfort level is determined by the prevailing mean outdoor temperature (for period of 7 to 30 days prior) and internal operative temperature. Increased air speed also affects comfort and allows higher operative temperatures on the basis of the cooling effect of air passing over the body. Figure 4.2.2 indicates the resulting comfort by a red pointer. When the pointer is inside the colored band thermal conditions complies with ASHRAE 55, which is the applicable comfort standard. The series of three images (A), (B) and (C) in the Figure 4.2.2 show the dependency of thermal comfort sensation on the mean air speed. Higher air speed increases the allowable operative temperatures band, by pushing the colored compliance band upwards, and therefore results in compliances at higher operative temperatures.

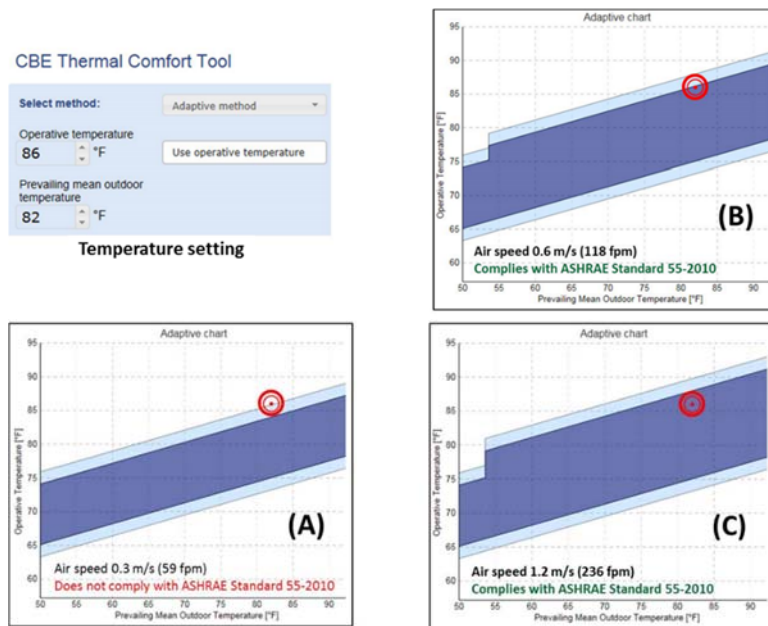


Figure 4.2.2: Adaptive comfort method – dependency on air speed to achieve code compliance (CBE adaptive comfort assessment tool)

Temperature setting: The prevailing mean outdoor temperature and the indoor operative temperature determine the resulting adaptive comfort level. The temperatures used in example (A) indicate that adaptive comfort level does not comply; here air speed 0.3 m/sec is used, which is a threshold below which air movement is considered not existing. Applying 0.6 m/sec (B) and 1.2 m/sec (C) of air movement past the body shifts the acceptance limits upwards and therefore adaptive comfort standards are met.

4.3 Scope of Work in Part 3 of the Research Project

The scope of work under Part 3 of the Research Project is illustrated in Figure 4.3.1. The work was divided into experimental and CFD simulation work. The primary objectives of experimental work under Part 3 differed from Parts 1 and 2 of the Research Project. In Parts 1 and 2 the experimental work was carried out mainly for validation of CFD simulation results. The experimental work under Part 3 was a stand-alone investigation. Some of the results, however, were also used for validation of CFD results.

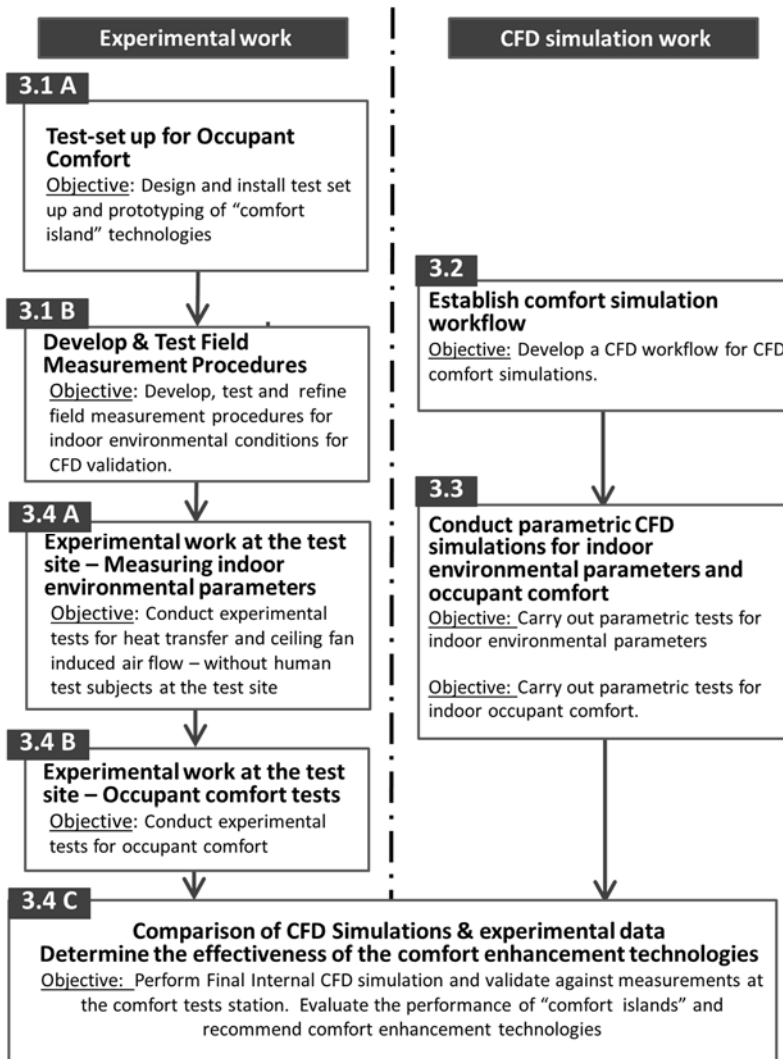


Figure 4.3.1: Scope of work performed under Part 3 of the Research Project

The experimental portion of Part 3 used a comfort test set-up which was specifically designed and installed for the project. The experiments included investigations of thermal performance of comfort enhancement technologies as well as comfort tests with human test subjects.

The CFD simulation work was performed in parallel to the experimental work. The work included the development of a generic workflow for comfort simulations.

The project work used **two comfort enhancement technologies** which can improve comfort levels in naturally ventilated buildings. The two technologies tested were:

1. **Install a ceiling fan** to provide a range of locally increased air velocities. The ceiling fan was a high performance fan with a range of fan speed velocities. The ceiling fan had the capacity to provide a “gentle shower” of air at a low fan speed.
2. Install **radiant cooling panels** that are actively cooled to a range of temperatures.

4.4 Test-set up for Occupant Comfort

The comfort test set-up was installed in Room HIG 204, which was temporarily converted to a “comfort station”. Room 204 is a windowless space that has one door to the exterior. The room configuration prior to the conversion into the comfort chamber is depicted in Figures 4.4.1. The room was rearranged to make space for the test set-up, which included two test desks that were separated by a textile covered room divider. The layout of the test site is shown in Figure 4.4.2.

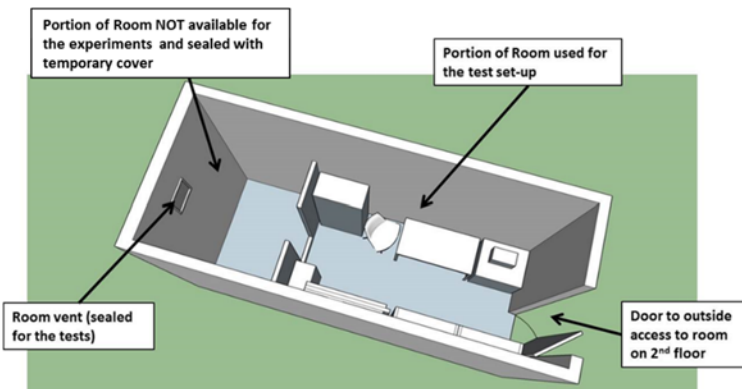


Figure 4.4.1: Room configuration of Room HIG 204 prior to tests

The room HIG 204 is an overflow office which is also used as a document storage room. The room was converted to a “comfort chamber for the duration of the tests

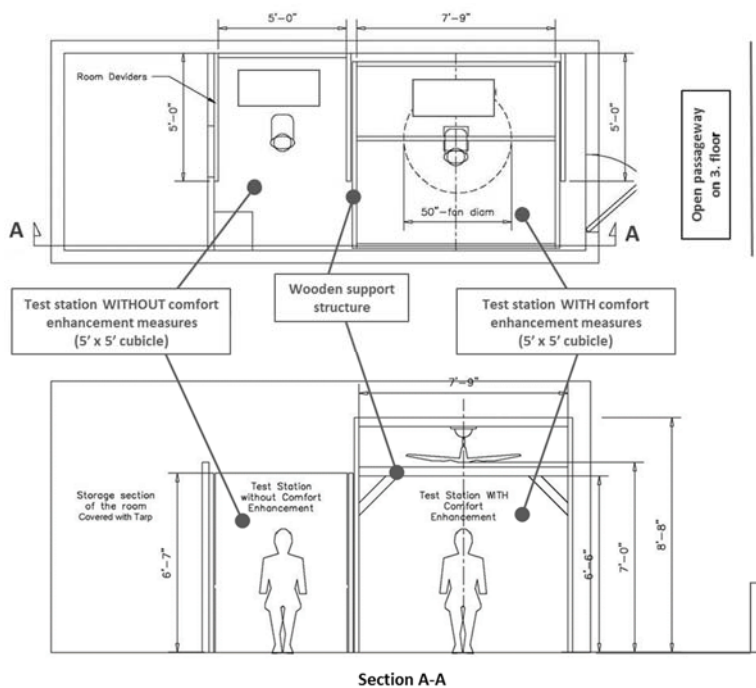


Figure 4.4.2: Layout of the test set-up in HIG 204

The room was equipped with two work spaces with one desk each, divided by a 6-foot high cubicle wall.

One work space (test station) DID HAVE and the other (control station) DID NOT HAVE comfort enhancement measures installed.

The wooden structure supported the following test equipment:

- A 50-inch ceiling fan installed on a cross beam
- An array of 10 actively cooled radiant cooling panels that were hung from the horizontal beams by means of support wires for vertical adjustment.
- Chilled water piping system to cool the radiant panels

Actively radiant cooling panels have not been used as comfort enhancement measures in unconditioned spaces. Due to high humidity levels in the unconditioned test space, the radiant panels had to be operated at relative high temperatures to avoid condensation on the panels and chilled water supply pipes. Two panel type were tested in initial scoping tests, one was a gypsum panel with Phase Change Material (PCM) and the other was a conventional aluminum radiant panel which is used in radiant cooling installations. The PCM panel has the important benefit of a high thermal mass, which can be used for energy saving night flushing cooling, when cooler air is passed through the space removing heat that builds up during daily operation.

Figures 4.4.3 and 4.4.4 show the two types of radiant panels which were tested in initial scoping test for their thermal performance.

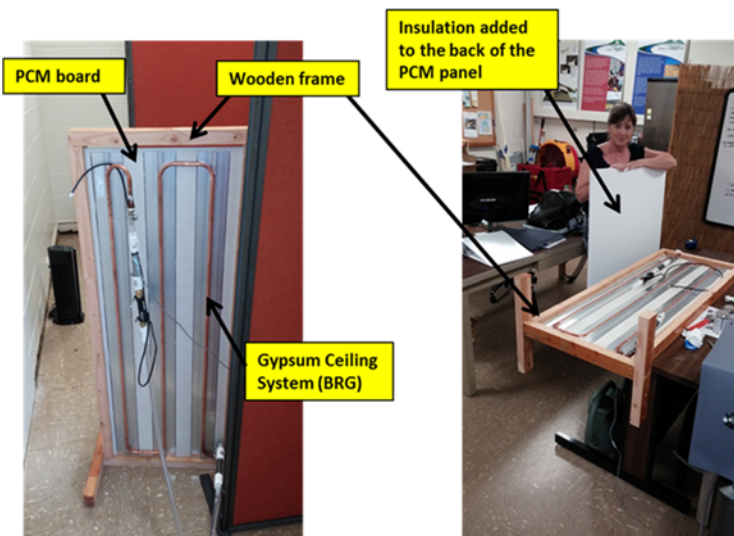


Figure 4.4.3: Completed PCM panel assembly.

A 2 x 4 feet PCM gypsum board was mounted on a wooden frame. The backside of the PCM gypsum board was equipped with a heat rejection rail (copper tubing meander) that was glued to the PCM board. Chilled water was pumped through the copper tubes. The chilled water transported heat away from the PCM board, cooling it.

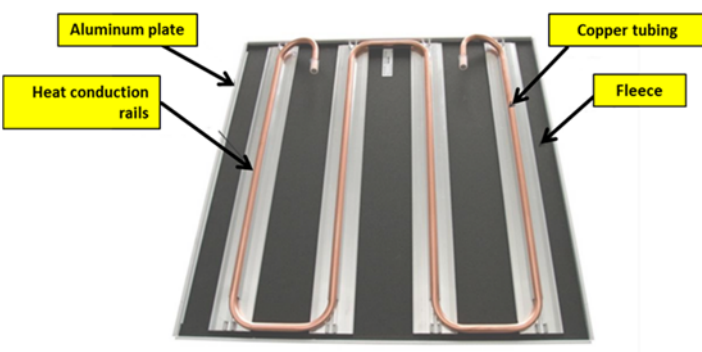
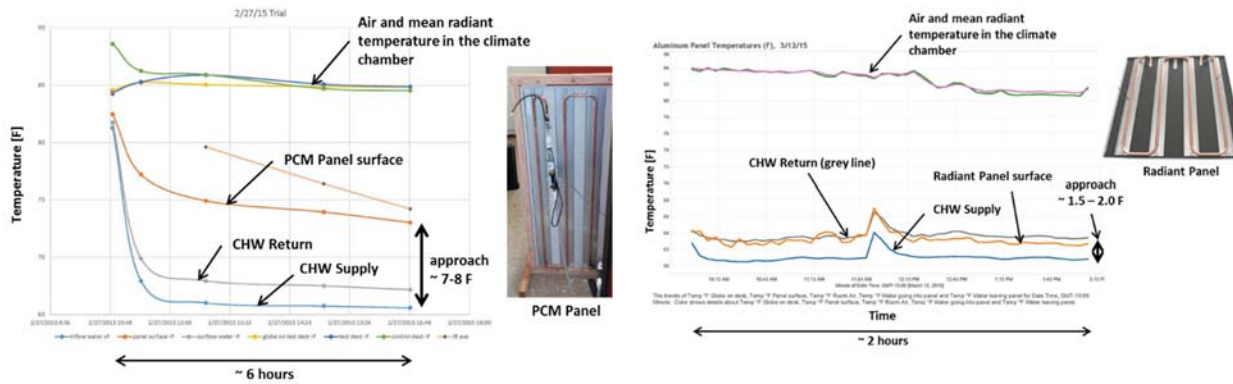


Figure 4.4.4: conventional aluminum radiant panel

Chilled water was pumped through the copper tubing meander to cool the panel. The picture does not show the Styrofoam insulation on the back of the panel.

The thermal performance scoping tests revealed that the PCM had a too high approach temperature to make it a viable option for the radiant panels. Approach temperature is the temperature difference between the panel front surface and the chilled water temperature. The PCM panel had an 8 F approach temperature and the aluminum radiant panels 2 F, respectively. Since the target radiant panel surface

temperature was around 70 F the high approach temperature of the PCM panels required chilled water temperatures of 62 F. This created significant condensation problems. The aluminum panels on the other hand could be operated with 68 F chilled water, which lowered condensation impacts to acceptable levels. Figure 4.4.5 shows the thermal responses of both types of panels.



Thermal response of PCM panel during scoping tests

Thermal response of radiant (aluminum) panel during scoping tests

Figure 4.4.5: Thermal performance of two types of radiant panels tests in the scoping tests

Figures 4.4.6 through 4.4.8 show the test set-up with the comfort enhancement measures of radiant panels and ceiling fan.

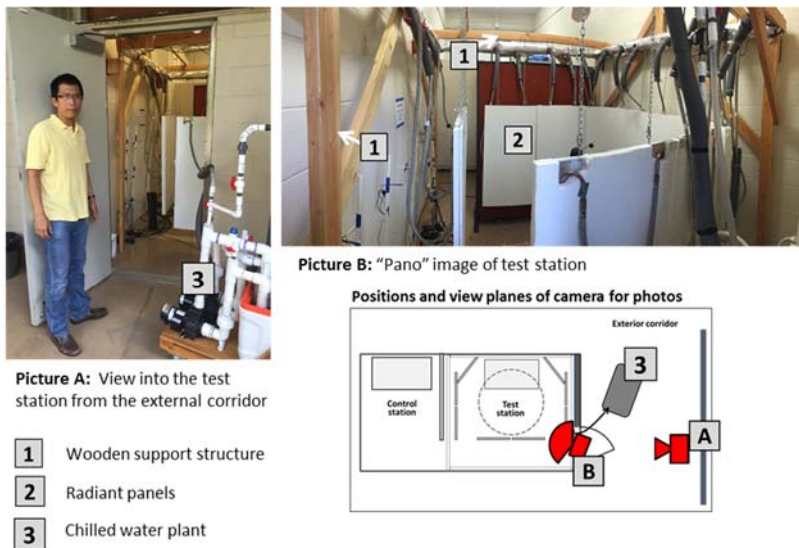


Figure 4.4.6: Test set-up in and outside room HIG 204

Picture A shows a view from the outside of room HIG 204. A small chilled water plant (3) was placed outside the room and the chilled water was pumped into the room

Picture B shows a view from inside the room. The radiant panels (2) were suspended from a wooden support structure

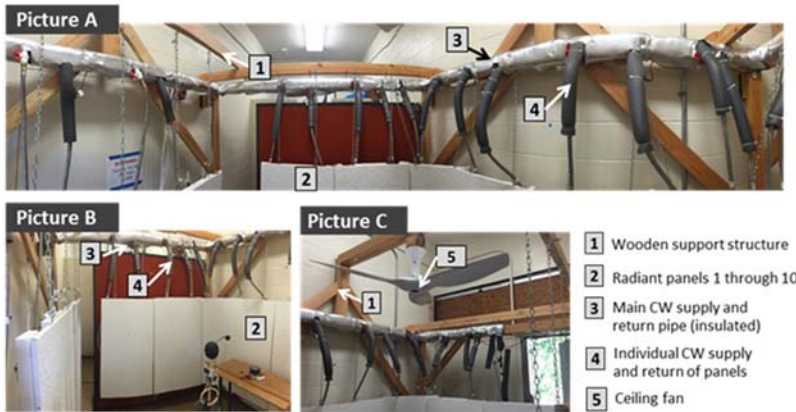


Figure 4.4.6: Test set-up in room HIG 204

Pictures A and B show radiant panels with chilled water system
Picture C shows ceiling fan installed on the wooden support frame

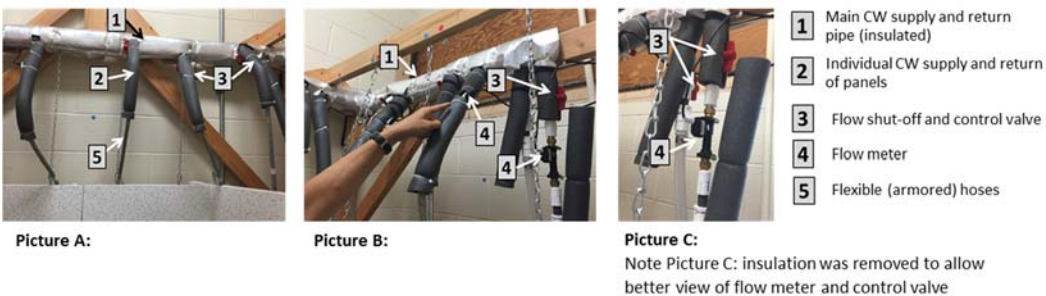
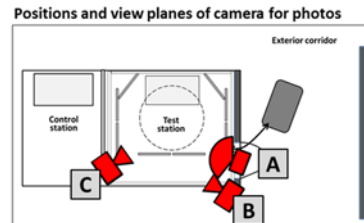


Figure 4.4.8: Test set-up in room HIG 204 – the chilled water pipes inside the comfort chamber were insulated. Each panel was individually flow controlled (valve) and instrumented (flow and temperature sensor)

The chilled water supply for the actively cooled radiant panels was generated by a chilled water plant that operated outside the comfort chamber. The chilled water supply was pumped into the comfort chamber. The heat sink of the chilled water plant was a conventional AC-window unit, which cooled the water by means of an air-to-water heat exchanger. An insulated tank served as a chilled water reservoir. Figure 4.4.9 shows the basic flow diagram of the chilled water system, which was used in the comfort tests. The comfort test set-up was instrumented with 62 sensors which measured the following environmental and equipment parameters.

1. Air temperature in room
2. Relative Humidity in room
3. Contact temperature (for chilled water pipe and panel surface temperature)
4. Flow sensor - for chilled water flow
5. IR temperature probe – for assessment of surface radiant temperatures of objects
6. Hot wire anemometer – to measure air velocities generated by the ceiling fan
7. Hand held anemometer – to make spot checks for air velocities
8. Carbon dioxide level to detect ventilation needs of the climate chamber

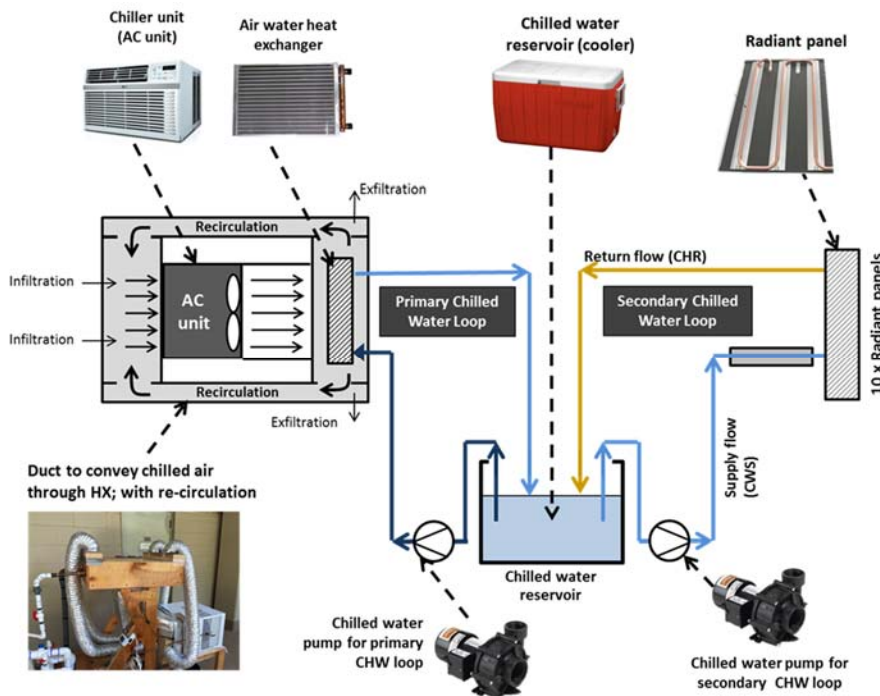


Figure 4.4.9: Basic flow diagram of the chilled water system

The chilled water system was divided into two loops, the primary and secondary chilled water loop. In the primary loop the water in the chilled water reservoir was continuously cycled through the AC unit, where heat was extracted. In the secondary loop, the chilled water was pumped from the reservoir to the actively chilled radiant panels inside the comfort chamber.

For the experimental work of Part 3 a tests set-up was used that was specifically designed, built and installed for this project. The test set-up created a “comfort chamber” inside a temporarily converted office space. The test set-up had two work spaces where human test subjects were sitting during comfort tests. One of the work spaces was equipped with comfort enhancement measures.

4.5 Generic CFD Workflow for Comfort Assessment

The development of a specific workflow for comfort simulations was necessary since the CFD software used for the Research Project did not have specific comfort assessment subroutines available. For the development of the generic comfort workflow the research team considered the following guidelines:

- The development and testing of a CFD simulation process used reasonable simplification of the computational process in order to make effective use of ERDL’s computational resources, yet produce quality simulation results that could be validated with the ERDL comfort test set up.
- A review of existing CFD approaches to model comfort levels in small spaces was conducted. The review suggested that many numerical prediction applications were concerned with predicting the comfort level in automobile and aerospace. The research team decided to develop a generic comfort simulation approach based on a combination of the common PMV comfort model, and

adding simulation CFD simulation routines. The commonly used PMV analytical model is based on steady state and uniform (or averaged) thermal condition of the surrounding environment.

- The experimental approach of the ERDL test set-up was based on using steady state values that were averaged over the whole body and included environmental and personal (of the test subject) conditions. Creating a whole body averaged thermal losses and an average description of the flow field adjacent to the human body was, however, a simplification of the numerical comfort prediction. The available ERDL instrumentation precludes the measurement of different body parts of the human test subject or an instrumented manikin and instead used averaged thermal parameters.
- The comfort simulation approach developed for this project considered sensible convective and radiative heat losses. The procedure was unique for the investigation of the effectiveness of the “comfort island” approach. The comfort island approach is based in increasing convective heat loss through ceiling fans and radiative heat loss through actively cooled panels, which are placed in close proximity to the human occupant.
- The research team benchmarked comfort simulation workflow against a PMV analytical model and concluded good data consistency of simulations results. Simulations were based on simplified boundary conditions and averaged environmental properties which were also typical for the PMV approach. These simplifications included uniform distributed temperatures of air and radiant surfaces. In the experimental tests of the ERDL comfort chamber, air and radiant surface temperatures were non-uniform.

A process diagram showing comfort simulation workflow developed for these investigations is depicted in Figure 4.5.1. The sequential steps are explained in the following:

- Step 1: An initial CFD simulation run was carried out to predict mean air temperature of the comfort chamber and mean air velocity close to the body, and mean radiant temperature from objects with direct line of sight to the body.
- Step 2: The analytical procedure of the PMCV model was carried out using the personal thermal parameters are used, including M metabolic rate (refer to Appendix F), W mechanical work (assumed as 0 w/m² for sedentary activity), skin area (assumed as an average 1.8m²), Clo clothing thermal insulation depending on clothing ensembles worn by the test objects (refer to Appendix G) as well as environmental parameters obtained from the initial CFD simulation run.
- Step 3: The skin temperature and clothing temperature considered for the test subject was used as boundary condition inputs for the virtual manikin’s surface of the final CFD simulation run.

Step 4: Four latent heat loss components, calculated from the PMV analytical calculation in Step 2, and two sensible heat loss components, convection C and Radiation R from CFD simulation in Step 3, were used to determine the PMV index.

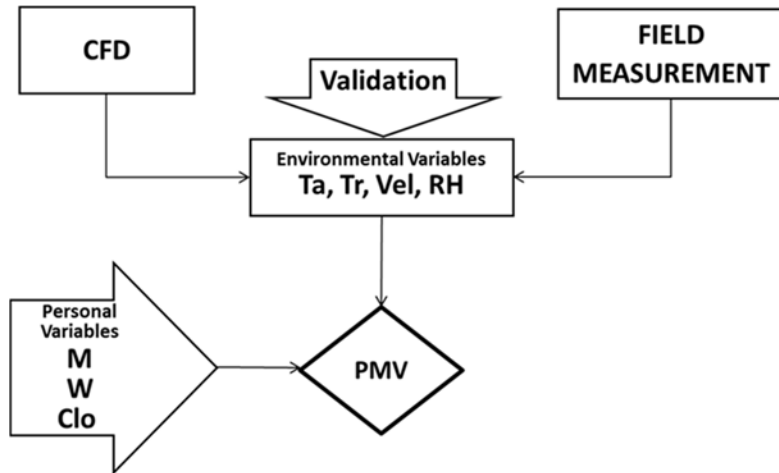


Figure 4.5.1: Basic flow diagram of comfort simulation workflow

Workflow of linking PMV and CFD approach.

CFD models and meshing used to carry out the simulations are depicted in Figure 4.5.2 and 4.5.3.

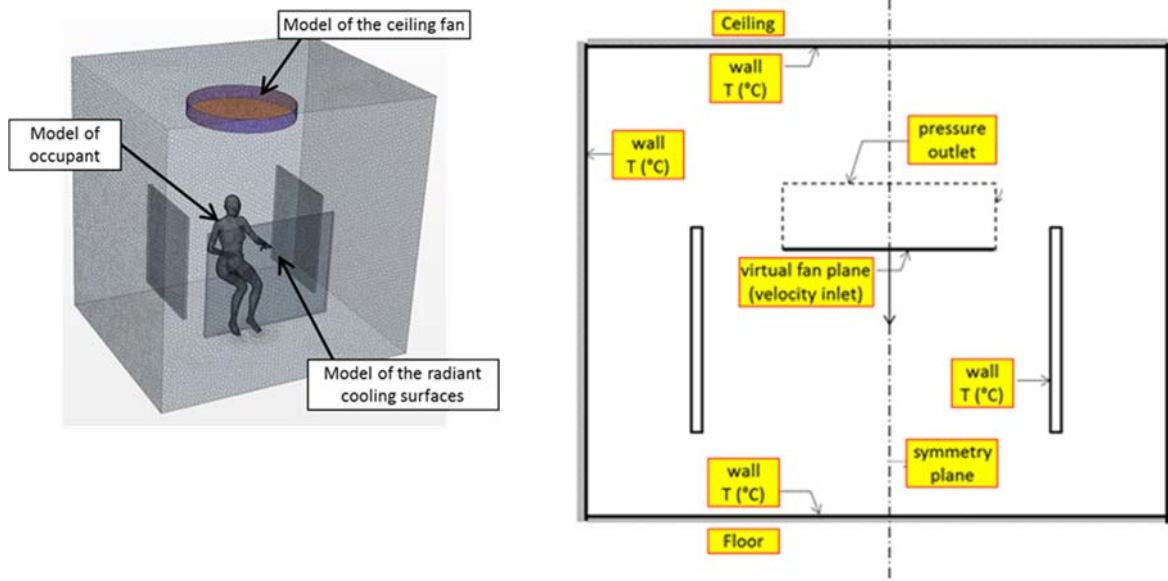


Figure 4.5.2: CFD Model and boundary conditions used to simulate thermal performance of the test set up

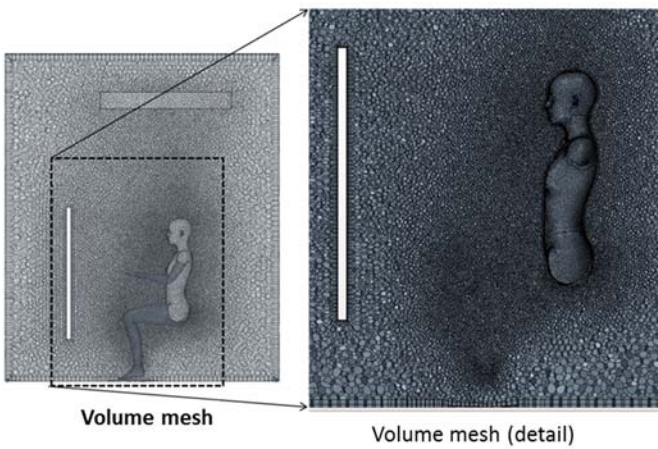


Figure 4.5.3: CFD volume mesh

3D virtual manikin model was split into 16 different parts to individually investigate parts of the body, such as called heat, torso, etc.

A sample of **qualitative results**, which means visualizations of the results, obtained from the CFD simulations are depicted in Figure 4.5.4 through 4.5.6.

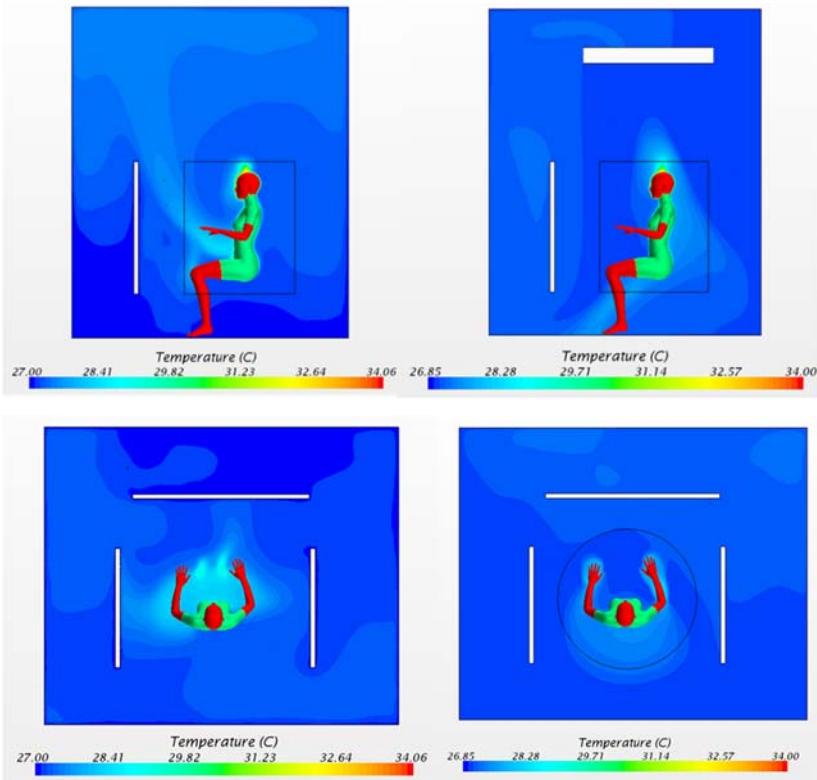


Figure 4.5.4: Visualization examples of temperature contours

Temperature contour map at **vertical** cross section plane when ceiling fan is off (left) and on (right)

Temperature contour map at **horizontal** section plane at 1m above the floor plane when ceiling fan is off (left) and on (right)

SECTION 4 - SUMMARY OF PHASE 3

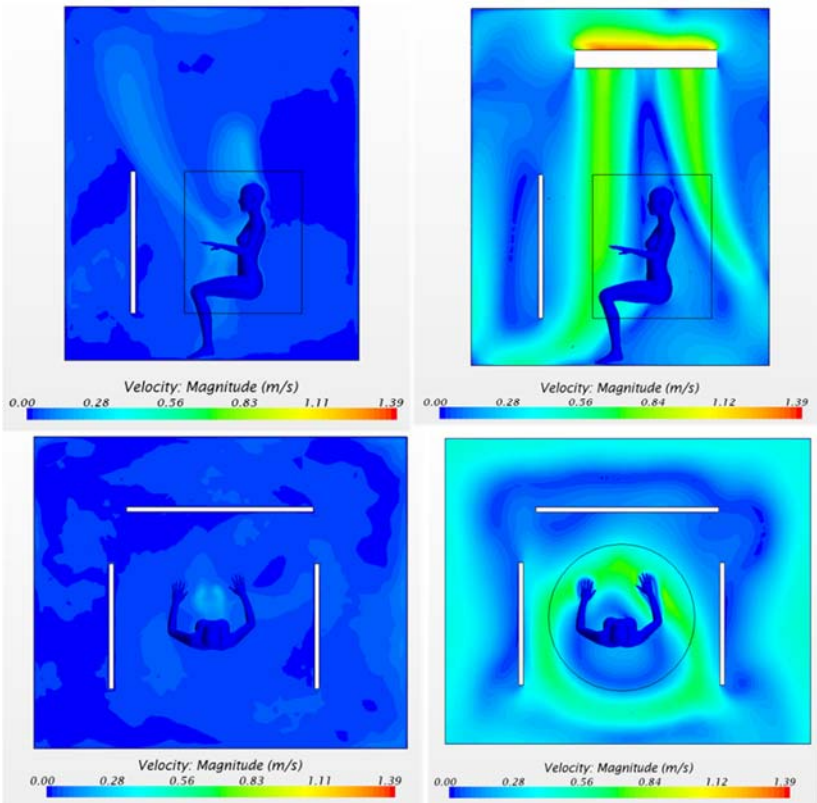


Figure 4.5.5: Visualization examples of air velocity contours

Air velocity contour map at **vertical cross section** plane when ceiling fan is off (left) and on (right)

Air velocity contour map at **horizontal section** plane at 1m above the floor plane when ceiling fan is off (left) and on (right)

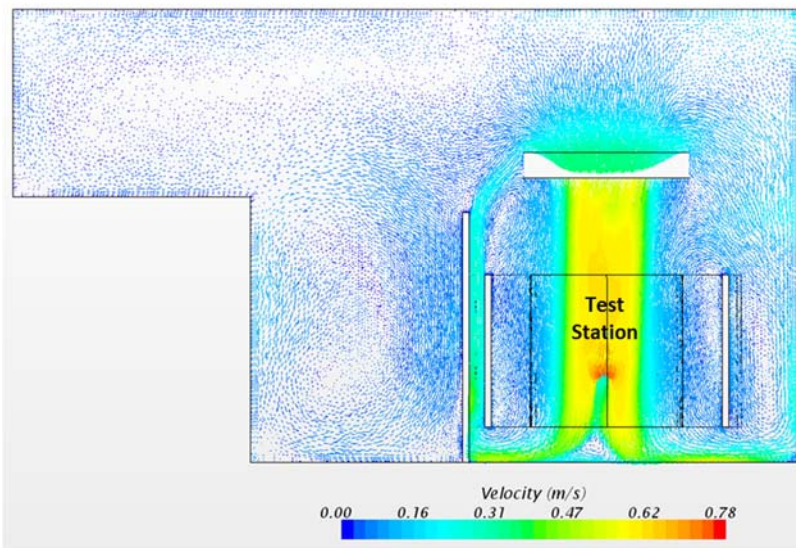


Figure 4.5.6: Visualization examples of air velocity streamlines

Qualitative results were obtained by placing a 3D-array of virtual probes around the manikin CFD model. Figure 4.5.7 illustrates the 3D-array as a 10x10x10 virtual probes matrix. The virtual sensors extract values at the designated locations in the computational grid. Individual values were then used to determine the representative average values. Main verification results are presented in Tables 4.5.1.

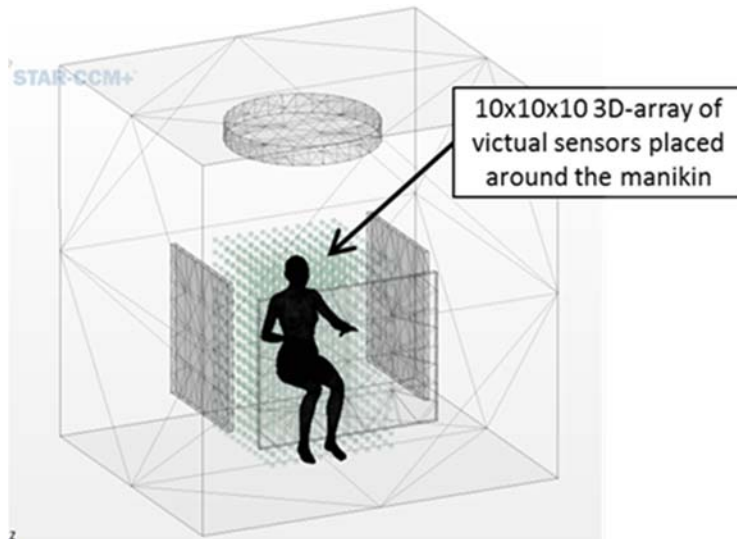


Figure 4.5.7: Array of virtual sensors used to extract localized values from the CFD solution

The green points represent the locations of the virtual sensors of the 3D-array.

The array of virtual probes is also referred to as a “presentation grid”.

	Scenario 1		Scenario 2	
	Convective heat transfer C (w)	Radiative heat transfer R (w)	Convective heat transfer C (w)	Radiative heat transfer R (w)
CFD approach	25.82	32.33	49.87	28.97
PMV analytical approach	25.70	33.70	43.06	28.33
Discrepancy	0.46%	-4.07%	15.81%	2.27%

Table 4.5.1: Validation of thermal performance convective

Comparison of convective heat transfer and radiative heat transfer between two approaches: CFD vs. PMV analytical approach: **Scenario 1 ceiling fan OFF, Scenario 2 ceiling fan ON**

The resulting errors between the two theoretical approaches CFD and PMV indicates only small data discrepancies.

Results of the development of the generic comfort simulation workflow suggested stable simulation performance. For CFD modelling the air movement induced by the ceiling fan a simplification was used in form of a cylinder, whose bottom face was defined as a velocity inlet with a discharge vector field. The vector field had rotational symmetry and was based on air velocity measurements downstream of the ceiling fan. The qualitative results by color contour visualizations indicated the temperature distribution and air flow patterns adjacent to the virtual manikin. Qualitative results suggest good verification results when comparing the CFD and PMV processes.

4.6 Air Flow Measurements Around Person

The assessment of comfort level on the basis of either the PMV or adaptive comfort requires the knowledge of the representative ceiling fan induced air velocity around the human test subject. This section describes the methodology and results of these air speed measurements.

The air velocities were measured with two types of anemometers, the Accusense F-900 (F-900) hot wire anemometer and the GrayWolf DirectSense AS-201 hotwire anemometer (DirectSense). Two F-900 sensors were rigidly installed and the single DirectSense was hand held. Figure 4.6. shows the location of the air velocity measurements.

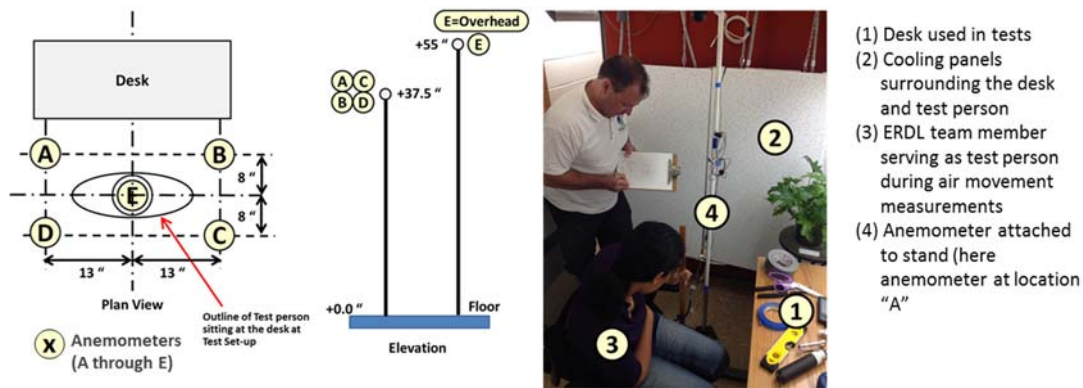
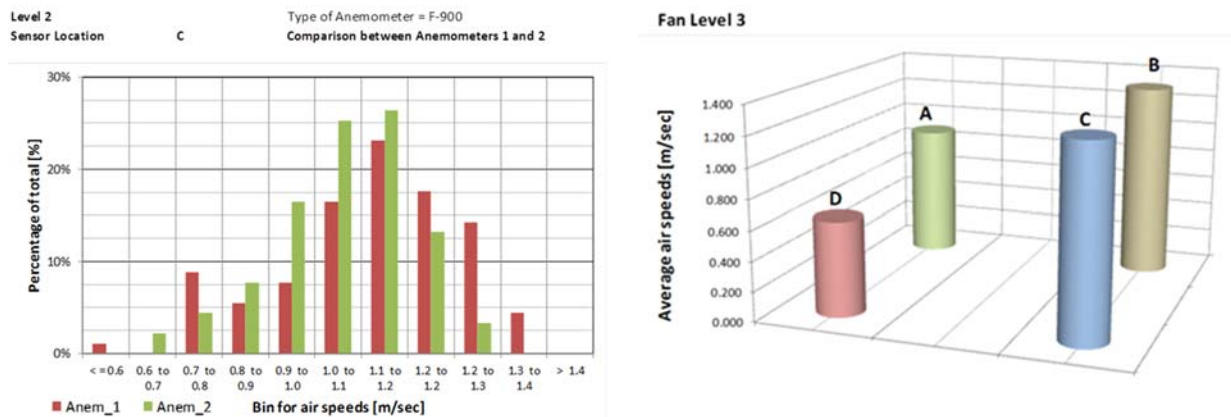


Figure 4.6.1: Measurements locations of air speed measurement around a test subject

Results of the air movement tests are shown in Figure 4.6.2 through 4.6.4. Figure 4.6.2 shows the probability density functions of air speeds (left) and the spatial distribution of air velocities (right).



Example of probability density functions of air speeds measured with two F-900 anemometers (air speed ranges were assigned probability frequency)

Spatial distribution of measured air speeds. The spatial distribution indicates a non-uniform distribution

Figure 4.6.2: Results of air speed measurements – examples of frequency and spatial distribution

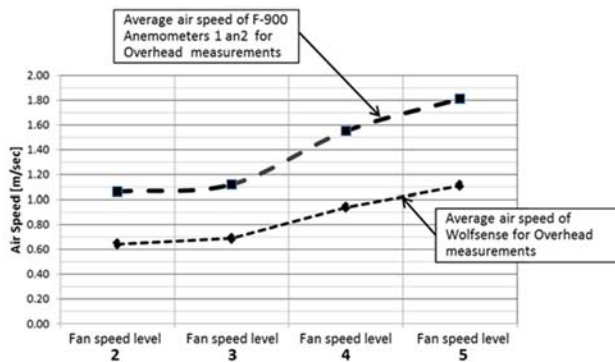


Figure 4.6.3: Comparison between overhead averages of F-900 and Graywolf DirectSense anemometers

The DirectSense results showed a systematic lower air speed than the two F-900 anemometers. The table below shows that there was a nearly constant factor between the measured data of the two F-900s and the DirectSense. The average factor was **1.64**.

	F-900 Overhead m/sec	Wolfsense Overhead m/sec	Factor [-]	adjusted wolfsense m/sec
Level 2	1.06	0.64	1.65	1.06
Level 3	1.12	0.69	1.63	1.13
Level 4	1.55	0.94	1.65	1.54
Level 5	1.81	1.11	1.63	1.82
			1.64	

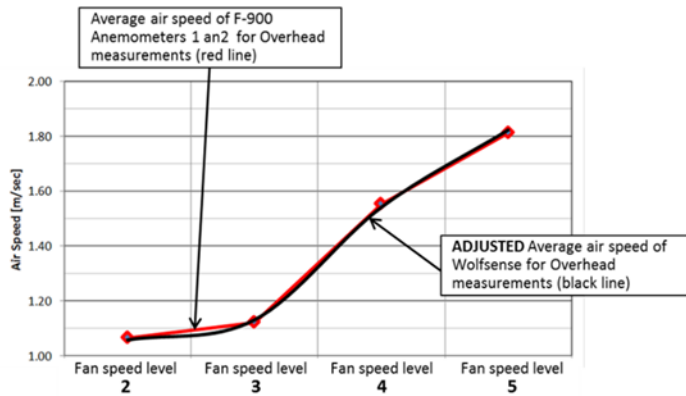


Figure 4.6.4: Adjusted overhead averages of F-900 and DirectSense anemometers

DirectSense results were adjusted by the factor 1.64. The resulting data of both anemometers were basically identically. The resulting air speeds for the fan speed level 2 and 3 were 1.05 and 1.14 m/sec, respectively.

F900 anemometer

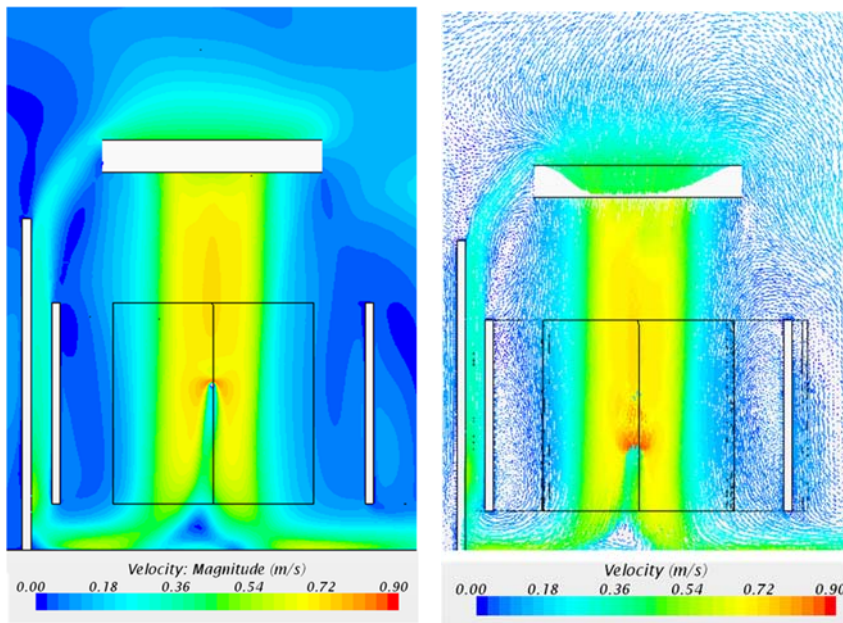
Fan level	Overhead [m/sec]	average A to D [m/sec]	Resulting [m/sec]
Level 2	1.06	1.03	1.05
Level 3	1.12	1.16	1.14
Level 4	1.55		
Level 5	1.81		

Ceiling fan induced air speeds around a test subject were measured. These air speeds were used in the subsequent comfort tests. The Graywolf DirectSense anemometer showed a consistent under presentation of air speeds. Adjustment of DirectSense measurements with a constant factor resulted in good data consistency.

4.7 CFD and Experimental Investigation of Air Movement without Test Subjects

Initial investigations of ceiling fan induced air movements at the test set-up were performed without the presence of human test subjects. The CFD simulations were validated by experimental data.

The visual representation of CFD air movement simulations are shown in Figure 4.7.1. Figure 4.7.2 shows the 3D presentation grid, a 7x7x7 point matrix, which extracted localized air velocities from the computational domain. Figures 4.7.3 and 4.7.4 show the methodology of the actual air speed measurements. Figures 4.7.5 and 4.7.6 show results of experimental data and the good comparison of CFD predictions and actual measurements.



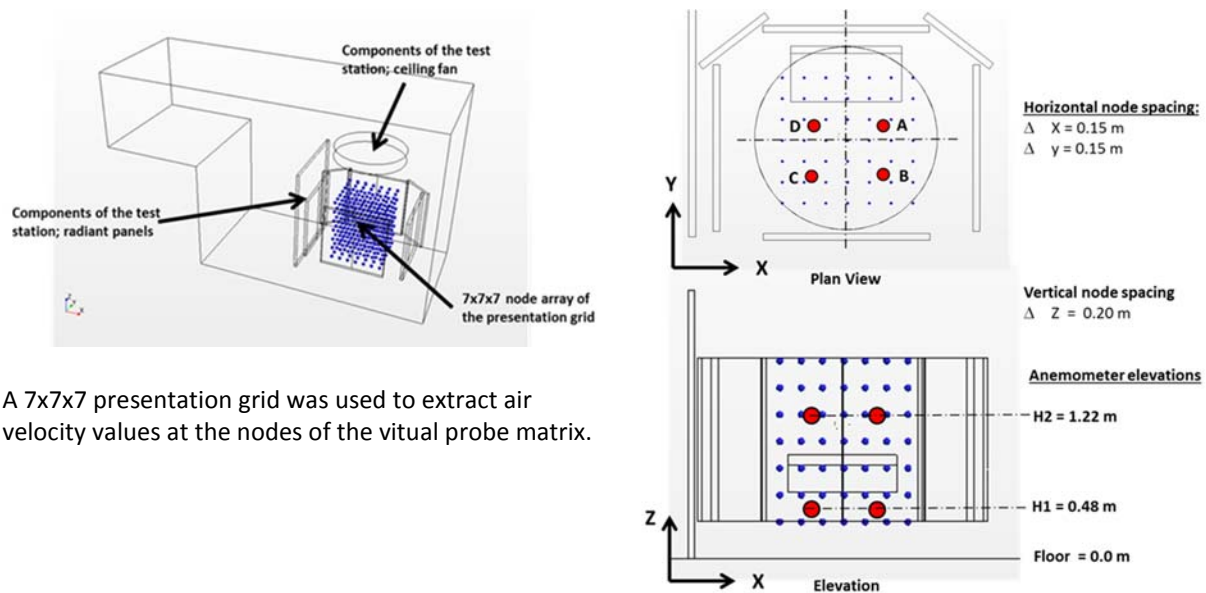
Velocity profile – contour map

Velocity profile – contour map with streamlines

Figure 4.7.1: Example of visual representation of CFD air speed simulation

The image shows the air velocity distribution at the central section of the test station. In the CFD simulation the ceiling fan is approximated as a cylinder, whose bottom face induces an air vector field which had a rotational symmetry.

The air flow discontinuity in the center of the flow field is a result of the globe thermometer geometry in the CFD model.



A 7x7x7 presentation grid was used to extract air velocity values at the nodes of the virtual probe matrix.

Figure 4.7.2 : 7x7x7 presentation grid for data extraction of CFD air speed simulations (left) 3D-view of the presentation grid, (right) locations of the actual anemometers superimposed on the presentation grid

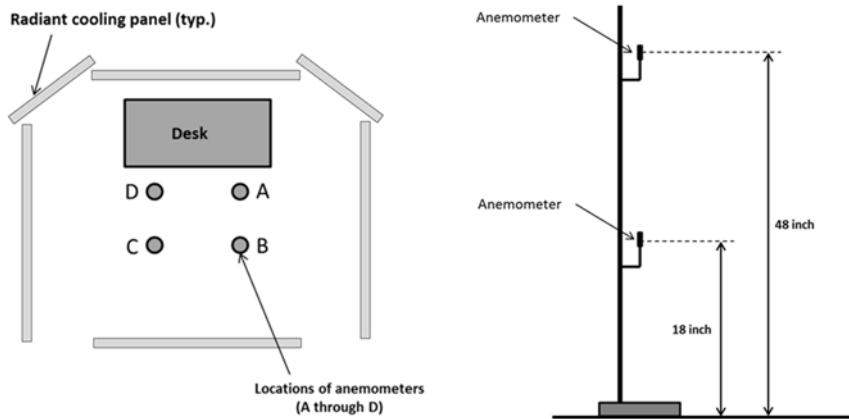
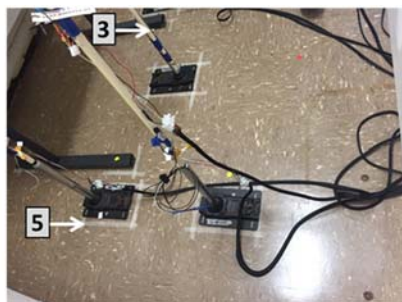
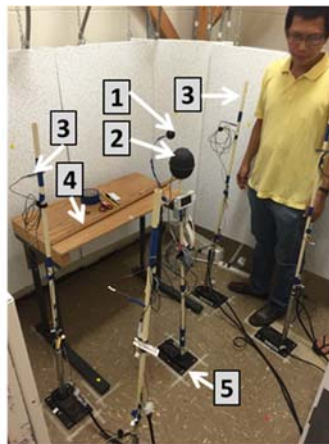


Figure 4.7.3: Description of the horizontal and vertical location of the eight anemometer used for the measurements

In Figure 4.7.2, the horizontal and vertical locations of F-900 anemometers were superimposed on the CFD presentation grid are the same locations of anemometers A through D (shown here in grey)



Picture A

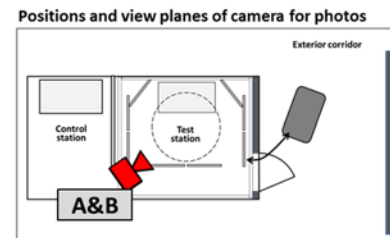


Picture B

Figure 4.7.4: Installation of the anemometers

Note: The globe thermometers (1) and (2) are also depicted.

- 1 Globe thermometer (large)
- 2 Globe thermometer (small)
- 3 Anemometer
- 4 Desk at which test person will sit
- 5 Marked instrument placements for globe thermometer and anemometers



Location B fan level 2 number of sample points 1,189
48 inch elevation of anemometer

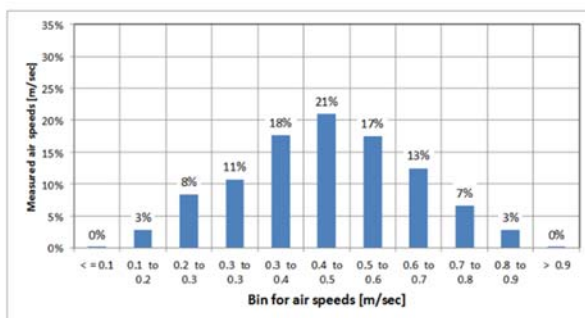
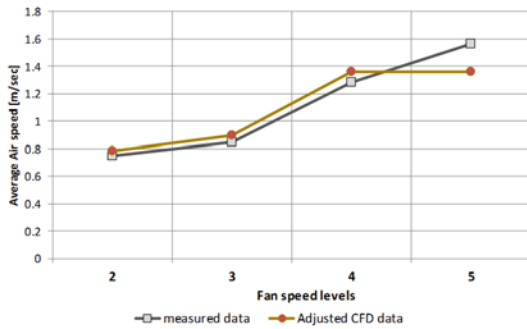


Figure 4.7.5: Example of results of air speed measurements at the test station for CFD validation

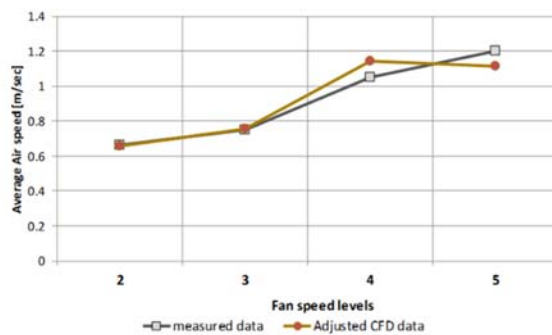
The frequency distribution of most of the data collected showed normal distribution of air speeds around the average

Adjusted CFD data points with an average and constant correction factors of 1.8
Average values for measured data and CFD
Actual and virtual anemometers at elevation 0.46 m



Comparison of ADJUSTED CFD simulation and measured air speeds – at sensor elevation of **0.46 m**

Adjusted CFD data points with an average and constant correction factors of 1.4
Average values for measured data and CFD
Actual and virtual anemometers at elevation 1.20 m



Comparison of ADJUSTED CFD simulation and measured air speeds – at sensor elevation of **1.22 m**

Figure 4.7.5: Validation of CFD simulation and measured air speeds at the test site

Ceiling fan induced air movement at the test site was investigated with CFD simulations. The air flow was simulated for four fans speed levels. The actual air speeds were measured at the site with an array of eight F-900 anemometers, located at four horizontal and two vertical positions. The CFD results compared very well with actual measurements of air speeds for different fan speed levels.

4.8 CFD Simulations and Measurement of Radiant Heat Transfer Without Test Subject

Radiant heat loss is the primary physical phenomenon of the comfort enhancing measure with actively cooled radiant panels. Since increased radiant heat loss decreases operating temperature without the need to lower the ambient air temperature energy can be saved to provide increased comfort. Radiant heat transfer at the test set-up was simulated with CFD and subsequently measured for data validation. The CFD simulations and measurements were carried out without a person sitting at the tests station. The objective of these tests of physical comfort contributing conditions was to validate the CFD simulation approach for thermal performance of the ERDL test set-up.

The CFD simulation determined the radiant heat transfer conditions for a “target” object, which was an inert object of the same dimension as the globe thermometer used in the actual heat transfer tests. The CFD simulation determined the average radiant temperatures that the target object was subjected to by integrating radiant temperatures over the target object surface. Figure 4.8.1 shows the “target” object which was placed into the CFD computational domain at the same horizontal and vertical location as the globe thermometer in the measurements.

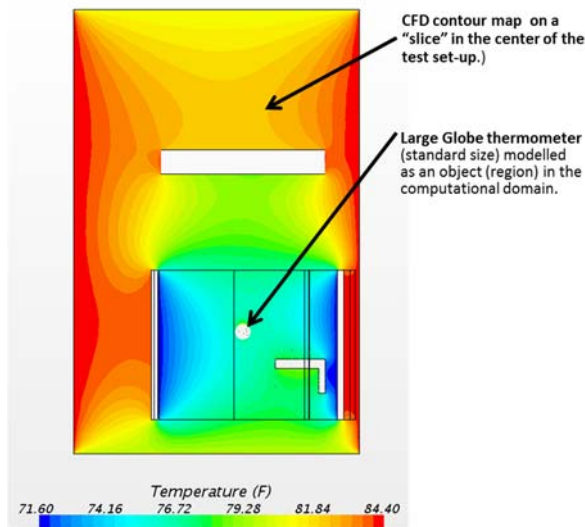


Figure 4.8.1: CFD simulation to determine the mean radiant temperature

The visualization show the temperature distribution on the center section of the test set-up.

Figure 4.8.2 shows the globe thermometer installed at the test set-up. The globe thermometer was installed along with eight anemometers for the test series without a person sitting at the test site. Image (A) in Figure 4.8.2 shows the globe thermometer situated at the center of the test station. Image (B) shows a detail of the globe thermometer installation with one large and one small globe thermometer. The large globe thermometer had standard dimensions of 150 mm and the small a diameter of 50 mm. The ERDL research team had built several small globe thermometers which were installed at different locations at the test set-up. The small globe thermometers were cost effective and allowed multiple measurements which were averaged in order to obtain more consistent radiant temperature data.

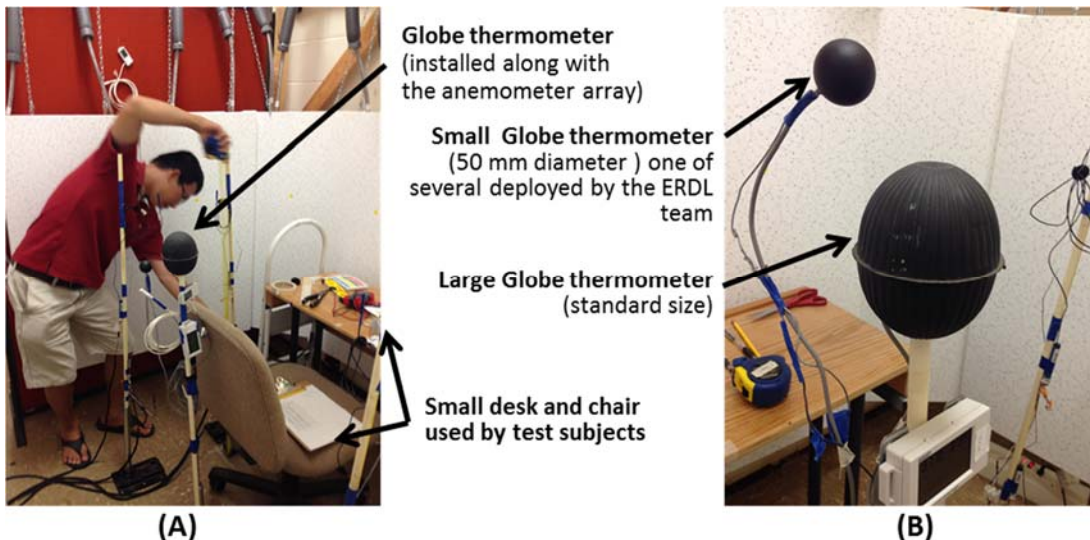


Figure 4.8.2: Test set-up with globe thermometer

The comparison of CFD simulation results of mean radiant temperature (MRT) and measured MRT is depicted in Figure 4.8.3. Figure 4.8.4 shows a comparison of CFD simulation results and measured air temperatures data. Figure 4.8.3 shows that the mean radiant temperatures obtained from CFD simulations (e.g. simulation) were smaller than those measured at the test set-up. Similarly, Figure 4.8.4, indicate that the predicted air temperatures were also smaller than the measured temperatures. Reasons for this data discrepancy could not be described with the available data.

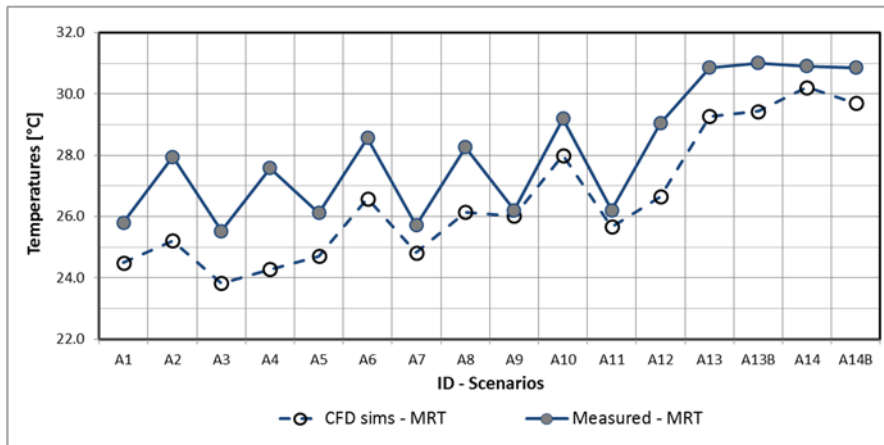


Figure 4.8.3: Comparison between CFD simulated and measured mean radiant temperatures

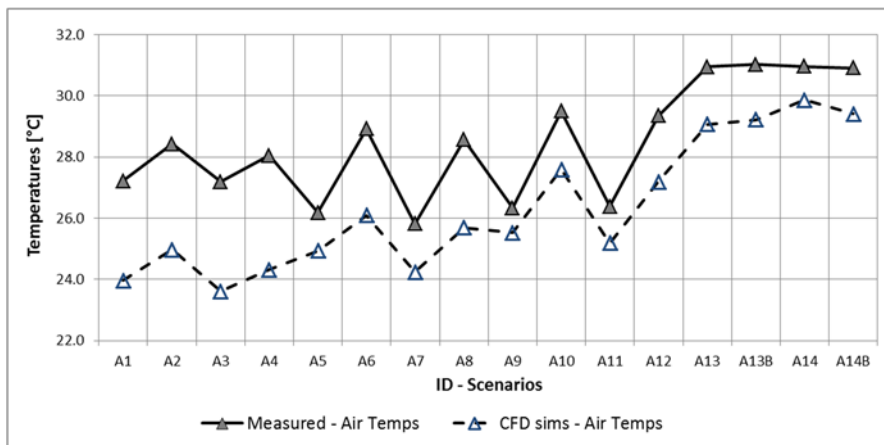


Figure 4.8.4: Comparison between CFD simulated and measured air temperatures

Radiant heat transfer was investigated with CFD simulation. The radiant heat transfer rates were compared with mean radiant temperatures (MRT) which were derived from globe temperature measurements. The comparison was carried out for 16 test scenarios. The comparison between simulated and measured MRT as well as simulated and measured air temperatures indicated slight data divergence.

4.9 Comfort Test with Human Test Subjects – Methodology and Results

Comfort tests were conducted over a period of four weeks at the test site in HIG 204. The approximately 40 tests participants (e.g. test subjects) were recruited from among University of Hawaii students and staff. The test participants followed a scripted test procedure which is described in Table 4.9.1. Test subjects experienced five test scenarios, which were four combinations of ceiling fan at different fan speed levels and radiant cooling panels. These test scenarios are described in Table 4.9.2.

Activity No.	Location of Activity	Description of activity	Duration min	Timeline min
1	Team office (HIG 205)	Subjects arrive at team office	0	0
2	Team office (HIG 205)	Subjects acclimate for 10 min; during that 10 min the get introduction and start fill our survey form	10	10
3	Control station	Subject stay at control station for baseline conditions; engages in directed activities	12	22
4	Test station	Subject moves from comfort station to test station; stays at test station during test scenario ("treatment"), subject engages in directed activities	12	34
5	Control station	Holding time at the control station while the test conditions ("treatments") are changed in the test station	2	36
6	Test station	Subject moves from comfort station to test station; stays at test station during test scenario ("treatment"), subject engages in directed activities	12	48
7	Team office (HIG 205)	Test subject is checked out and completes filling out the survey forms	2	50
Total length of test subject at the tests site			50	

Table 4.8.1: Sequence of activities by test subjects

The test subjects participated in one test sequence on one day. One tests sequence investigated the occupant thermal comfort experience for two scenarios with comfort enhancement measures plus the baseline scenario.

Table 4.8.2: Four test scenarios and one baseline scenario used in comfort tests

No.	Title of test scenario	Description of test scenarios	Type of comfort enhancement measures
1	Baseline	Condition in the control station of the test set-up	No measures operating
2	Fan 2	Only ceiling fan is operating	Ceiling fan at level 2
3	Fan 3	Only ceiling fan is operating	Ceiling fan at level 3
4	Panels	Only radiant panels are operating	Radiant panels
5	Panels + Fan 2	Radiant panels and ceiling fan are operating	Radiant panels and ceiling fan at level 2

Table 4.8.3 summarizes results of the comfort tests. The values in Table 4.8.3 include values derived from measurements of environmental data and numerical values of metrics derived from the comfort surveys completed by the test subjects.

Summary Report of the Research Project and Presentation of Results of Part 3

SECTION 4 - SUMMARY OF PHASE 3

Table 4.8.3:
Results of the comfort tests

The table presents values derived from measurements of environmental data and numerical values of metrics derived from the comfort surveys completed by the test subjects

Averages of values:	Baseline - Control Tests	Test with Fan at Level 2	Test with Fan at Level 3	Test with Radiant Panels NO Fan	Test with Radiant Panels and Fans at Level 2
PMV [-]	1.62	0.37	0.35	1.18	0.27
Temperature perception WARMER than or EQUAL to PMV prediction [%]	33%	35%	15%	10%	25%
Temperature perception COLDER than PMV prediction [%]	68%	65%	85%	90%	75%
Percentage of conforming general comfort (PPD) [%]	0%	60%	60%	5%	55%
Percentage of NON-conforming general comfort (PP) [%]	100%	40%	40%	95%	45%
Thermal sensation value >>> [-]	1.40	-0.10	-0.55	0.15	-0.50
<i>description >>>></i>	Closer to Slightly warm than Warm	Closer to Neutral than Slightly cool	Closer to Neutral than Slightly cool	Closer to Neutral than Slightly warm	Closer to Neutral than Slightly cool
Thermal acceptance value >>> [-]	0.40	1.95	2.20	1.25	2.00
<i>description >>>></i>	Closer to Neutral than Slightly acceptable	Closer to Moderately acceptable than Slightly acceptable	Closer to Moderately acceptable than Highly acceptable	Closer to Slightly acceptable than Moderately acceptable	Closer to Moderately acceptable than Moderately acceptable
Air movement acceptance value >>> [-]	-0.10	1.60	1.65	0.20	1.80
<i>description >>>></i>	Closer to Neutral than Slightly unacceptable	Closer to Moderately acceptable than Slightly acceptable	Closer to Moderately acceptable than Slightly acceptable	Closer to Neutral than Slightly acceptable	Closer to Moderately acceptable than Slightly acceptable
Air movement preference value >>> [-]	0.90	0.20	-0.10	0.90	0.05
<i>description >>>></i>	Closer to Want MORE air movement than Want No change	Closer to Want No change than Want MORE air movement	Closer to Want No change than Want LESS air movement	Closer to Want MORE air movement than Want No change	Closer to Want No change than Want MORE air movement
Numerical assessment of adaptive comfort:					
Conformant with adaptive comfort 80% criterion [%]	100%	100%	100%	100%	100%
NOT Conformant with adaptive comfort 80% criterion [%]	0%	0%	0%	0%	0%
<i>All values are averages:</i>					
Middle (e.g. expected) value of comfort standard °C	26.5	26.6	26.6	26.5	26.5
Upper limit WITHOUT correction for air motion: °C	30.0	30.1	30.1	30.0	30.0
Upper limit WITH correction for air motion: °C	30.1	32.1	32.2	30.0	32.0
Correction of upper limit due to air movement °C	No correction	2.0	2.1	No correction	2.0
Applicable upper limit °C	30.1	32.1	32.2	30.0	32.0
Operative temperature °C	29.6	29.6	29.6	28.2	30.1
Absolute deviation from middle °C	3.0	3.1	3.0	1.7	3.6
Percentage of deviation from applicable upper limit [%]	85%	56%	53%	50%	65%

The comfort tests were conducted with the participation of 40 test participants, who were students and staff members of the University of Hawaii. There were four test scenarios with comfort enhancement measures and one baseline scenario. Test participants (also referred to as test subjects) provided responses to their comfort experiencing of four test scenarios with comfort enhancement technologies and the one baseline scenario. The comfort tests produced important conclusions on the performance of comfort enhancement technologies and the general concept of “comfort islands”.

4.10 Performance and Ranking of Comfort Enhancement Measures

This section ranks the performance of comfort enhancement measures in regard to their potential of increasing occupant comfort in comfort islands.

A ranking procedure was created and applied to the comfort tests results. The ranking procedures involved a two tiered ranking method. In the first tier overall weights were assigned to each ranking criterion. The sum of all overall weights for all criteria was 100%, or unity. In the second tier of ranking alternative comfort enhancement measures (e.g. alternatives) ranking factors were assigned for each ranking criterion. The product of overall weight and ranking factor determined the resulting rank for each ranking criteria; and the sum of all resulting ranks was the overall rank of the alternative. The alternative with the highest rank was defined as having the best performance. Figure 4.10.1 illustrates the methodology of assigning overall weights. The overall weights in the first tier were identical for all test scenarios.

Ranking group and individual criteria	Group ranking	Criterion ranking	Overall weight
PMV	30%		
PMV value		50%	15%
Ratio of conforming to non conforming		50%	15%
Adaptive comfort conformance assessment	25%		
Percentage of operative temperature deviation from applicable upper limit		100%	25%
Response to thermal conditions	30%		
Temperature perception		15%	5%
Thermal sensation		25%	8%
Thermal acceptance		60%	18%
Response to air movement conditions	15%		
Air movement acceptance		60%	9%
Air movement preference		40%	6%
sums	100%		100%

Figure 4.10.1: Definition of ranking criteria and assigning of overall weights; the figure shows two levels of ranking, the first level is the group level and the second level is the criterion ranking.

The table illustrates that the group ranking and the overall weights add up to 100%. The basis of the ranking is a relative comparison.

In Table 4.10.2 individual ranking factors were determined for each ranking criterion and for each of the four comfort enhancement measure alternatives plus the baseline case. The result is the overall rank of the comfort enhancement alternatives is the multiple factor of the baseline control tests (benchmarking).

The ranking results of the performance test scenarios is presented in Table 4.10.3. The most effective test scenario alternative of comfort enhancement measures was scenario “Fan at Speed Level 3” and the least effective scenario was “Radiant Panels NO Fan”.

Table 4.10.3: Rank of performance of comfort enhancement measures

Comfort enhancement alternative	Rank of performance of increasing comfort level
Fan at Speed Level 3	1
Fan at Speed Level 2	2
Radiant Panels and Fan at Speed Level 2	3
Radiant Panels NO Fan	4

The ranking of the result of the comfort tests suggests that **both scenarios with “only the fan in operation” obtained the highest rank**, followed by the combination of cooling panels and fans and the scenario with only the cooling panel.

The physical phenomenon of using a fan to increase air movement over the body (or better skin) results in a higher convective heat loss due to an increased convective heat transfer coefficient. The heat transfer coefficient increases due to a thinner boundary layer when air passes the body with higher velocities. A higher heat transfer coefficient, in turn, increases the amount of heat that can be rejected from the body. This is the so-called “cooling effect” of the ceiling fan. The physical phenomenon of using actively cooled radiant panels results in the lowering of the radiant temperatures of adjacent surfaces and therefore in the lowering of the operative temperature.

Both physical phenomena of increasing air movement over the skin (ceiling fan) and lowering the radiant temperatures of adjacent surfaces (radiant cooling panels) result in the same occupant perception of being exposed to a lower operative temperature.

Conclusions derived from the present comfort tests suggested that the cost benefit ratio of using a ceiling fan is higher than installing an elaborate chilled water system with actively radiant panels. However, observation during the experiments indicated that the relative warm side walls and ceiling that surrounded the test station kept the mean radiant temperature higher than anticipated from initial scoping tests and CFD heat transfer simulations. Furthermore, all heat transfer simulations did not include the heat output of the test subject. Future tests should consider the installation of a radiant barrier to shield the test station from unwanted radiant heat gain from surrounding walls and ceiling.

SECTION 5 – OVERALL CONCLUSIONS OF THE RESEARCH PROJECT

The ranking of the two comfort enhancement technologies, ceiling fan and radiant panels, indicated that ceiling fans are the more effective method to increase comfort levels in spaces that are not cooled and dehumidified.

In fact, under test conditions that represent typical summer conditions detected in naturally ventilated spaces rooms at the University of Hawaii, acceptable comfort levels can be achieved using ceiling fans only or in combination with radiant panels.

Conclusions from these comfort tests indicate that ceiling fans are the best and most cost effective comfort enhancement technology. Using ceiling fans in naturally ventilated spaces can create comfort islands with acceptable indoor comfort conditions.